Smart building energy management system for improved energy efficiency.

by

Natheem Jacobs

A thesis submitted in partial fulfilment of the requirements for the degree

MEng: Energy (coursework)

in the Faculty of Engineering and Built Environment

at the Cape Peninsula University of Technology

Supervisor: Dr Marco Leroy Adonis

Bellville

November 2021

DECLARATION

I, Natheem Jacobs, declare that the contents of this dissertation/thesis represent my unaided work and that the dissertation/thesis has not previously been submitted for academic examination towards any qualification. Furthermore, it represents my own opinions and not necessarily those of the Cape Peninsula University of Technology.

Signed **Date**

ACKNOWLEDGEMENTS

All thanks and praise is due to Almighty Allah for his guidance and blessing in my time during this research. Without the hand of His blessing upon my life, I would have been unable to overcome the many challenges faced from the day I began higher studies.

I want to acknowledge my indebtedness and render my warmest thanks to my supervisor, Dr Marco Adonis, who made this work possible. His friendly guidance and expert advice have been invaluable throughout all stages of the work. The discussions and valuable suggestions have significantly contributed to the improvement of the thesis. I would also like to extend my thanks for being considered adequate to receive financial assistance during my research period.

My thanks are extended to my mother and father, who has sacrificed immensely during their lifetime to bring me to a stage where I am financially stable to engage in many things others cannot. I have a professional career, engage as a part-time researcher in my field of engineering and have the pleasure of being responsible for a beautiful family, all by the prayers and work of my beloved parents.

I wish to thank my beloved wife further, Zayaan Tommy, who has supported me immensely through our marriage which spanned throughout my Master's research. Without my wife, I would be lost in the darkness of my many responsibilities. She had assisted me with her patience, perseverance and constant positivity when everything seemed too challenging.

I want to thank Liquid Telecom (Pty Ltd) and the Cape Peninsula University of Technology for providing me with financial support, which has assisted me in completing this research without any financial challenges.

ABSTRACT

A thermal analysis was selected as a dissertation topic due to insufficient data from published scientific journals on detailed glazing thermal performance in parametric façades. Three glazing types, NC52, NC60E and NC55E, were analysed for this application. In South Africa, HVAC engineers' work is limited to professional fees, thus, the opportunity to value engineer an architectural design through thermal analysis is not always available. This dissertation clearly explains why thermal modelling should be adopted in every façade building design.

The Capitec head office building engineering team was required to perform a thermal analysis of the building at an early design stage. The main aim was to inform the architectural team how a parametric façade could be optimally designed to reduce the internal cooling requirement below a design threshold of 180W/m^2. A thermal comfort study was thus done to investigate the thermal performance following the GreenStar standard and SANS regulations.

The software *DesignBuilder™ with EnergyPlus™* was used to evaluate four glazing types; clear glazing as a baseline, NC60E, NC55E and NC52 performance glazing. The analysis provides detailed information on thermal performance for total cooling loads, internal and external solar heat gains, and various psychrometric values such as temperatures and humidity. The thermal comfort study aims to identify the Fanger predicted mean vote and discomfort hours, summarised as a weighted average for the best and worst-performing zones.

The thermal analysis showed that clear glazing is not practical for a façade and can result in 40% higher internal heat gains. Low emissivity glazing is high-performance glazing, and the application needs to be justified against the higher cost over a less expensive performance glazing. NC52 glazing can be significantly improved through energy-efficient passive architecture such as parametric facade design combined with external shading. Optimisation of the roof heat transfer through a green roof was done via a thermal heat transfer coefficient which showed no significant energy savings compared to a well-optimised building.

Thermal comfort was measured in each zone as a weighted average. It showed insufficient thermal acceptance levels in most zones as the dissatisfaction percentage was too high. Further data optimisation requires the application of computational fluid dynamics, data-driven models analysis, zone control and spatial distribution in multi-zoned areas, airflow optimisation and night ventilation. In addition to this, only measurement and verification can genuinely confirm the accuracy of a predictive simulation model.

DEDICATION

This thesis is dedicated to my dear mother and father, **Ferial & Ali Jacobs**. They worked effortlessly to provide me with the opportunity for higher education and always believed in my ability to achieve success.

I sincerely appreciate my dear wife, **Zayaan Tommy**, for the moral support she offered, to which I could not complete this work without.

This thesis is further dedicated to Rania Jacobs, my unborn daughter of 6months, who passed away during my research period.

Lastly, to the light of my life, Liyana Jacobs, my rainbow baby daughter who smiles at me each day, lightening my burden of responsibility.

TABLE OF CONTENTS

TABLE OF FIGURES

LIST OF TABLES

GLOSSARY

AHU -	Air handling unit
ASHRAE -	American Society of Heating, refrigeration, and air-conditioning engineers
AT -	Air temperature
CFD -	Computational fluid dynamics
CLO60 -	Clothing insulation of 0.6 used in thermal comfort simulations
CLO95 -	Clothing insulation of 0.6 used in thermal comfort simulations
ENE-1 -	Green Star credit for greenhouse gas emission
ESG -	External solar heat gain
GBCSA -	Green building council of South Africa
HVAC -	Heating, ventilation, and air conditioning
IEQ -	Indoor environmental quality
IEQ 9-	Indoor environmental quality thermal modelling standard Green Star
ISG -	Internal solar heat gain
IWEC -	International Weather for Energy Calculations
LC -	Latent cooling load
O&M -	Operations and maintenance
ODBT -	Outdoor dry bulb temperature
OT -	Operative temperature
PMV -	Predicted mean vote
SABS -	South African Bureau of standards
SANS 204	South Africa national standards
SANS 204 –	South Africa national standards (Energy efficiency in buildings)
SANS 10400XA -	South Africa national standards (Energy use in buildings)
SC -	Sensible cooling
SHGC -	Solar heat gain coefficient
TC -	Total cooling
TCA -	Total cooling per 1 metre square of area
UFAD -	Underfloor air distribution

CHAPTER 1: INTRODUCTION

1.1 Background of the study

Rational energy modelling is a science that requires a basic understanding of the combined effects of thermal heat transfer and architectural design. This process in building simulation allows one to estimate the building energy efficiency & thermal comfort inside a building. The thermal performance of various glazing types needs to be analysed for a building façade to understand the effect of overheating and peak load reduction to reduce the HVAC cooling plant room requirements. Rational energy design and optimisation applications need to be investigated to understand best practice for various scenarios encountered in a design stage.

1.2 Statement of the research problem

The published research on energy modelling is vast in the context of whole-building energy analysis, however, there is not enough data available for South African glazing manufacturers data in applied case studies. The software *DesignBuilder™ with EnergyPlus™ is* currently being used in many research publications and is the leading software for building thermal analysis. The façade thermal analysis simulation data on this software is very limited in published research. The study recognizes a parametric façade as the best opportunity to provide insight into the performance characteristics of these glazing types in a South African project. The value engineering process that was done during the design phase of the project, had to be further detailed regarding thermal overheating studies of each zone along the façade. Thermal comfort modelling also needs to be demonstrated as it is essential to a zone thermal analysis.

1.3 Justification of the research study

HVAC energy modelling has become a mandatory requirement for approving any council plans, as shown by SANS (2010b). Understanding how to reduce the final HVAC load estimates through progressive façade design is essential. A building and façade should thus be designed to maintain minimal energy consumption levels. These HVAC loads are also directly influenced by regulations and energy codes that need to be well understood as they play a role in how an energy model is prepared and analysed. Design optimisation is necessary to improve the energy efficiency of the thermal performance of the façade, and clarity is required to provide clear direction on how the most effective and appropriate assumptions can be made at an early design stage. The Capitec head office in Stellenbosch was selected for this purpose, and this study aims to reproduce the facade analysis done by the building engineering team.

1.4 Outline of the context

Chapter 1

This chapter covers the introduction of the thesis topic and discusses the main aims and objectives of the research topic.

Chapter 2

This chapter provides a literature review of the resources used in the thesis. The basic theory of thermal load analysis and HVAC design is analysed, and a critical review of relevant literature is done over the scope of energy modelling and thermal performance analysis

Chapter 3

The experimental framework comprises various research components that lead toward a completed thermal simulation model. This chapter discusses the basic engineering theory behind thermal load calculations and the experimental framework of the model development, it also provides the relevant energy modelling parameters used in the simulation.

Chapter 4

This chapter reviews the simulation and experimental results for the glazing performance analysis, optimisation and thermal comfort studies.

Chapter 5

This chapter concludes the results and discussion of the thesis.

1.5 Research aims and objectives

The analysis aims to measure glazing performance and its role in cooling load and thermal comfort in a building. The basic theory behind the cooling load simulation theory is discussed.

1.5.1 Energy modelling

1.5.1.1 Research aims

Model and simulate the performance of four different glazing types to analyse the effects of internal space heat gain on a façade.The HVAC cooling plant size is also required for a comfortable space temperature that adheres to the ASHRAE guidelines on thermal comfort.

1.5.1.2 Research objectives

a) Measure the Conduct a peak simulation load and glazing performance analysis of a parametric façade.
b) Carry out a sustainable design optimisation of a building architectural design for improved energy performance, and;
c) Perform a thermal comfort analysis to understand the importance of psychrometric charts.

CHAPTER-2: LITERATURE REVIEW

2.1 Heating, ventilation, air- conditioning and refrigeration

The American Society of refrigeration and air conditioning (ASHRAE) has significant influence in the modern world as a leading authority of theoretical research and practical applications in building services engineering. The literature published by ASHRAE forms the foundation upon which most of the current technical expertise in HVAC & refrigeration has developed. Numerous ASHRAE publications cover a broad spectrum of technical information related to thermal comfort control in all sectors.

The 2013 ASHRAE handbook by ASHRAE (2013a) covers most of the theoretical design considerations for thermodynamics and fluid heat transfer applications in the HVAC industry. The most relevant chapter investigated the psychrometric chart's variables, which involved a thorough review of the formulae used to calculate both thermodynamic properties for moist air and the various humidity parameters. The introduction of these parameters on a psychrometric chart led to a few examples of basic air conditioning processes relevant to HVAC design. The analysis of these air conditioning fundamentals is further reviewed to assist one with understanding how each variable plays a role in the load estimation process of HVAC design.

There are more than enough theoretical aspects covered in ASHRAE literature, however, the actual examples of how different psychrometric charts work are not adequate to assist a reader in understanding how to extract information from a graph using any known variables. Thermal performance analysis of a façade depends wholeheartedly on understanding how air properties change with outdoor air conditions and the thermo-fluid interaction with the building envelope, and this cannot be done without understanding the psychrometric chart.

In summary, the approach is entirely theoretical in the 2013 ASHRAE handbook. The literature aims to refresh the memory of a professional engineer, as one is expected to understand how to calculate thermal air properties from basic principles. Noting all the above, the information on psychrometrics is highly relevant, and the entire chapter is summarised in this dissertation.

The research by Howell et al. (2013) provides a revised and updated edition of the 2013 ASHRAE handbook. This detailed review covers every chapter relevant to the principles of HVAC systems. The most pertinent chapter that benefits this study is noted as the “Design Conditions”. Thermal comfort is discussed at great length. It was found that internal body temperatures are well regulated compared to that of the external skin, which is unregulated and can vary from between 31 – 36°C, depending on the activity and environmental conditions.

The psychological aspects of thermal comfort are shown to have an essential role in comfort acceptance, and it is a key component that drives the standard of acceptable temperature differences. A comfortable temperature of 33°C is the ideal mean skin temperature regardless of clothed or unclothed, and a temperature fluctuation of 1.4°C contributes to no discomfort. A further recommendation for acceptable humidity levels inside a space is noted at 30%.

The discussion of skin comfort temperatures leads to an analysis of the sensation of comfort, which forms the basis of the ASHRAE thermal sensation index scale, better known as the Fanger predicted mean vote index, which uses numbers from -3 to 3 to describe acceptable levels of comfort. There are also details on metabolic rates, which notes that men have 30% higher metabolic rates than women in all activities. The differences between males and females are usually not considered in thermal studies as office environments are mixed, and designing on the higher male metabolic rates is deemed sufficient for all occupants. The overall perspective is that the research is well presented as the finer aspects of thermal science, and the amount of data available covers the broad spectrum of thermal studies, making this reference one of the more valuable resources as thermal studies.

A similar research approach was shown in the research done by Grondzik (2007), who has provided a summarised manual HVAC design. More particularly, the chapter on thermal comfort includes further information on the ideal parameters on which an HVAC system should operate to ensure an acceptable level of comfort by the occupants, as recommended by ASHRAE 55. Metabolic rates (MET) are accepted at an average of 1.2 MET, and relative humidity is acceptable between the ranges of 40% - 50%, with an upper limit of 60%. The ideal indoor temperatures for summer and winter are noted as 22.2°C and 25°C, respectively.

These basic assumptions provide a yardstick for the average design conditions to which thermal simulations can better understand how an internal space's psychrometric properties impact the HVAC system design. This resource does however, only summarise basic thermal studies and not enough discussion on the Fanger PMV scale and how it plays a role in HVAC design.

A significant amount of time was invested by Gatley (2013) to help the reader understand the fundamental and advanced concepts involved in psychrometrics. As energy modelling relies on weather data files and algorithms to calculate the psychrometric properties of air, the site location parameters affect the final cooling and heat load simulation. It was noted that

ASHRAE published these psychrometric charts at varying sea levels, namely; 0m, 750m, 1500m & 2250m above sea level and each height with its respective barometric pressure.

These psychrometric charts allow one to derive any psychrometric parameter based on the site location. Thus, in summary, the advanced studies of psychrometrics were discussed in great detail, and each parameter is carefully explained and derived from the first principles, which sets a baseline for all HVAC designs and energy modelling simulations.

Load calculations are covered by Splitler (2014), who has provided a thorough review of the fundamentals of thermodynamic heat transfer with complete data sets of heat transfer materials to assist with load calculations. As seen in Table 3.7 of the thermal properties tables, single clear glazing provides solar heat gain coefficient for various incidence angles across the glazing pane. Under normal circumstances, a single value would be provided alone for a thermal simulation. The amount of thermal performance detail in this reference is so vast that it is impossible to simplify a single material's thermal properties. This information thus serves as a valuable asset to this research where a thermal energy model will require input parameters that are not necessarily available from a manufacturer directly.

Underfloor air distribution (UFAD) heating systems are used in certain climates, and more specifically, when there is an advantage of utilising this method to assist standard HVAC systems operation in improving energy efficiency. UFAD systems are covered by ASHRAE (2013e), who meticulously outlines UFAD systems and their role in practical applications. A room air distribution model is analysed that summarises how these systems function in an office environment, and there are three thermal zones noted. The lower mixed, middle stratified, and upper mixed zones exhibit different temperatures and air velocities. The erratic movement of airspeed temperature can be somewhat quantified with error using computational fluid mechanics and thermal modelling techniques.

Thermal comfort is an essential aspect of UFAD systems as the level of comfort acceptability is much higher than that of conventional overhead supply air grilles. The idea is that a UFAD design delivers the required air temperature and speed directly into the occupant zone from below the floor, and this is based on a 20% dissatisfaction rating with a 10% safety factor.

This reference provides a solid theoretical component into the thermal distribution of a UFAD system, however, some more research could be provided on more practical applications through case studies and performance analysis. Concerning a façade thermal analysis,

sufficient information guides the results and discussions to make an informed study on how thermal comfort acceptance is measured and concluded.

A detailed guide is provided by Simmonds (2015) for tall building design following ASHRAE fundamentals for commercial and high rise residential applications. HVAC systems design and tall buildings have additional risk factors such as the stack effect, which influences indoor and outdoor temperature conditions. The stack effect occurs when tall building experiences cold weather, and the building acts as a chimney which causes naturally ventilated fresh air from the lower levels to rise up to release warmer air in the upper regions of the building through a pressure difference caused by the building height. The reverse of this phenomenon is known as the reverse stack effect and has an opposite effect. It is noted that this effect regularly causes issues on lower levels during the heating season and elevator doors have problems with closing due to the pressure differential. From a power consumption point of view, it can be proven that there would be considerably more power inefficiencies thus, providing additional heating load is generally recommended on the lower level in high rise buildings.

This literature offers a more practical approach with more case studies referenced, it is also well balanced in both the theoretical and practical approaches. Relative to a facade analysis study, the stack effect may be considered for further research in a large open plan office environment. Energy modelling aims to quantify the various building physics problems that are not generally understood without software tools. This research will contribute towards understanding how to balance the design requirements for acceptable comfort levels.

The 2013 ASHRAE handbook by ASHRAE (2015a) covers most of the practical design considerations for HVAC systems over a wide range of applications. The chapter on commercial and public buildings provides guidelines on HVAC design criteria based on the occupation type. These internal design requirements are critical to an energy model as all load calculations depend on how internal space conditions are defined. For a typical office environment, it is recommended that during the winter period, an indoor temperature of 20.3˚C - 24.2˚C and indoor humidity of 20% to 30% are the conditions that will satisfy the occupants during this period. During the summer period, it is recommended that during the winter period, an indoor temperature of 23.3˚C - 26.7˚C and indoor humidity of 50% to 60% are the conditions that will satisfy the occupants during this period. The office environment is also recommended to operate at 8.5 L/s and 5 people 100 m² with occupation hours from 08:00 am to 06:00 pm.

The literature is quite thorough in providing the latest information and research on HVAC system design, with little or no discussion left open to interpretation, these internal conditions will be used as a yardstick when designing the research methodology for this dissertation.

The 2016 ASHRAE Handbook by ASHRAE (2016) is a highly detailed reference that focuses on applied HVAC systems. Everything is considered, from the primary design considerations to maintenance and commissioning. A direct expansion (DX) split system is analysed as to how it functions, and the essential components of the indoor unit that make up this system are noted as the evaporator coils, heating coils, filters, valves and a fan. The main advantages are that the cost is low, tenant metering is easy, little or no ducting is required, reduced power consumption and service installation is easy and maintainable without elevated cost. This resource will guide further research into detailed HVAC systems analysis as understanding every detail of the internal aspects of HVAC and refrigeration equipment are required on a component level.

District cooling is a popular method of providing cooling loads utilising thermal energy distribution with chilled water from central sources to various residential, industrial, commercial and other sectors. The technical guidance provided by ASHRAE (2013b), systematically addresses the complete background and benefits of district cooling in HVAC applications. The central plant facility is discussed with regards to its design requirements, and this information is quite helpful to a façade analysis because it provides general assumptions of what may be required to improve the energy efficiency of cooling systems.

It was noted that the primary condition in the overall operation of a chilled water plant is the temperature difference between the supply and return water. The temperature and flow rate are found to affect energy performance. The flow rate should be kept to a minimum to keep pump power running efficiently, and supply temperature would thus be required to run as high as possible and return as low as possible. The information provided in this resource is both advanced in the theoretical and practical approach, and it will be of benefit to assist with average design assumptions for an energy model.

District heating is a popular method of heating loads through hot water or steams from thermal energy distribution with chilled water from central sources to various residential, industrial, commercial and other sectors for space heating. The technical guidance provided by ASHRAE (2013c), systematically addresses the complete background and benefits of district heating in HVAC applications. The central plant facility is discussed with regards to its design requirements about heating loads, it is recommended that a 95% diversity factor between

design and peak load be the standard design criteria for district cooling plant operations, also the occupied and unoccupied periods be included in a schedule parameter that would represent both summer and winter periods.

The importance of diversity schedules in these larger plant rooms plays a significant role in the energy efficiency of the entire facility, and it notes that energy models require a well-researched occupancy schedule that includes the diversity of operation in the various seasons. The information provided in this resource is both advanced in the theoretical and practical approach, it will be of benefit to assist with occupancy schedule assumptions and future studies.

As data centres play a significant role in the modern age, continuous steady operation demands active cooling over the life cycle of these facilities. The limitations of air cooling can be overcome by liquid cooling, as noted by ASHRAE(2015c), who provides the necessary tools an engineer requires for the functional design of liquid cooling systems. The most relevant chapter analyses psychometric properties of a data centre environment concerning temperature and humidity, and it is recommended that a low-end environment design be specified at 20 ˚C, and 40% relative humidity (RH) and a high-end design be specified at 25 ˚C and 55% RH.

These are fundamental design assumptions as the operational level changes on a cooling load requirement and simultaneously reacts to the outdoor environment. This resource is directly related to a façade study. The amount of information provided on psychrometrics is highly detailed. There is also a well-researched methodology for analysing optimal temperature and humidity levels on a dynamic system. A parametric façade would have various results that need to be interpreted, and this resource may be used to analyse thermal simulation data.

The basic concepts of fluid engineering mechanics provide the basis for understanding how fluid travels in HVAC systems. One of the most respected resources available is that by Çengel et al.(2006), which covers in great detail everything from fundamentals to advanced principles of how fluids react in various states and applications in a real-world environment. The most relevant chapter, fluid kinematics, attempts to clarify the Fourier law heat transfer equation and its applications, which is referred to in this dissertation.

This resource is theoretical and serves the purpose of providing the necessary background equations and illustrations for understanding heat transfer and fluid mechanics, however, the lack of case studies or applied examples make it difficult to understand the concepts on a more advanced level. It is however, sufficient for simplifying the physics-based models that energy modelling software utilises on a more complex level.

One of the other respected resources available by Çengel et al.(2001) has provided the necessary theoretical information for the various applications of thermodynamics and fluid mechanics. The most relevant chapter, energy transfer, attempts to clarify the heat conduction transfer and thermal conductivity, more often known as the k factor, referred to in this dissertation. The temperature differential in the thermal conductivity formula is noted as the most crucial factor for HVAC design, as the outdoor dry bulb temperature and indoor space temperature requirement determine what air conditioning equipment is selected. This resource is more theoretically inclined and serves the purpose of providing the necessary background equations and illustrations for understanding thermal conductivity, however, similar to all publications done, there is a lack of applied examples which makes it challenging to understand the concepts on a more advanced level. It is however, sufficient for simplifying the physics-based models that energy modelling software utilises on a more complex level.

Thermal fluid science is the primary literature that is used in HVAC design as air-fluid movement and heat transfer describe the nature in which a fluid reacts to a system design. This is addressed by Çengel et al. (2008), who explains the laws of conduction, convection, radiation and condensation. The seamless integration of fluid mechanics and thermodynamics make this book the ideal approach to understanding the thermal performance characteristics in building physics. The chapter titled “basic concepts of thermodynamics” looks at the multiple types of radiation thermal radiation and their applications. The thermal resistance is focused on as this drives the design of a building envelope to which an HVAC system operation responds to achieve optimal thermal comfort. The literature is highly theoretical as there are primarily derivations and fundamental analysis covered, so there is sufficient information to explain the essential principles of energy modelling. This resource is directly related to this study as heat transfer and fluid science is the fundamental aspect of load calculations used in HVAC sizing.

Heat and mass transfer have their place in HVAC systems as the primary objective of HVAC design is to transfer heat through mediums and utilisation of mass transfer. This is addressed in detail by Çengel et al. (2007), who explains how the laws of fluid systems interact with thermodynamic systems in each of the detailed chapters. The seamless integration and adaption of formulae make this book the ideal approach to understanding heat and mass transfer building physics. The chapter titled “energy transfer” looks at the basic adiabatic heat transfer equation and its applications. The temperature differential component is focused on as this drives the entire plant equipment sized for an HVAC system design. The literature is highly theoretical as there are primarily derivations and fundamental analyses, so there is sufficient information

to explain the essential principles of energy modelling. This resource is directly related to this study as heat transfer is the fundamental aspect of thermal load calculations.

Regardless of its purpose, every mechanical system requires some form of control; otherwise, it would become inefficient and impractical to operate. HVAC and refrigeration systems have a wide range of controls in real-world applications to manage how the systems function for temperature control in various environments. A vital resource is provided by McDowall et al. (2011), where a detailed study into control systems, particularly for HVAC systems, is broken down meticulously into its various components. The fundamentals of control modules and their requirements are well detailed. The controls themselves have been investigated in detail for; self-powered, electric, pneumatic, and analogue electric-powered devices.

The software consideration and control protocols have also been explained how systems function to support one another. This area of study is directly related to energy modelling in that an HVAC system relies on control systems to control the temperature, airflow, and pressure of the fluid it is moving. Detailed energy modelling, which would be a prelude to this dissertation, would require an understanding of control system logic as it can be modelled to account for energy usage, however, it is not expected that it would be significant enough compared to the energy utilised in an HVAC plant room.

The resources utilised for HVAC and refrigeration systems are the most complete and up to date information on modern-day engineering practice and how it ties up theory combined over years of research and development into actual installed, tested and maintained systems. The amount of information is vast yet shows a seamless combination of physics applied in real-world applications. The ability to identify and estimate heating and cooling requirements has been standardised even though it is a highly complex process that demands a basic understanding of all the elements involved in moving fluids and heat transfer. Focusing on these disciplines' theoretical background will allow for a smooth transition into the more advanced topics, namely energy modelling and computational fluid dynamics.

2.2 Energy modelling

Energy simulation and modelling is a science that encompasses most, if not all, of the technical disciplines within the built environment. Estimating the building energy utilisation, specifically regarding the HVAC energy consumption, is a unique skill that demands a high level of understanding of the different elements involved in how an HVAC system operates within a building envelope. The literature available for energy modelling has significantly been

developed to provide the necessary skill set required to understand the process behind predictive modelling of building thermal performance.

A broad approach towards energy modelling is represented by Anderson (2014), who detailed the energy modelling process over all aspects of the building physics applications. The most relevant chapter refers to comfort and controls, where thermal comfort is discussed for energy modelling. The acceptable levels of external environmental temperatures are noted at an average of 21˚C, and these comfort levels are experienced by the metabolic rate and clothing insulation value, where 0 is nude, and 1 is a business suit. These values are critical to the energy model inputs and will be compared to the initial assumptions. The resource is quite basic in its approach to thermal comfort, and the introduction is brief. A further simplified computational fluid mechanics study on thermal comfort and spatial distribution is also studied. The research is sufficient to introduce thermal comfort studies, and the additional information provided allows for further referencing into the methods that may be utilised in a façade thermal analysis.

The limits of thermal comfort are analysed by Nicol (2013), where the fundamental aspects of comfort and overheating have been studied for European buildings. One of the more essential findings suggests that temperatures exceeding 28 ˚C for longer than 1% of working hours is classified as overheating, however, in colder temperatures such as the United Kingdom, this may be acceptable in the upper limits of the Fanger thermal comfort scale. It was noted that while the limiting values of indoor temperature may be used to provide a sample of measurement for overheating, the severity is not quantified with temperature scales alone. A space with 1˚C over the limit might have less overheating of a similar space of 4˚C even if the hours of discomfort was longer in the case of 1˚C temperature difference.

The formulation of the weighted average is thus the acceptable unit of measurement on the discomfort scale and has been well researched in both CIBSE and ASHRAE technical guidelines. The risk of overheating is an essential topic of this resource as it directly relates to a façade analysis thermal simulation results, this resource presents a well-researched outlook on thermal comfort as the thermal simulation technical design guideline codes and standards are well researched and tested over the broad spectrum of thermal comfort studies.

A complete guide to the DesignBuilder™ interface was done by Garg et al. (2017), who provides a comprehensive breakdown of the initial data required to do basic heat load estimations. The materials and construction data are carefully broken down into their respective categories and roles in the simulation and is one of the more essential aspects of a thermal

simulation. A building consists of various constructions, such as a floor, roof, walls, windows, and openings. These components are represented by a graphical object and a thermal resistance that the software measures the area and volume to compute the various simulations.

Many other thermal and fluid variables are noted to calculate the different building physics simulations with the envelope, such as thermal bridging and condensation. The elemental construction thermal resistance focusing on glazing is noted as the most crucial factor for this dissertation. The resource mainly aims to provide theoretical examples on how to use and set up the various variable requirements of an energy model in DesignBuilder™ and serves as an invaluable source of guidance in this regard.

The modelling methodology is essential to understand how to achieve accurate simulation results, the scientific methods behind energy modelling are detailed by Underwood et al. (2008), with this resource focusing on the mathematical approach. The most relevant chapter investigates heat transfer through a glazing plane, it was shown that there are three significant properties from the sun's interaction between the external glazing surface to provide external heat gain and the internal surface, which provides internal heat gain. These three variables are summarised as reflectance, absorption, and radiation.

These variables will be used to explain the fundamental approach that energy modelling utilises to complete a load calculation based on the glazing thermal resistance and solar heat gain coefficient. This resource is theoretical and does not provide applied examples or case studies. In this regard, the information is only sufficient to introduce the building physics formulae and explain the mathematics behind them, thus further work is required for understanding the various applications on a parametric façade.

The effects of double and tripled glazing were investigated by Al Touma et al. (2008), this paper provides a novel analysis on glazing performance in offices in hot climates. The study uses measurement and verification of fully louvred and blinded compartments compared to glazed enclosures with no passive architectural features. A key aspect noted is that the total convective heat gain for all room types is always more significant than the total radiation energy transmitted through the façade surface. Although the best performance was noted on a triple-glazed façade, the addition of shading devices and double and triple glazing mean that the external surface temperature on the façade is always high.

Room	Total Convective Heat Gain (kWh)	Total Solar Radiation Transmission (kWh)	Total Cooling Load (kWh)
Room 1	254.8 ± 15.1	82.2 ± 9.7	337.0 ± 24.8
Room 2	196.9 ± 15.1	143.9 ± 9.7	340.8 ± 24.8
Room 3	248.3 ± 15.1	60.1 ± 9.7	308.4 ± 24.8
Room 4	153.9 ± 15.1	80.8 ± 9.7	234.6 ± 24.8

Figure 1: *Calculated cooling loads in four rooms* (Al Touma et al., 2008)

The analysis is very well done in terms of measurement and verification of an experimental setup, however, it lacks an analytical approach or a basic thermal simulation to which the results can be compared to identify the accuracy of a thermal model. The reference will significantly benefit this study as the temperatures and cooling loads analysis of a façade zone is particularly important, as interpreting results requires previous research.

The influence of solar shading in office building cooling loads was investigated by Damian et al. (2020), there are four sun shading scenarios considered where S0 is the base case without any additional passive design features, S1 is a vertical aluminium blinds on the inside window face, S2 as horizontal blinds, S3 with a dynamic sun shading system that is made up of aluminium lamella and S4 which utilises the shadowing effect of the neighbouring south-facing building. The most important observation is that S3 produces the lowest cooling load requirements and electrical consumption when compared to the other scenarios.

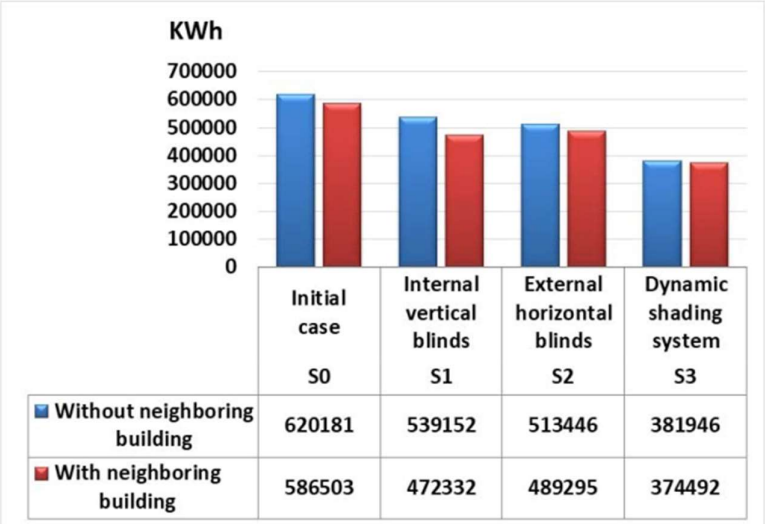

Figure 2: *Annual cooling loads analysis* (Damian et al., 2008)

The research presented on the various scenarios provides essential insight into thermal zone directions and façade design. The paper, however, is limited in the respect that it does not focus on multiple performance glazing types but looks at blind performance in thermal modelling. This limits the analysis to provide additional information on how various glazing systems can also reduce thermal loads along the façade zones. This information is beneficial as blinds are an essential design feature of residential and office blocks to ensure a passive reduction of internal heat gain. The analysis will assist with understanding what other methods can be used to increase the thermal efficiency of a parametric façade.

The comparison of mean radiant temperature thresholds and predicted mean vote limits was investigated by Song et al. (2022). This resource explains the limitations of mean radiant temperature concerning internal thermal comfort according to the PMV scale. The PMV values equal to +- 0.5 and +- 1.0 are the thresholds at which the mean radiant temperature can deviate towards 90% and 75% satisfaction of occupancy comfort. Figure 3 presented in this research provides the optimal measurement scale for applying the Fanger index comfort scale. It is understood that the most optimal environment is when the air temperature is closer or equal to the mean radiant temperature.

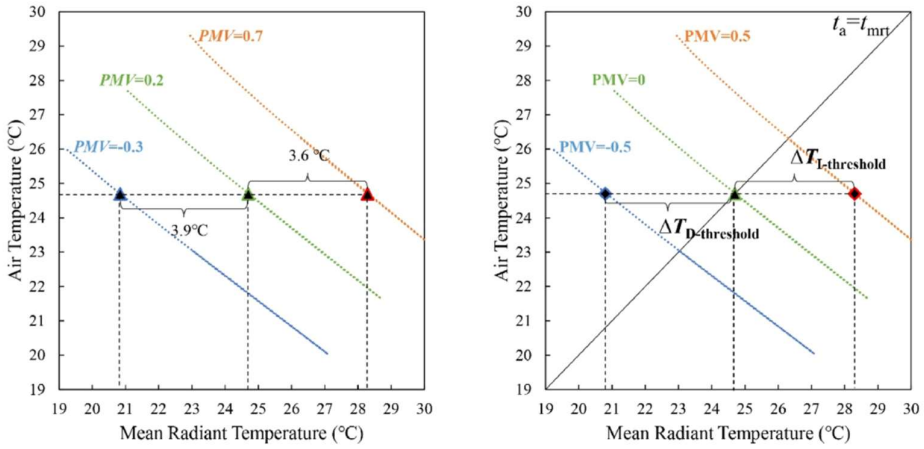

Figure 3: *Mean radiant temperature and PMV comparison* (Song et al., 2022)

This resource is limited because it provides an impressive theoretical background on the subject of temperatures in a space. The application of a case study or real-time analysis is not present. The results need to be understood as to the deviation between a mathematical model and a real-time environment. Futher, the highly relevant information will be provided and compared as temperature performance concerning this thesis.

2.3 Regulations, codes and standards

.The South African National Standards (SANS) developed by the South African Bureau of Standards (SABS) has guided the building environment practice in South Africa. These strict regulations form the basis of deemed to satisfy council approval and provide the option of rational design and govern all aspects of building engineering.

The most relevant standard to this dissertation is that by SANS (2010b), who provides the lighting and ventilation standard of South Africa. The design regulation presents fundamental requirements and guidelines to rational energy modelling assessments for approval by the local council. The standard covers the building envelope requirements and design assumptions, whereby this study will consider the relevant 10400XA energy assessment procedure guidelines. The design assumptions are provided in the "Air requirements for different types of occupancies" section, where the various spatial types are regulated with their ideal minimum outdoor air requirements in air changes per hour and litres per second per person.

A significant difference found between SANS and ASHRAE is that SANS only requires the highest ventilation rate to be designed for between the two types of air requirements, and ASHRAE combines these as a minimum design standard. ASHRAE would thus be a better standard to follow however, the dissertation is for a project in South Africa so that SANS would be the more appropriate option. This resource sets the essential requirement for an energy model as fresh air provides the ventilation heat load.

This ventilation standard is directly linked to SANS (2010b), known as SANS 204, where the entire construction planning guideline is provided. This includes; climatic conditions and fenestration requirements for the applicable space requirements. The most important information noted for this dissertation is the summary of worst-case glazing, there is single clear, single tinted and double clear glazing rated. Single glazing has to be the worst-performing thermal performance in both heat transfer and solar heat gain coefficient, thus it would serve as the base case for comparison in a façade thermal analysis presented in this dissertation. The standard is highly technical and provides enough information on glazing performance, however, the standard was published in 2010, and improved glazing performance cannot be found in an updated directory. The standard will be thus used as a guideline to what is appropriate in an energy model for glazing performance.

Green Star is a unique energy design procedure that encompasses the entire built environment, The technical manual of new office buildings version 1 is provided by GBCSA. (2010) who

sets the standard for energy credit systems for every aspect of the design and as-built stages of the project. The design guideline recommends two simulations be done, one for a 0.60 insulation clothing value and another for a 0.95 clothing value, each with their own respective air velocities. Thermal satisfaction is measured using the simulated weighted average hours on the dissatisfaction scale. Compared to other literature, the thermal modelling standard is oversimplified as velocity and insulation values are dynamic in reality. A CFD assessment is required to thoroughly assess thermal comfort to a scientific level of research acceptance. The IEQ-9 standard is sufficient for building performance modelling and will be used as needed.

The technical manual has a broad scope beginning with the introduction into the credits available and the rating tool for office buildings which lead into the certification process. This is an in-depth system that is always open to interpretation. The IEQ9 thermal modelling standard will be utilised to assess thermal comfort for the internal zones of the parametric façade, and the relative velocities and insulation values will be adopted.

2.4 Optimisation methods

An energy simulation reliability study is done for further application in indoor environmental predictions. This study is directly related to a parametric façade analysis as the building utilised in this dissertation has already adopted a parametric façade design, which reduces the glazing in some areas and increases in other places along the façade. The limitations of this resource are that it considers colder climates in Tibet, which is the opposite of the South African weather, however, the results provide meaningful insight into what can be expected in different climates.

The Optimisation of HVAC systems has various strategies that can be implemented to achieve efficient operation during the life cycle. Optimising a system can be planned at the design phase and through routine maintenance and upgrades. This study aims to identify methods that are limited to the following methods at the design phase, noting that these are only a few of many solutions available to the HVAC industry.

This key focus area provides the necessary information to conclude acceptable assumptions on how passive cooling can improve a building design. This research is highly relative to this dissertation because the energy model simulates both temperature and ventilation rates. Further research on this topic can guide research into acceptable assumptions of average space temperature reduction where passive cooling is used and will be utilised in the literature review.

Evaporative cooling is an environmental friend cooling process that utilises water and air as heat transfer mechanisms. As per figure 4, water is pumped through a cooling pad, and mechanical ventilation pulls through cooled air into the space requirements.

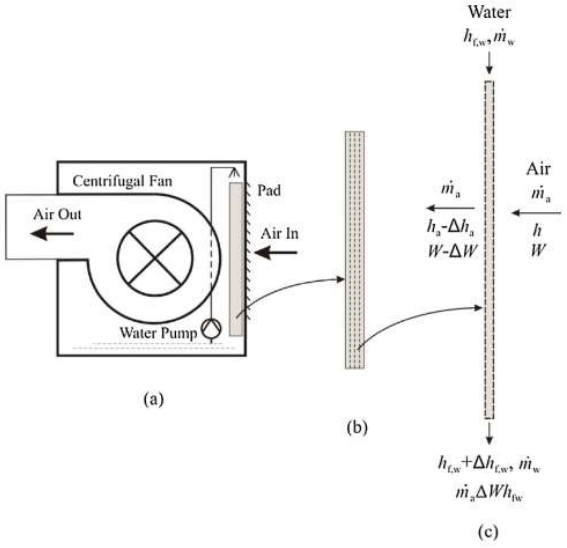

Figure 4: *Evaporative cooling process* (Santamouris, 2008)

Two processes exist, classified into direct evaporative cooling, where water and air are mixed through a durable pad changing the humidity and temperature. The second process is indirect evaporative cooling, where a thin med separates air and water, which allows the moisture to remain constant. During indirect evaporative cooling, the benefits of such a system allow for pre-cooling and heat recovery (Santamouris, 2008). The relevant aspect of this resource is noted the essential elements of passive cooling in residential homes. In combination with a whole house fan, interior air sealing and elastomeric roof coating, the solar gains were decreased by up to 80%, and a 2.5°C decrease in internal temperature was noted. This resource is well researched, and the topics cover the fundamental theory behind the various cooling methods. There are also numerous case studies and further detailed analyses present to cover the broad topic of passive cooling. The reduction of solar heat gain and internal temperature is of great importance to this study as it is the main aim of a façade analysis.

This energy storage method ensures the system operates at the lowest cooling setting, drastically improving energy performance. The resource is highly detailed in that it provides extensive information into thermal energy storage systems and analyses applied examples and case studies, allowing one to gain confidence in its application. The relevance is of high

importance as the building in this dissertation utilised an ice bath thermal energy storage system in the HVAC cooling system, and this reference will assist in further research discussion.

An introduction into natural ventilation studies is done by Wood et al. (2017), who discusses its importance to building design for improved energy efficiency. This resource provides a case study for the Deutsche Messe AG building, and the natural ventilation method utilises a double skin façade and a sliding window of each level of the façade, and stale air is exhausted through a duct in the ceiling void via the stack effect. The double skin façade results in an air buffer with incoming pre-tempered air, increasing energy efficiency. The natural ventilation technique improves air conditioning performance, and the heat from stale air is sent through a heat recovery system, improving the chiller performance. This resource focuses extensively on case studies and applied examples in the operational buildings. This focus provides confidence in a natural ventilation design approach and suggests an additional way to improve façade thermal performance. Natural ventilation is covered in the openings & infiltration model input in the thermal analysis software.

Wind-induced natural ventilation is a passive method that is researched by Haw et al. (2012), who focuses on an experimental analysis of wind-induced natural ventilation, the results show that an average external wind speed of 0.1 m/s flowing over an inverted airfoil connected the building architecture can generate approximately 10000 m^3/s with an average of 57 air changes per hour for comfort cooling via ventilation and improved air quality.

Figure 5: *Wind-induced experimental house* (Haw et al., 2012)

These are exceptionally high flow rates and can provide the best solution for façade overheating and improving HVAC system performance. This resource gives much attention to an actual example along with measurement and verification. It would usually be challenging to quantify ventilation rates through software tools, thus this resource motivates why further studies are

required on at least one ventilated area of the parametric façade in this dissertation. The external wind velocities of 0.1 m/s will be used to rationalize an appropriate velocity for the comfort simulation, in conjunction with the relative IEQ-9 code.

Desiccant cooling and its effects on indoor air quality are researched by Ahlem et al. (2015), who discusses the utilisation of solar thermal heat collection for thermal-based desiccant air conditioning systems. A key finding of this research is that the optimal method of achieving the desired temperature in a space can be performed with great accuracy if an HVAC system humidifies the air after the cooling process is completed. This is relevant because the energy model allows for both temperature and humidification settings to be applied, and one can be decided as the driving parameter on which the air conditioning system operates. The temperature setpoints should ideally be focused on a façade analysis study vs humidity, as the latter would only be of concern in detailed thermal comfort studies. The resource is mainly based on mathematical modelling. It does not consider case studies or a more technical approach. In this respect, it lacks the realistic approach to a host of environmental and operational variables that may be present. For this dissertation, the focus on temperature set point would thus be deemed as the primary focus area to reduce overheating.

Direct evaporative cooling (DEC) and chilled water systems are researched by Al-Badri et al. (2017). who focuses on psychrometrics in air conditioning design and develops an analytical model to predict mass and heat balance performance. The mass flow rate ratio is tested in simulation conditions that assist provide various conclusions of the applications of direct evaporative cooling in humid conditions climates, the end goal being increased energy performance of an HVAC system. The key aspect of this research concludes that decreasing the mass flow rate while relative humidity is high improves the energy efficiency of a DEC HVAC system. This is important to this study as heat loads and mass flow rate of heat rejection or absorption are directly related. Although mass flow rates are not the key focus of this dissertation, it would be of great value to take note of the significance of mass flow rates vs heat balance in a façade analysis. DEC is also a typical strategy used in fan coil units.

Indirect evaporative cooling (IEC) systems are analysed by De Antonellis et al. (2017), who provides an overview of experimental analysis in summer outdoor conditions. The main focus is placed on an IEC utilised in air handling units of an HVAC system, and the results show that chiller operation is greatly improved by reducing the fraction of evaporated water and primary air temperature of the system. IEC research is relevant to this dissertation as the experimental analysis focuses on temperature performance in and out of the boundary conditions.

The research is limited to a single experiment in summer conditions and does not consider various other design parameters and winter conditions. For this study, the primary inlet temperature conditions of a summer design will focus on how it is affected in a façade analysis as the weather file extrapolates numerous outdoor dry bulb temperatures in all seasons.

Green roofs are used as passive techniques to improve the building performance as it is complemented by their cost-effectiveness and building aesthetics. The study by Ran et al. (2017) provides an insight into real-time field experiments to analyse thermal performance on roof structures with the combined effects of natural ventilation. Building energy simulations have been conducted in DesignBuilder™ to compare model data with the tested results. This research shows that intermittent ventilation and a green roof can reduce acceptable temperature levels by up to 27% compared to an insulated roof with mechanical ventilation. The analysis provided is in-depth in its approach towards thermal analysis of green roofs and offers the best resource for simulation comparison as the software utilised is the same for this study. This research is essential because a green roof analysis is included in this dissertation.

Natural ventilation is a standard method of providing air at atmospheric conditions to spaces through infiltration into the building envelope, Ran et al. (2017) analyses the performance of combining green roofs and natural ventilation. The study reveals that intermittent ventilation and improving the heat transfer through a green roof can reduce system energy requirements by up to 27% on average.

The combination of green roofs and ventilation to achieve cooling is discussed by Jiang et al. (2017), where the main objective is thermal performance and energy efficiency improvement. A building simulation using energy modelling software is done for a building in China, showing the cooling and energy performance potential in both hot and cold climates using the combined method of passive improvement. The conclusions drawn provide valuable information on how ventilation studies and simulation models can improve building performance during a summer day by reducing internal temperature and reduce overall solar heat gains. An entire season is simulated with intermittent ventilation, and the data supplied from simulation results guide one on how building performance improves energy efficiency. This is a well-researched analysis as there is an experimental case study, measurement and verification data, and a mathematical model to compare site performance data. A green roof is modelled in this façade analysis of this dissertation, and this resource will provide the data required to quantify the simulation results.

A further study into the performance effects of green roofs is analysed by Kotsiris. et al.(2012), who discusses specific heat transfer values used in a simulated in an experimental building structure, where the research aims to study how energy performance is improved with various green roof constructions. It is noted from this study that green roof compounds with substrates of rock wool of coarse aggregate produced the lowest thermal transmission, and the green roofs with rock wool or 20cm pumice had significant performance improvements. This was approximated at 60.5% - 62.5% overall increase over a non-insulated roof. The research is well thought out, with both a mathematical model and a live building structure to measure actual performance, it provides a well-rounded approach to what is the best heat transfer properties to use in a façade analysis and will be used for that purpose in this dissertation.

Computational fluid dynamics (CFD) is relevant to this dissertation as detailed thermal comfort studies rely heavily on CFD as a tool to model the expected airflow and temperature within a zone. A CFD analysis was researched by Zhang et al.(2016), where a factory plant system for food production has been made the area of focus. The ventilation method of forced convection and circulation systems are often used in these factories to arrive at the desired climatic conditions for successful industrial storage of the perishables at hand. Stagnation effects of poor air quality can be responsible for lousy crop development of vegetables such as lettuce by the low transpiration rate. A detailed 3-D CFD analysis has been done to validate improved airflow performance within the boundary conditions. An improved solution to a warehouse shelf's thermal and fluid requirements was also simulated. Unlike with product design, CFD analysis should typically be done more often in HVAC building engineering design. CFD is mainly done if the necessary budget and time are available is a tool that can help with these complex relationships. Each building envelope could be improved in the design phase to ensure the highest operational efficiency of an HVAC system. The results concluded assist with the predictions to passively improve energy performance.

The design improvement simulates four cases with perforated tubes as the primary method to improve air performance. Notably, the most crucial aspect of this research study is that air distribution is shown to improve with additional airflow ducts implemented into the design. Insufficient airflow is proven to have adverse effects on air distribution across the room, known as dead spots, and the temperature profiles indicate that thermal comfort improved. This is important to a façade overheating analysis as thermal comfort acceptance is second on the list of priorities, and a poorly designed HVAC system will operate at higher inefficiencies.

The velocity profiles of this study will be used to gauge the average airflow velocity used in the thermal comfort simulation, along with the relevant green star energy design guidelines. The limitations of this analysis are that it is restricted to a particular application that is not similar to this dissertation, however, the interpretation of results will be focused on and used to quantify thermal simulation results.

The improvement of thermal comfort by controlling airflow around the building envelope was investigated by Mochida et al.(2005), who discusses cross ventilation as the technique used to achieve better comfort standards in the occupied space. Although not widely utilised anymore, it offers an insight into passive strategies in vernacular architecture that can drive building performance towards improved sustainability. CFD research has thus attracted much attention to the concept of cross-ventilation in future building design. The method of variable control of window openings to alleviate temperature fluctuations is presented with a predicted mean vote (PMV) as the control variable. The conclusions of this research suggest that by adjusting the mass airflow rate to suit window positions and planting a tree in strategic locations to change wind loads, a CFD analysis can be used to predict airflow and load operation in the applications above and significantly improve thermal comfort. The utilisation of the comfort scale is significant to this façade analysis as interpreting thermal comfort data is not just limited to temperature and humidity changes. Knowing how other research applies the comfort scale allows one to gauge how results should be interpreted. This analysis is limited to a basic comfort analysis and does not focus on heat gain and its effects thereof concerning comfort acceptance, but for understanding the comfort scale applications, it is sufficient in this regard.

Building simulation combined with CFD has been analysed by Colombo et al.(2017), who focuses on designing a double-glazed façade using CFD. The method utilised evaluates a warm day cycle and interior thermal comfort performance, focusing on temperature and heat gain on glazing and surface boundaries along with highly sensitive temperature loads. The model also displays the potential to increase energy efficiency by varying parameters, including the absorptivity of glazing, area, and ventilation slots. The key component of this research indicates that surface temperatures on the internal face are simulated at approximately 30°C, while the external blind temperature is almost 70°C.

The reduction of temperature from the outside glazing to the inside glazing is significant to a façade analysis, as the interaction of solar radiation is the focus of this dissertation. The CFD analysis is well researched, and the approach is effective to understand the various elements of

façade components and solar radiation, however, there is only one glazing type used, and this limits a thermal study to provide a broader understanding into glazing performance.

Simulation of HVAC systems has provided the ability to utilise modelling strategies to improve energy efficiency. The discrepancies of a model vs reality have been analysed by Trčka et al. (2010), who details these inefficiencies. The are various components involved in HVAC design, and there is significant research being done on the performance of the components in an HVAC plant. This resource summarises multiple case studies and provides insight into how efficient modelling can be when a system is commissioned. Engineers would thus allow for estimations into the accuracy of model validation against real-world applications. In particular, in this façade analysis, peak performance will not be considered the final design requirement. A significant factor of safety (FOS) is required to finalize the HVAC system design. This analysis is limited to case studies and literature reviews; however, no modelling supports the claims, and a higher FOS will be considered for the theoretical research even if overdesigned.

Modelling can significantly reduce overall energy consumption, and with sophisticated software tools, the effects of all the variables each have a significant role in the overall simulation results. A brief yet detailed study is provided by Afram et al.(2014), who shows the complex relationships involved in HVAC operation and the various measurement and verification processes. The ability to control temperature, pressure and velocity of the heat transfer medium is studied and chilled water temperature setpoints. All the data provided allows for a most accurate simulation considering the physical phenomenon of all boundary conditions. The conclusion is drawn to give information on data-driven models, physics-based models techniques focusing on utilising scientific formulae as the research model.

This research is mainly mathematical modelling which uses many complex data-driven models to arrive at assumptions on control strategies for HVAC systems, and the relationship between a façade analysis and control systems analysis is the focus on the multitude of physics-based parameters available in this text. This information is thus relevant to the literature review of this dissertation as the relevant parameters noted for thermal model inputs will be confirmed, noting temperatures, thermal resistance and energy gain as detailed in the model inputs. In terms of the research approach, it is highly theoretical, and no case studies or applied examples are present, thus the focus on model parameters becomes the key focus of this research paper.

A data-driven approach to reduce energy utilisation of HVAC systems is presented by Kusiak et al.(2014), who detailed this process to maintain thermal comfort. The dynamic effects of

occupancy changes significantly impact performance modelling, and the Poisson model is utilised to represent these conditions. The data presented an opportunity to form a multi-layered perception mathematical model that can accurately predict an HVAC system's performance based on historical data and control settings. In addition to the energy model parameters used to confirm what variables are required, for example, outdoor air temperature, the accuracy of modelling is noted as the key aspect of this research, with the improvements of 20% recorded.

This models accuracy is essential to a façade thermal analysis as it proves the importance of considering the most relevant modelling parameters, the better the simulation results and the lower the chances for a poorly designed HVAC system. The approach is mainly focused on mathematical modelling, however, this information is primarily related to the literature review and energy modelling inputs, thus it does not require further research outputs in future studies.

A similar optimisation energy-saving method is taken by Seo et al.(2014), who focuses on developing an algorithm to examine performance and energy savings for an apartment HVAC system. The optimal performance characteristics of an HVAC system is extracted using a complicated algorithm focusing on heating and cooling load demands. Simulation data has confirmed that by utilising an operation plan and algorithm-based simulations, energy savings can be increased regarding the equipment used in these systems. This analysis is similarly a mathematical approach with no case studies, however, it further supports the literature review study and assists with modelling parameters assumptions that are of greater importance.

The energy map of HVAC systems is presented by Lombard et al.(2011), who shows the various types of systems available in the industry. The key aspect of this research focuses on thermal comfort as the driving factor of an HVAC design, noting that a well-designed HVAC system would ensure that the design is following ASHRAE-55 and in doing so, the most effective ventilation rate is maintained in the design process. The demand for comfort design is relevant to a façade analysis because ventilation codes are utilised for typical office spaces, and the model inputs determine the ventilation loads. For this reason, the highest possible ventilation change rate will be used to ensure that energy efficiency according to this resource follows the necessary design guidelines.

This resource uses a mathematical modelling approach to arrive at its design recommendations, but no case studies or applied examples are found. This lack of comparative data would mean that it is impossible to quantify which strategy is the best for an energy model unless all the scenarios were considered, which is not in the scope of this dissertation.

Adaptive control as an energy-saving technique is presented by Bhaskoro et al.(2013), who discusses how adjusting setpoint temperatures within an air-conditioned space allows for energy savings in heating and cooling periods. This adjustment creates an opportunity for over utilisation and underutilisation to be effectively managed as a control strategy within the HVAC system design. The findings also suggest that a significant amount of energy is saved by intermittent cooling techniques. Thus occupancy schedules play an essential factor in the simulations to ensure the cooling systems simulates these considerable energy savings.This study is relevant as set point temperatures are the basic requirements of a thermal cooling load simulation. There is a specific focus in a typical Malaysian climate on a glazed structure where the cooling load is analysed with the proposed energy management technique. Results are validated and compared with an actual building design, and the data on temperature performance is accurate to within 1.5°C of the simulated model. This analysis is relevant to a façade analysis as the accuracy allows for a workable reference for interpreting the simulations in this dissertation. The overall approach of this resource is a well-researched study that identifies all the possible parameters of a mathematical model and uses this data to arrive at a highly accurate comparative analysis.

Computational fluid dynamics, as mentioned previously, has proven its ability to improve comfort conditions by identifying the temperature and velocity profiles in a space. A performance analysis is done by Youssef et al.(2017), who simulates the flow conditions of cold air at varying temperatures velocities and thermal loads within a space. One of the more important conclusions of this analysis notes that higher jet velocities decrease thermal comfort and increases the possibility of cold drafts. The velocity used in a comfort simulation is the dynamic parameter that defines thermal comfort performance, the basic assumption of entry velocity thus requires well-researched assumptions for improved thermal comfort simulations. The overall research is theoretical, and no case study is done, however, the fundamental conclusions on velocity and temperature will be considered in the comfort simulations.

In an attempt to lower the consumption of a building, the proposal of a control strategy by combining variable air volume and indoor positioning systems is presented by Wang et al.(2017), who provides a well-researched CFD application by combining both the theoretical aspect and measurement and verification data. The method focuses on dynamic spatial distribution, and monitoring occupation variation allows for live detection of the area to rapidly improve energy reduction. This is done by matching the thermal service distribution of occupancy and redefining occupancy as a dynamic spatial distribution matrix. This method is

tested with on-site data and compared with CFD simulations which provide the results of energy savings of up to 20%. These innovative solutions have to be introduced into HVAC system engineering as operational efficiency is unused. Cold air systems are similar to air conditioning systems, but they operate at lower temperatures, typically around 4-10°C. Another key result is that lower temperature and velocities reduce air diffusion performance. A thermal analysis will provide temperatures and velocity data, a crucial variable of thermal comfort and air distribution. This information needs to be interpreted correctly, taking into account information provided by relevant CFD studies as the data is too complicated to arrive at basic conclusions. The importance of spatial planning is also key to a façade analysis as zone planning would ensure that each thermal zone meets the acceptable comfort levels.

A CFD simulation of a passenger coach was done by Aliahmadipour et al.(2017), who presented an experimental analysis that verifies the performance of the model results inaccuracy by focusing turbulent airflow of the HVAC system. This analysis is done in a confined space of a passenger coach, taking into account a variation of temperature distributions. The comparison variables, velocity and temperature profiles, are discussed as to how an inappropriate design within the space can negatively affect passengers' thermal comfort conditions, proving the necessity for CFD to form part of the design process for confined airflow. This research is vital to a façade analysis as the ability to interpret temperature data is best done from CFD research. This resource is well-researched and presents many key findings that assist in understanding the complexity of temperature distribution.

Ventilated walls were previously implemented in buildings to reduce moisture and weather degradation. A novel brick wall with ventilation properties is presented by Buratti et al.(2018), who introduced a design for a prototype brick wall built in a controlled test chamber. In this facility, the heat transfer and velocity were investigated for ventilated and unventilated conditions. This approach allowed ventilation performance to be closely monitored for the novel design assisted by CFD simulations. The resource provides a well-researched approach as the testing facility is state of the art, and measurement and verification is done and compared with simulated data. The data and conclusion will be used as part of the literature review to elaborate on temperature fluctuation and thermal comfort simulations data.

CHAPTER-3: EXPERIMENTAL FRAMEWORK

3.1 Psychrometrics in energy modelling and HVAC design

Psychrometric charts use thermodynamic properties to estimate the conditions and processes involved in moist air conditions (ASHRAE, 2013a). As the purpose of HVAC processes is primarily to deliver air in a changed thermo -fluid state, the study of psychrometric charts is of significant importance to thermal studies.

3.1.1 Air compositions

Atmospheric air is composed of water vapour and miscellaneous gaseous, according to ASHRAE (2015a) gaseous contaminants in the air must sometimes be removed to prevent harmful exposure to occupants. Not much attention was given here as HVAC processes are concerned with dry and moist air conditions.

Dry (d) air is atmospheric air with no contaminants and most of the water vapour removed, the universal gas constant (R) is noted as:

$$R(d\ air) = 287.042\ \frac{J}{kg(d\ air)\cdot K} \qquad \text{Equation (1)}$$

Moist (w) air is a mixture of dry air and water vapour. The water vapour content ranges from zero (dry air) to maximum moisture level, noting temperature and pressure as the variables determining its state. The universal gas constant of water vapour is given by:

$$R(w\ air) = 461.524\ \frac{J}{kg(w\ air)\cdot K} \qquad \text{Equation (2)}$$

These formulae are a crucial component of psychrometrics known as the universal gas constant, commonly used thermo-fluid applications.

3.1.2 Standards atmospheric conditions

Atmospheric temperature (T) and barometric pressure (P) changes with several variables, ranging from; geographical location, altitude and weather conditions (ASHRAE, 2013a). The basic formula of pressure and temperature in varying altitudes is given by:

$$P = 101.325\ (1 - 2.25577\ x\ 10^2 Z)^{5.2559}\ (kPa) \qquad \text{Equation (3)}$$

$$T = 15 - 2.25577\ Z\ (^{\circ}C) \qquad \text{Equation (4)}$$

where

Z = atmospheric altitude (m)

Atmospheric conditions such as temperature and pressure play a key role in HVAC design, as is the case with cooling tower systems, where there is a significant effect on hydraulic design, pump selection and sizing. The coil selection of chiller units also considers the atmospheric air composition, following the equipment testing phase where dry simulations cannot be done in high altitude conditions (ASHRAE, 2013a). These formulae are accurate from -5000m to 11000m, higher altitudes have other tables which are applied.

3.1.3 Parameters of humidity

The basic humidity parameters are essential in understanding the state of air during an HVAC cycle, and the following parameters are derived in a psychrometric chart for cooling load calculations (ASHRAE, 2013a).

Humidity ratio (W), is defined by the ratio of the mass of water vapour (w) to that of dry air (da):

$$W = Mw/\,Mda \ \ (unitless) \qquad \text{Equation (5)}$$

Specific humidity (γ), is defined as the ratio of water vapour to total moist air mass:

$$\gamma = W/\,(1 + W) \ \ (unitless) \qquad \text{Equation (6)}$$

Absolute humidity (Dv), is defined as the ratio of water vapour mass (w) to volumetric total (V):

$$\mathrm{Dv} = Mw/\,V \ \ (unitless) \qquad \text{Equation (7)}$$

Density (p), is defined as the ratio of total mass to the total volume of moist air

$$\mathrm{p} = (Mda + Mw)/V \ \ \left(\frac{m3}{kg(d\ air)}\right) \qquad \text{Equation (8)}$$

When moist air reaches saturation, the respective formulae are similar, and figure 6 would be extrapolated:

Saturation humidity ratio (Ws (t,p)), is defined as the ratio of humidity of saturated moist air for water at the same pressure(p) and temperature (t)

Degree of saturation (μ), is defined as the ratio air of the humidity of air (W) to that of moist air (Ws)

$$\mu = W/Ws \mid \mathrm{t,p} \qquad (unitless) \qquad \text{Equation (9)}$$

Relative humidity (φ), is defined as the ratio of water vapour mole fraction (Xw) to that of moist air (Xws)

$$\varphi = Xw/Xws \mid t,p \qquad (unitless) \qquad \text{Equation (10)}$$

Dew point temperature (td), is defined as the temperature of saturated moist air at a pressure (p) defined, which has the same ratio of humidity (W) to that of moist air in a given sample

$$Ws\,(p, td) = W \qquad (unitless) \qquad \text{Equation (11)}$$

In addition to HVAC design in general, the dew point temperature has a crucial role in pant stacking district cooling plants as flue gases must remain below this for stable operation of the systems ASHRAE (2013c).

3.1.4 Moist air thermodynamic properties

Moist air applications are driven by thermodynamic properties, as shown in figure 6. The following properties can be used to derive specific values based on an initially known variable such as temperature (ASHRAE, 2013a). The temperature range is between -60°C to 160°C

Table 2 Thermodynamic Properties of Moist Air at Standard Atmospheric Pressure, 101.325 kPa (*Concluded*)

Temp., °C	Humidity Ratio	Specific Volume, m^3/kg_{da}			Specific Enthalpy, kJ/kg_{da}			Specific Entropy, $kJ/(kg_{da}\cdot K)$	
t	W_s, kg_w/kg_{da}	v_{da}	v_{as}	v_s	h_{da}	h_{as}	h_s	s_{da}	s_s
15	0.010694	0.8159	0.0140	0.8299	15.087	27.028	42.115	0.0538	0.1525
16	0.011415	0.8188	0.0150	0.8338	16.093	28.873	44.966	0.0573	0.1624
17	0.012181	0.8216	0.0160	0.8377	17.099	30.830	47.929	0.0607	0.1726
18	0.012991	0.8245	0.0172	0.8416	18.105	32.906	51.011	0.0642	0.1832
19	0.013851	0.8273	0.0184	0.8457	19.111	35.107	54.219	0.0676	0.1942
20	0.014761	0.8301	0.0196	0.8498	20.117	37.441	57.558	0.0711	0.2057
21	0.015724	0.8330	0.0210	0.8540	21.124	39.914	61.037	0.0745	0.2175
22	0.016744	0.8358	0.0224	0.8583	22.130	42.533	64.663	0.0779	0.2298
23	0.017823	0.8387	0.0240	0.8626	23.136	45.308	68.444	0.0813	0.2426
24	0.018965	0.8415	0.0256	0.8671	24.142	48.245	72.388	0.0847	0.2560
25	0.020173	0.8443	0.0273	0.8716	25.148	51.355	76.503	0.0881	0.2698
26	0.021451	0.8472	0.0291	0.8763	26.155	54.646	80.801	0.0915	0.2842
27	0.022802	0.8500	0.0311	0.8811	27.161	58.128	85.289	0.0948	0.2992
28	0.024229	0.8529	0.0331	0.8860	28.167	61.812	89.979	0.0982	0.3148
29	0.025738	0.8557	0.0353	0.8910	29.174	65.708	94.882	0.1015	0.3311
30	0.027333	0.8585	0.0376	0.8961	30.180	69.829	100.009	0.1048	0.3481

Figure 6: *Thermodynamic properties of moist air at atmospheric pressure* (ASHRAE, 2013a)

Water at saturation may occur at equilibrium as a saturated vapour and liquid, the various properties of moist air are used to determine the water vapour saturation pressure. Saturation temperature and pressure have a crucial role in heating capacity in district cooling systems (ASHRAE, 2013b). Refrigeration design also relies significantly upon the water vapour parameters as states of matter change from one thermodynamic cycle to another. Pressure drop considerations will also affect coil sizing in refrigerant pipes which are essential to the movement of the fluid which moves heat in and out of a refrigerant loop (ASHRAE, 2013b).

Table 3 Thermodynamic Properties of Water at Saturation (*Continued*)

Temp., °C t	Absolute Pressure p_{ws}, kPa	Specific Volume, m^3/kg_w			Specific Enthalpy, kJ/kg_w			Specific Entropy, $kJ/(kg_w \cdot K)$		
		Sat. Liquid v_f/v_f	Evap. v_{fg}/v_{fg}	Sat. Vapor v_g	Sat. Liquid h_f/h_f	Evap. h_{fg}/h_{fg}	Sat. Vapor h_g	Sat. Liquid s_f/s_f	Evap. s_{fg}/s_{fg}	Sat. Vapor s_g
3	0.7581	0.001000	168.013	168.014	12.60	2493.80	2506.40	0.0459	9.0306	9.0765
4	0.8135	0.001000	157.120	157.121	16.81	2491.42	2508.24	0.0611	8.9895	9.0506
5	0.8726	0.001000	147.016	147.017	21.02	2489.05	2510.07	0.0763	8.9486	9.0249
6	0.9354	0.001000	137.637	137.638	25.22	2486.68	2511.91	0.0913	8.9081	8.9994
7	1.0021	0.001000	128.927	128.928	29.43	2484.31	2513.74	0.1064	8.8678	8.9742
8	1.0730	0.001000	120.833	120.834	33.63	2481.94	2515.57	0.1213	8.8278	8.9492
9	1.1483	0.001000	113.308	113.309	37.82	2479.58	2517.40	0.1362	8.7882	8.9244
10	1.2282	0.001000	106.308	106.309	42.02	2477.21	2519.23	0.1511	8.7488	8.8998
11	1.3129	0.001000	99.792	99.793	46.22	2474.84	2521.06	0.1659	8.7096	8.8755
12	1.4028	0.001001	93.723	93.724	50.41	2472.48	2522.89	0.1806	8.6708	8.8514
13	1.4981	0.001001	88.069	88.070	54.60	2470.11	2524.71	0.1953	8.6322	8.8275
14	1.5989	0.001001	82.797	82.798	58.79	2467.75	2526.54	0.2099	8.5939	8.8038
15	1.7057	0.001001	77.880	77.881	62.98	2465.38	2528.36	0.2245	8.5559	8.7804
16	1.8188	0.001001	73.290	73.291	67.17	2463.01	2530.19	0.2390	8.5181	8.7571
17	1.9383	0.001001	69.005	69.006	71.36	2460.65	2532.01	0.2534	8.4806	8.7341

Figure 7:*Thermodynamic properties of water at saturation* (ASHRAE, 2013a)

The equations used to determine the relationship between pressure and temperature are more complicated vs. the moist air equations (1) & (2) above and can be found in ASHRAE (2013a).

3.1.5 Thermodynamic dew point and wet bulb temperature

The dew point temperature is defined as the temperature at which water vapour reaches the point of saturation (ASHRAE, 2013a). The dew point temperature has a significant role in sizing equipment using psychrometrics. The refrigerants dew point is essential to HVAC design as the gas boils inside a refrigerant circuit, and it will not fully evaporate and obtain bubble temperature until the dew point is reached. Similarly, the condensing process will reach subcooling at bubble temperature. Condensation and evaporation are crucial phases in HVAC systems as they facilitate heat transfer.

The wet-bulb temperature is defined as the temperature at which water (solid or liquid) brings about adiabatic saturation at constant pressure and the same temperature through evaporation of moist air at dry-bulb temperature (ASHRAE, 2013a). This parameter has a crucial role in HVAC chilled water systems, as the operation is affected by low wet-bulb temperatures. A condenser coil can cool the chilled water through a heat exchanger instead of a full refrigerant plant operation (ASHRAE, 2015a). The wet and dry-bulb temperature is clearly defined in design standards where the type of heat exchanger has a specific entering design condition for the application. From a condenser operation design perspective, the approach can be fundamentally a wet or dry bulb based system. The wet-bulb method functions by evaporating air at lower temperatures, and it is thus possible to gain energy-efficient operation at cooler water temperatures. The dry bulb system works on a temperature difference in the condenser

water loop. The outdoor ambient dry-bulb temperature and heat transfer would thus achieve by operating the condenser loop at a much higher temperature (ASHRAE, 2013a).

3.1.6 Psychrometric charts

A Psychrometric chart presents the thermodynamic properties of moist air in graphical format, the purpose is during a thermodynamic evaluation of air properties at a given temperature and pressure. It would thus be possible to derive the required variables of moist air for a specific HVAC process (ASHRAE, 2013a). ASHRAE has developed five types of psychrometric charts which operate are various conditions, each chart utilises enthalpy and humidity ratio coordinates to arrive at these thermodynamic approximations.

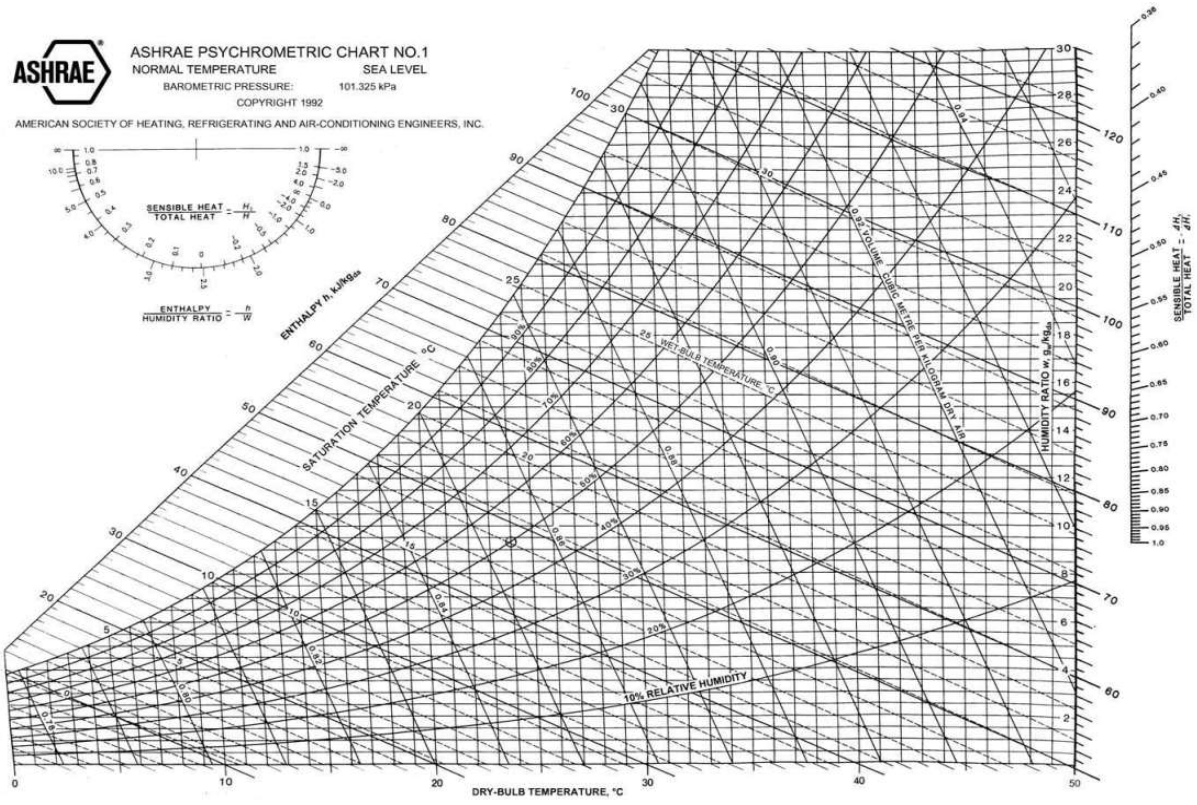

Figure 8:*Psychrometric chart at atmospheric pressure of 101.325 kPa* (ASHRAE, 2013a)

As shown in figure 8 above, chart 1 applies to an average atmospheric pressure of 101.325kPa. According to ASHRAE (2015a), the chart that works for an altitude of 2440m is thus crucial in the design process. Cooling tower design in HVAC applications relies significantly on the thermodynamic properties derived from a psychometric chart (ASHRAE, 2013a).

Data centre applications require specific guidelines regarding the relative humidity (RH) ratio within the space, ASHRAE (2015c) identifies that high RH values are to be avoided to ensure

electronic components do not have a high failure rate. On the contrary, lower RH values are also to be avoided as the rate of electrostatic discharge is much higher in arid indoor climates. The acceptable temperature conditions also require that high temperatures be avoided to increase reliability, and overcooling should be avoided. The use of a psychrometric chart determines these design criteria in a given temperature and pressure conditions.

3.1.7 Typical air conditioning processes

HVAC design works on simple thermodynamic processes involving moist air, and the following underlying principles are used for processing moist air to the desired condition:

Moist air sensible cooling and heating are processes where a temperature change occurs (ASHRAE, 2015c). This process exhibits no humidity, thus it is shown as a single horizontal line on a psychometric chart.

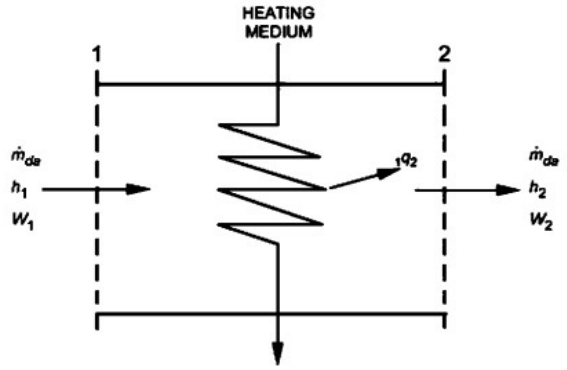

Figure 9: *Heating moist air process schematic* (ASHRAE, 2013a)

The schematic in figure 9 shows the basic process of sensible heating (Q) and is described by equation 12 by multiplying the enthalpy (h) change by the coil's mass flow rate ($\dot{m}_{da}$).

$$Q = \dot{m}_{da}(h_2 - h_1) \qquad (kW) \qquad \text{Equation (12)}$$

According to ASHRAE (2013a), to effectively carry out sensible cooling, thermal displacement ventilation mixed with strategically designed grille placement can ensure lower cooling requirements as some spaces might not require cooling. In principle, the cool air is supplied at a lower level, velocity and the air is returned at a higher level, the mixture always remains cooler at occupants level as heated air rises into the return air plenum void.

Cooling of moist air and dehumidification is when moist air is cooled to the desired temperature below a space's dew point.

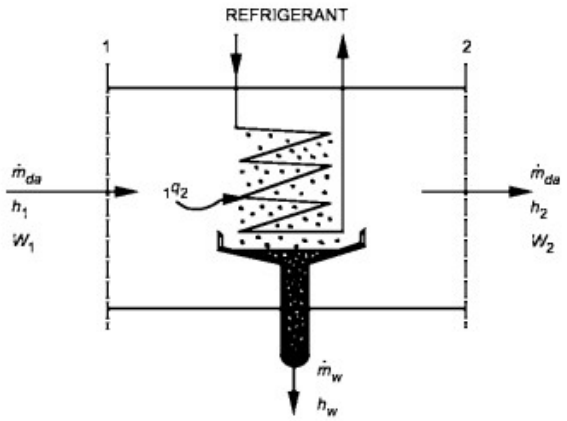

Figure 10:*Cooling moist air process schematic* (ASHRAE, 2013a)

The schematic in figure 10 shows the basic process of moist air cooling and dehumidification (Q) and is described by equation 13 by multiplying the enthalpy ($h_{1,2}$) change minus the work change to remove the moisture from the air by the coil ($W_{1,2}$ x $h_{w1,2}$).

$$Q_2 = \dot{m}_{da} \left[(h_2 - h_1) - (W_1 - W_2) h_{w2} \right] \quad (kW) \qquad \text{Equation (13)}$$

According to ASHRAE (2013b), mission-critical facilities manage peak cooling loads using thermal energy storage in conjunction with moist air cooling and dehumidification. Piping architecture utilises chilled water cooling networks by removing the heating load through underground pipe networks linked to a computer room air-conditioning unit (CRAC). According to ASHRAE (2015c), some data centres use chiller-less installations with supplemental cooling such as evaporative cooling.

Adiabatic mixing of moist air airstreams is defined as the process whereby two or more moist airstreams mix to form a combined stream at the desired velocity, airflow rate and pressure with no heat flow change to the surroundings (ASHRAE, 2013a).

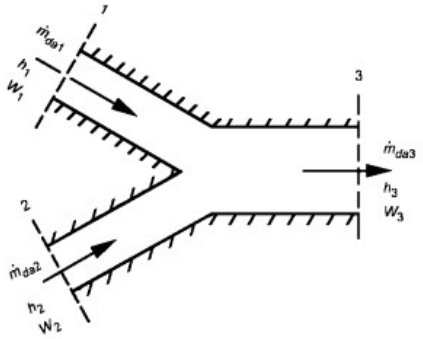

Figure 11: *Adiabatic mixing of moist air airstreams schematic* (ASHRAE, 2013a)

The schematic in figure 11 shows the basic process of adiabatic moist air stream mixing and is described by equation 13 by adding the flow together to arrive at a relationship that allows variables to be found.

$$\frac{h2 - h3}{h3 - h1} = \frac{W2 - W3}{W3 - W1} = \frac{\dot{m}da1}{\dot{m}da2} \qquad \text{Equation (14)}$$

According to ASHRAE (2013e), mixing airstreams often happens in a space where thermal displacement ventilation is more complicated as heat transfer occurs at different levels within the room itself. Subzone variable volume systems combine the above effect by mixing the air back into an air handling unit, causing a balance of temperature, airflow, and pressure to ta spaces required conditions. According to ASHRAE (2016), turbulent flow design impacts are essential in the larger energy scheme as adiabatic mixing occurs in ducts. The static pressure increases as the fan runs at a higher frequency to maintain the operating flow rate and pressure.

Adiabatic mixing of water into moist air/humidification is defined as the steam of liquid injected into moist air to raise the humidity.

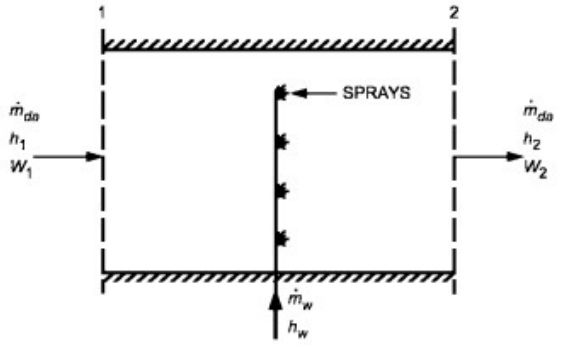

Figure 12: *Adiabatic mixing of water into moist air* (ASHRAE, 2013a)

The schematic in figure 12 shows the basic humidification process described the rate of enthalpy (h_w). If the mixture occurs as an adiabatic process, equation 15 defines how the working relationship of the variables by dividing the enthalpy ($h_{1,2}$) difference by work change ($W_{1,2}$).

$$h_w = \frac{h2 - h1}{W2 - W1} \quad (kj/Kg) \qquad \text{Equation (15)}$$

According to ASHRAE (2015c), humidification in data centre applications is always to be designed against as equipment failure rates drastically increase with humidity ratios above 60%. On the other hand, lower humidity ratios result in high static electricity discharges, resulting in equipment failure. According to ASHRAE (2013e), thermal comfort standards

such as “ASHRAE standard 55” note the importance of 65% RH's upper limits to ensure occupants inside a space do not feel too humid, which also presents the risk of prolonged moisture content in the air. Humidity control is also responsible for system operation as outdoor climate factors change the psychometric properties in an HVAC process, this is essential for commissioning an HVAC system as multiple parameters may drive indoor thermal conditions.

Space heat absorption and moist air moisture gains is the process of conditioning the space to the desired moist air conditions, including the rate of heat gain and removal. Sensible heat gain is the most significant factor in thermal loads for a typical air conditioning process. It measures the energy added to the system to change the temperature without considering the lower energy contributions to humidify the space.

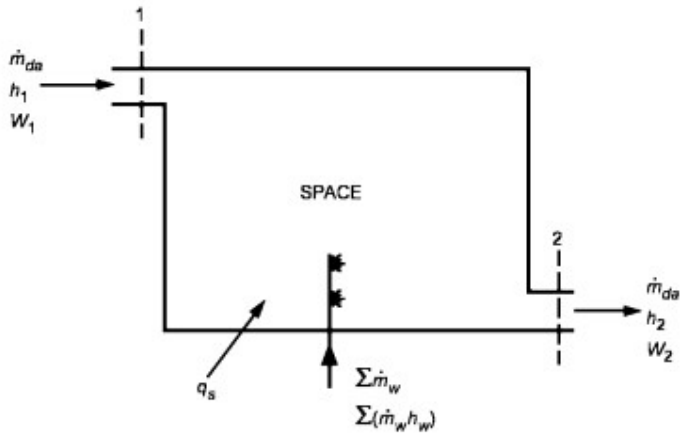

Figure 13: *Space heat absorption and moist air moisture gains* (ASHRAE, 2013a)

The schematic in figure 13 shows the basic air conditioning process and identifies the total energy required to complete the process, and it is described by equation 16 by equating the enthalpy ($h_{1,2}$) change over the work change ($W_{1,2}$) to the total energy required.

$$\frac{\sum (\dot{m}w \times hw)}{\sum (\dot{m}w)} = \frac{\Delta h}{\Delta W} = \frac{h2 - h1}{W2 - W1} \quad (kW) \qquad \text{Equation (16)}$$

It is shown by Gatley (2013) that altitude has an impact on psychometric conditions. As higher altitudes of air result in changes of the specific volume of the air, the heat gain and loss calculations as less dense air allow for more radiant intensity due to lower dust particles present. The HVAC engineer must exercise caution when using the weather data and consider if the building is of significant height to utilise psychrometric charts for higher altitudes.

According to Cengel (2006), fluid flow is a science developed to describe how a fluid reacts with the environment by widely accepted mathematical relationships. HVAC engineering encompasses all these variables noting that every aspect of fluid movement is affected. The heat transfer rate significantly focuses on how a system is designed in a particular building envelope. Noting the importance of heat transfer in HVAC applications as the main aspect of cooling and heating loads forms the basis of an HVAC design. Space heat absorption and moisture gains inside the boundary of figure 13 are examples of the Bernoulli equation where air travels while conservation of flow, potential and kinetic energy is observed.

Steady airflow movement is the primary focus of this study to simulate peak cooling loads, as is the case with basic recommendations and design assumptions (Howell et al., 2007). During designing an HVAC system, one would generally consider air movement velocities, pressure and temperatures as the key focus to drive the delivery from outdoor air to acceptable of the required indoor air conditions. In conjunction with the climatic conditions, these three parameters are the starting point of the system's functioning given the application, building envelope regulatory guidelines and recommendations per region.

3.2 Thermal load theory in HVAC design and energy modelling applications

Thermal loads form the basis of the HVAC design, and the process involves using the psychrometric chart with general external conditions in the form of historical weather data to obtain a heat load estimate of the building structure. The method of deriving a heat load is a science that identifies the effects of heat and mass transfer on the glazing area and determines the power required to cool a specific zone to the required indoor conditions. Thermal comfort is another consideration that is taken into account in the design process before equipment selection is made to do the work to cool or heat a volume of air.

3.2.1 Heat transfer

Heat transfer is one of the essential aspects of HVAC design, the difference in temperature from one medium to another is the main focus of heat transfer. Air is the medium whereby thermal comfort is achieved in HVAC applications. A liquid is used as the functional medium in the HVAC plant room to transfer heat in a refrigerant or chilled water /glycol pipe network. According to Cengel et al. (2006), heat transfer is mainly conduction, convection and radiation, with sensible and latent heat forming the primary heat transfer component in HVAC systems equipment selection. Negligible heat transfer (adiabatic) processes have become an important design aspect of conserving energy in a ducting design. Fourier's law of heat conduction

provides a relationship of conductivity heat transfer (Qcd) concerning a surface's thermal conductivity (k) and temperature difference (dT) over the surface area (A) over distance (dx).

$$Qcd = -k.A.\frac{\mathrm{dT}}{\mathrm{dx}} \qquad (kW) \qquad \text{Equation (17)}$$

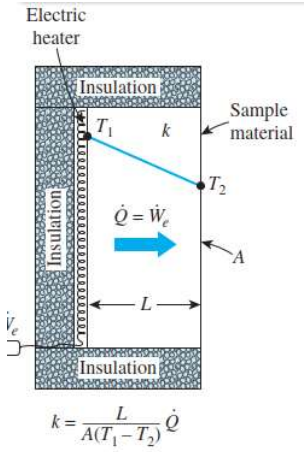

Figure 14: *Heat conduction* (ASHRAE, 2007)

To assess the convective the heat transfer rate (Qcv), Newton's law of cooling is utilised for forced and natural convective heat transfer. The rate of heat transfer is given by the convective heat transfer coefficient (h) multiplied by the surface area (A), multiplied by the temperature difference (dT) (Cengel et al., 2001).

$$Qcv = -h.A.dT \qquad (kW) \qquad \text{Equation (18)}$$

According to Cengel et al. (2007), the thermal conductivity of a material is described as the rate of heat transfer through a unit thickness of the material per unit temperature difference. This is the most important factor to consider in an HVAC system, material heat transfer is the component that drives the cost-effectiveness and energy performance of the operation of a system during its life cycle. In a building design, heat transfer through glazing influences the overall HVAC equipment sizing, which drives the capital and operational cost as the power requirements increase with more considerable thermal losses.

To assess the rate of steady-state heat transfer through a plane (Qcw), the temperature change (dT) is divided by thermal resistance (Rw), which is given by the length of thermal movement (L), divided by the thermal conductivity (k) multiplied by the surface area (A),

$$Qcw = \frac{\mathrm{dT=(T1-T2)}}{\mathrm{Rw}} \qquad (kW) \qquad \text{Equation (19)}$$

Where

$$Rw = \frac{\mathrm{L}}{\mathrm{kA}} \qquad (K/W) \qquad \text{Equation (20)}$$

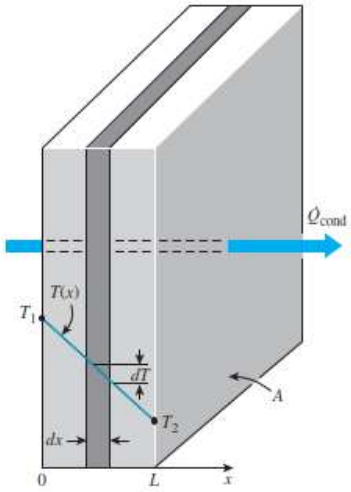

Figure 15: *Heat transfer through a plane* (ASHRAE, 2007)

According to Cengel et al. (2001), the second law of thermodynamics states that processes occur in a specific direction, as seen in figure 15 above, thus thermal resistance is continuously being improved through the use of composite materials. The method of improving resistance is done by stacking a series of composite materials to form a thermal resistance network (Rc), this is represented in equation 21 by adding the resistance value in series. The overall heat transfer coefficient (U) is used in heat load calculations with great focus window glazing performance, which uses the total thermal resistance to calculate the heat transfer (Qcomp cw) through a particular area of a given composite or single material (Cengel et al., 2008).

$$Qcomp\ cw = \mathrm{U.A.dT} \qquad (kW) \qquad \text{Equation (21)}$$

Where

$$Rc = \frac{\mathrm{L1}}{\mathrm{k1A}} + \frac{\mathrm{L2}}{\mathrm{k2A}} + \ldots \qquad (K/W) \qquad \text{Equation (22)}$$

And

$$U.A = \frac{1}{\mathrm{Rtotal}} \qquad (W/K) \qquad \text{Equation (23)}$$

These formulae are noted for heat transfer from the fundamental basis for advanced performance analysis of HVAC systems, as done in the detailed simulation of glazing performance of any building architecture.

3.2.2 Glazing properties

Glazing is considered the first line of defence against the sun's direct radiation into a building space. Without the correct glazing to protect the occupants, any building would become thermally uncomfortable.

According to Underwood (2008), heat transfer through glazing undergoes the following types of processes;

- Radiation can be reflected, absorbed and transmitted via diffusion or through direct solar radiation.
- The absorbed solar radiation in the ambient naturally begins a process of convection and conduction, which occurs along the surface area of the glazing pane.
- The temperature difference between indoor and outdoor results in convection and conduction.
- The internal surfaces are exposed to radiant heat fluctuations.

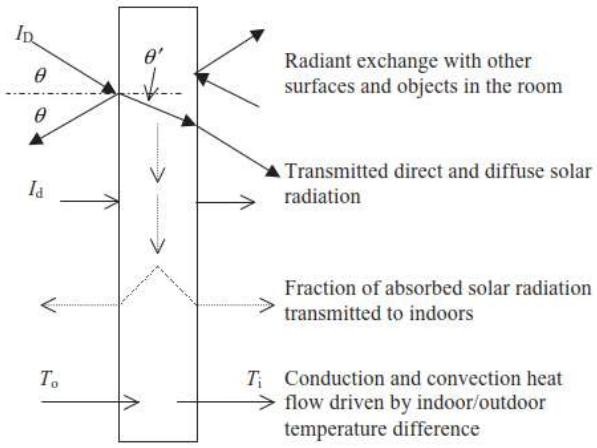

Figure 16: *Heat transfer processes through glazing* (Underwood, 2008)

Low emissivity coating glazing reduces thermal losses by radiation, improving thermal insulation properties. The coating on the glass may absorb or reflect light and heat, which reduces the solar heat gain coefficient (SHGC).

Energy modelling involves the simulation of cooling and heating loads over a year, the purpose is to analyse the peak solar gains, with glazing contributing a more considerable heat gain that

the cooling system needs to remove. Thermal considerations for glazing in high rise buildings are noted by Simmonds (2015), where it is shown that the taller buildings are exposed to higher levels of solar radiation /solar gains. The suburb settings are similar to low rise buildings. This is a benefit as surrounding buildings offer decreased cooling load requirements, however, reflections from glazing of the surrounding structures can increase solar heat gains.

Mean radiant losses are mainly sky view (SVF) factors affecting the internal solar heat gains. Low rise buildings have more SVF's which increases the heat loss during cold winter nights, thus, low rise buildings predominantly radiate to surrounding structures at higher than normal temperature conditions than the actual sky itself and lower the cooling energy in summer. Finally, the thermal conductance of glazing in facades increases with higher elevations due to more significant wind speeds. As larger wind velocities decrease the boundary layer, higher heat transfer rates between the envelope and the environment are present (Simmonds, 2015).

For this study, the main aspect of glazing, which is focused on is the thermal conductivity (U) value, the solar heat gain coefficient (SHGC), and shading coefficient (SC), as these affect heat load calculations the most, along with the area of glazing designed in the building envelope. These SHGC values are readily available in a manufacturer's specification sheet

3.2.3 Cooling and heating loads

Cooling and heating loads are the main focus of this study and HVAC design in general. The reason being is that HVAC equipment such as the fan coil unit determines the plant room power requirements. The initial step in cooling load calculation involves using the psychrometric chart, outdoor weather conditions, and the desired thermal requirements to arrive at an estimated sensible cooling and heating load applied to the envelope.

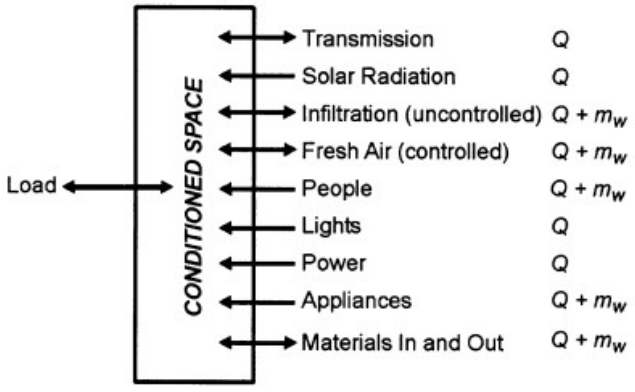

Figure 17: *Cooling and heating load components in a space* (Howell et al., 2013)

Figure 17 shows the basic HVAC heat transfer processes and identifies the total thermal load required to cool or heat a space inside a building. The formulae described by equation 24 & 25 provides the fundamental reference for the sensible cooling/ heating load (Qs) formula. This is done by multiplying the airflow rate (Qa) by the density(p) and specific heat (Cp) of air which is then multiplied by the indoor temperature difference (dT). For the latent (Ql) cooling/ heating loads, this is obtained by multiplying the airflow rate (Qa) by the density(p) and specific heat (Cp) of air which is then multiplied by the indoor minus outdoor humidity change (dW), and then further multiplied by the latent heat of water (Hfg), (Howell et al., 2013).

$$Qs = \text{Qa. p. Cp. dT} \quad (kW) \qquad \text{Equation (24)}$$

and

$$Ql = \text{Qa. p. Hfg. dW} \quad (kW) \qquad \text{Equation (25)}$$

Infiltration also forms a key component to cooling and heat loads, and the air leakage impacts the final thermal load estimation. The simple formula used to represent the infiltration load (Qi) is given by the recommended infiltration air changes per hour rate (ACH) multiplied by the space volume (V). For cooling loads, the main concern is with windows and doors, however, it plays a more significant role in the heating season, with care taken in cooling loads to avoid the revered chimney effect (Howell et al., 2013).

$$Qi = \text{ACH. V/50} \quad (m^3/s) \qquad \text{Equation (26)}$$

According to Howell et al. (2013), shading control substantially reduces the cooling requirement and is essential in building envelope requirements. This is one factor to consider in commercial applications, however, in residential buildings, the following unique features applied to the calculation of thermal loads are to be observed as they affect the overall design.

- The internal heat gains are generally smaller, reducing thermal load requirements.
- The particular use varies along the usable area, and this affects fresh air rates and equipment sizing
- Fewer zones thus air conditioning loads are moderated due to internal heat storage
- Distribution losses are greater than average as duct leakage is a common factor
- Partial loading operation is common, and so oversizing an HVAC system has a negative effect

- Dehumidification negatively affects the equipment as excessive sensible loads lead to short cycling
- Detached family spacing thus cooling loads require separate analysis per space.
- Multifamily spacing requires the opposite approach in the cooling load analysis
- Complex cooling loads are complicated as building and space design have varying thermal effects

The cooling load design guidelines in ASHRAE are constantly revised due to the complex nature present, as stated above, while heating loads mainly focus on the worst-case scenario and size equipment accordingly.

3.2.4 Thermal comfort

The thermal environment inside an occupied space is based on several complex variables interacting with the surroundings and the HVAC system's design, construction, and operation. Each individual perceives the environment with a different perception of thermal acceptability, various factors affect how comfort is felt between the body and the surroundings (Howell et al., 2013). The ASHRAE standard 55, as shown in figure 18, clearly defines how thermal conditions inside space will be acceptable to 80% of the occupants, with the temperature and humidity ratio being the dependent variables.

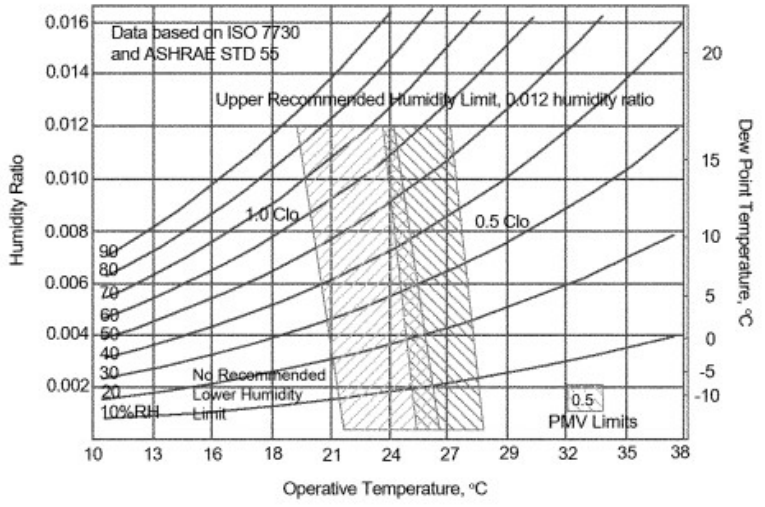

Figure 18:*Cooling and heating load components in a space* (Grondzik., 2007)

According to Nicol (2013), ASHRAE and Bedford comfort standards use numerical equivalents to determine the comfort level known as voting standards, and energy modelling

generally uses the predicted mean vote/Fanger index where most energy codes reference the ideal index value per space type (Nicol, 2013).

ASHRAE comfort scale		Bedford comfort scale	
+3	Hot	7	Much too hot
+2	Warm	6	Too warm
+1	Slightly warm	5	Comfortably warm
0	Neutral	4	Comfortable
−1	Slightly cool	3	Comfortably cool
−2	Cool	2	Too cold
−3	Cold	1	Much too cold

Figure 19: *Comfort Standards* (Nicol, 2013)

The operative temperature (Top) is found by the average of the air temperature (Ta) and the radiant temperatures (Tr) along with air velocity (V), which is negligible at lower airspeeds (Nicol, 2013).

$$Top = \mathrm{Tr} + \mathrm{Ta} / 2 \quad (°K) \qquad \text{Equation (27)}$$

The operative temperature should, at all times, lie within the acceptable ranges for all locations within the space boundary.

3.2.5 HVAC equipment selection

HVAC equipment selection has many considerations when selecting a system design; the selection can be based on a simple heat load calculation, and the cooling load required would reflect the size of air conditioning equipment. According to Simmonds (2015), the minimum design considerations should include the following in the planning stage:

- Capital cost
- The occupancy requirements now and in the future
- External and internal environmental requirements
- The acoustic levels acceptable to the occupied areas
- Seismic requirements (If applicable)
- Energy consumption and depletion
- Annual maintenance and operational cost
- Smoke and fire management

According to Grondzik (2007), the design engineer, in the early design phase of HVAC systems needs to evaluate the impact of the following:

- Energy code compliance
- Green building design considerations
- Lighting and internal load analysis
- Spatial efficiency with regards to available space, acoustics and aesthetics

The selection of equipment depends on the outdoor air conditions, according to Howell et al. (2013), the 0.4%, 1.0%, and 2.0% dry bulb and coincident wet bulb conditions on the psychometric chart of a given area will determine the size of the chiller and air-conditioning equipment, it is because the highest temperature is observed, and the cooling load will peak at this point. It is thus critical to obtain accurate weather data during the design phase.

The importance of controls in HVAC systems is highlighted by McDowall et al. (2015), noting that the conditions of an operating system require some motorized control to regulate airflow in the ducting and refrigerant or water in the plant room. These systems are typically monitored through a building management system. This would include a range of ancillaries that are used to regulate and or measure pressure, temperature and flow rates, and the following are examples of applied control technology:

- Sensors and devices can measure things like psychrometric variables of a live system
- Powered controls are mainly system powered valves
- Electrical controls which include a wide range of measures and verification
- Pneumatic controls are similar to other types of controls but use hydraulics
- Analogue electronic controls for all valves and ancillaries

3.3 Software simulation tool

3.3.1 DesignBuilder™with EnergyPlus™

DesignBuilder™with EnergyPlus™ is a leading energy modelling software that originates from the united kingdom, the utilisation of this resource has received much attention from the international community due to the accuracy and simplicity of the graphical user interface based thermal modelling software.

Figure 20: *DesignBuilder™ with EnergyPlus™ logo* (DesignBuilder, 2021)

According to Garg et al. (2014), the software works by using a weather file, a data log of the historical weather conditions of a required geographical location anywhere across the globe. The user has to model the building geometry from a cad or pdf file, considering 3-dimensional geometry and shading devices.

The building services HVAC system can then be modelled from a detailed performance or standard cooling and heating load based generic model. The HVAC model considers occupancy loading & schedules, lighting loads, equipment loads, thermostatic setpoints & HVAC operation schedules. A simulation will derive heating and cooling loads through a building physics simulation process that uses psychrometrics and weather data:

Energy modelling through DesignBuilder™with EnergyPlus™ offers a range of benefits:

- Directly reduce an HVAC system's cost by analysing the facade and making recommendations on the best alternative design approach.
- It is possible to simulate thermal comfort in the building, daylight studies, solar studies & shading
- The software can also benefit a building design by reducing energy usage and carbon emissions by utilising Green Star or LEED certification
- Regulatory approval for any rational architectural design as opposed to the strict mandates in SANS 204 by following the SANS 10400XA approach can be achieved with thermal modelling
- Computational fluid mechanics for natural ventilation studies is also a task that can be carried out
- The thermal and energy performance of detailed HVAC simulations can be carried out on most complex designs with the graphical user interface

Building physics computations are highly complex, and elements such as heat exchange between the surfaces and reflective radiant heat will take an unrealistic amount of time with hand calculations. DesignBuilder ™ with EnergyPlus™ can achieve the most sophisticated energy modelling analysis within a relatively short time.

The Fanger thermal comfort model is a complex and helpful tool to measure thermal comfort. This software can also retrieve the Fanger performance with minimal effort, among other physics-based thermal models.

3.4 Experimental methodology

3.4.1 Façade analysis experimental method

Energy modelling simulations can yield a plethora of data depending on what information is required regarding how the building envelope interacts with the surrounding environment thermal conditions. According to Anderson (2013), the assessment of comfort inside the envelope and energy efficiency performance goals are tested regarding the interaction of numerous building physics variables. The data derived from the energy model relevant to a façade analysis are as follows:

- The peak cooling and heating load over an annual simulation period
- Compare building geometry options, glazing size, location and thermal properties
- Test energy efficiency measures to improve building energy performance
- Validate performance of a design to comply with relative energy codes and regulations

Thermal calculations in energy modelling mainly use the balance point method, where the heat gains are equal to the heat loss within a space over a given time, this results in interior temperature data, which then is used to determine the acceptance of thermal comfort relative to a standard (Anderson, 2013). Thus, temperature data provides both the temperature change from external to internal, which informs us of comparative work required for cooling and heating loads, respectively. Typical input data needed for a thermal energy model noted below, are confirmed as key requirements indicated in greater detail. The bullet points (1-4) include climatic data-based thermal loads, and bullet points (5-9) include internal thermal loads:

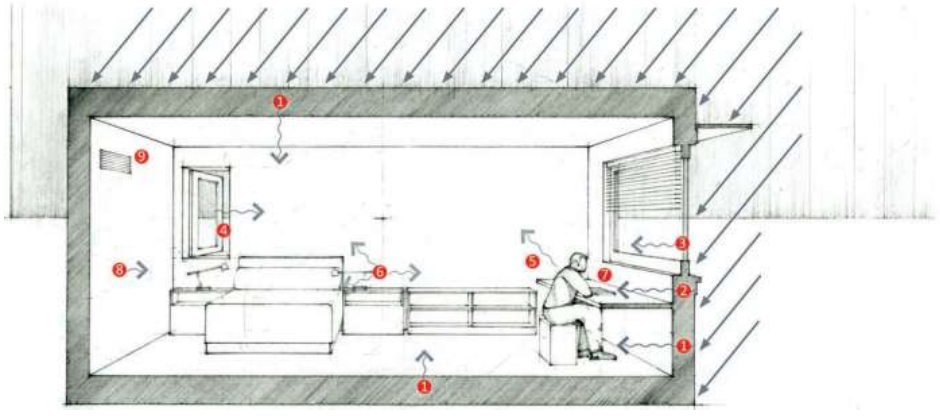

Figure 21: *Thermal model load inputs* (Anderson, 2013)

1. Conduction heat transfer through the building envelope, including ground and sky thermal radiation
2. Air leakage through gaps in the building design, infiltration and exfiltration
3. Solar energy transmittance through opaque assemblies and glazing panels
4. Outdoor fresh air delivered by mechanical or natural ventilation
5. Metabolic thermal rates by the heat given off by people and activity level
6. Electric lighting loads
7. Ancillary equipment loads, which includes all types of equipment requiring electrical power
8. Process loads which include loads required for building operation
9. Heat transfer through the adjacent interior through air and partitions

The experimental framework incorporating all the above has been done on an energy model of the Capitec Bank head office in Stellenbosch. The thermal model was used to simulate various output data, which was interpreted relative to the HVAC system energy efficiency operation:

Figure 22: *Capitec Bank head office panoramic site view 1* (Capitec, 2021)

Figure 23: *Capitec Bank head office site view 2* (Capitec, 2021)

Figure 24: *Capitec Bank head office site view 3* (Capitec, 2021)

1. A 3-dimensional thermal model of Capitec Bank head office in Stellenbosch was reconstructed.

2. The model inputs, including all factors as per figure 21 above, are regulation and code guidelines defined in this section.
3. Zoning of the façade (1m perimeter zone) was drawn and showing direction facing relative to the sun
4. Façade variables were considered in respect of glazing types and external shading devices. Internal shading devices such as blinds are not considered.
5. Peak cooling and heating loads are calculated along the façade, and the best performing glazing specification is selected according to the best thermal performance. Overheating was also analysed.
6. The thermal performance of selected zones was analysed in more detail, and this includes an analysis of variables on the psychrometric chart.
7. The distribution of all relevant heat loads was analysed further concerning the peak solar load.
8. Thermal comfort acceptance was analysed utilising the Fanger thermal index.
9. Some changes to the building envelope design were considered based on the energy model results, and the effects thereof measure and discussed how HVAC system sizing is reduced.
10. Some of the sustainable optimisation methods described in chapter 3.3 were modelled into the thermal model to measure the benefits of thermal loading.

3.5 Modelling methodology

The modelling methodology explains the most critical parameters needed to model a thermal cooling and heating simulation correctly, and these steps consider points 1-4 in the experimental method.

3.5.1 3-dimensional thermal modelling

The model geometry was provided by the architectural team DHK during a pre-design phase to value engineering the façade design to limit the HVAC cooling load requirement to a maximum of 180 W/m². The image below is the thermal model that was done in DesignBuilder™ with EnergyPlus™. The second floor was focused on as there is more exposure to the sun in the simulation, and the roof thermal heat gain ensures a higher cooling load requirement. Appendix A is the first-floor layout received from the architect.

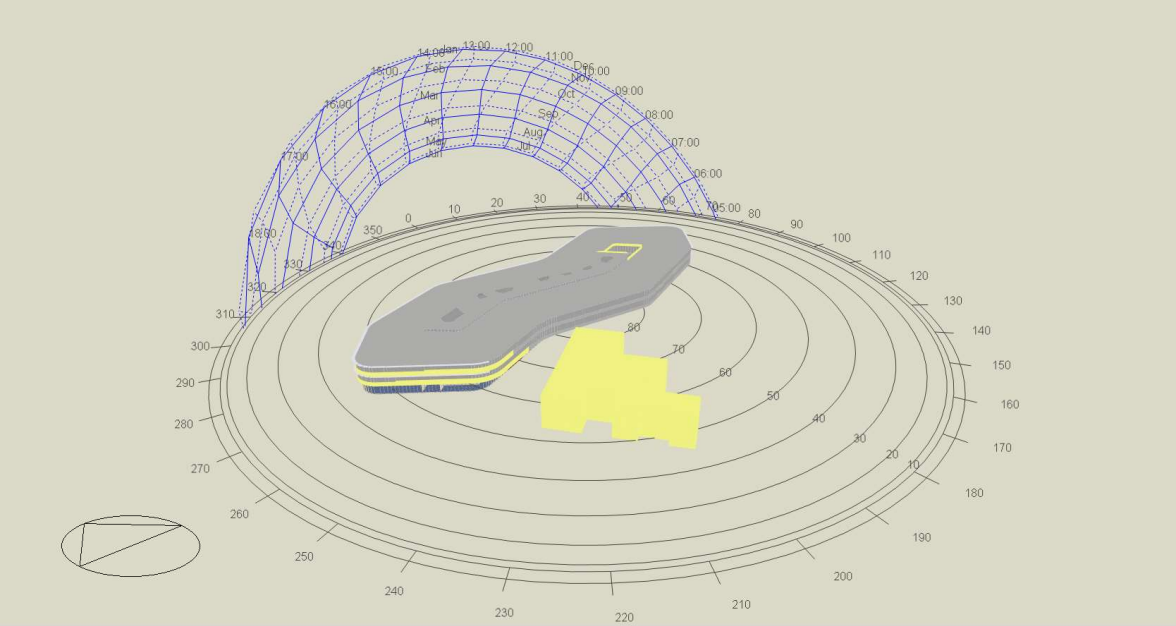

Figure 25*: Capitec Bank DesignBuilder™ with EnergyPlus™ thermal energy model*

3.5.2 Model inputs

The information loaded into the thermal energy model was derived from engineering regulations and design standards. DesignBuilder™ with EnergyPlus™ has input tabs in the software that allow the thermal model to provide various data over the simulation period.

The site was situated in the Stellenbosch area thus, weather data from the International weather for energy calculations (IWEC) database was simulated in the cape town location. The summer design day and winter design day are temperature extremes. The building site orientation was taken from the architectural design layout provided by the architect. This is one of the key parameters of an energy model as the solar azimuth is calculated for each orientation on a compass, which corresponds to a relative solar radiation value calculated by the software.

Table 1: *Site data model inputs*

ITEM	COMMENT
Weather data – Site	Cape Town, International Weather for Energy Calculations
Summer design day	35˚C dry bulb temperature and 23 ˚C Wet-bulb temperature
Winter design day	5˚C (IWEC, 2021)
Building site orientation	339˚ North (Architect layout) – see circular arrow in figure 25

The activity data sets the various parameters that affect all the thermal calculations, and these values are taken from multiple engineering standards and design recommendations.

Table 2: *Activity data model inputs*

ITEM	COMMENT
Operating hours	06:00 am – 18:00 pm, typical office hours (GBCSA, 2021)
Schedules	GBCSA schedules for occupancy, equipment and lights (GBCSA, 2021). See Appendix B
Equipment loads	18.75 W/m² [150 (W/desk) /8 (m² per person)] - (Splitler, 2014)
Lighting loads	10 W/m² (GBCSA., 2021)
Occupancy loads	8 m²/person (SANS, 2010b)
Outside air	10 l/s/p (SANS, 2010a)
Indoor temperature point	20-23˚C in Office areas (GBCSA, 2021) & (SANS , 2010a)
Metabolic activity factor (thermal comfort studies)	IEQ 9 Case 1 MET rate 1.2= 123 watts / person (GBCSA, 2021) Winter Clothing Case 1 (CLO) = 0.6 (GBCSA, 2021) Summer Clothing Case 1 (CLO) = 0.6 (GBCSA, 2021) Airflow velocity Case 1 (m/s) = 0.3 (GBCSA, 2021) IEQ 9 Case 2 MET rate 1.2= 123 watts / person (GBCSA, 2021) IEQ 9 Case 2 Winter Clothing (CLO) = 0.95 (GBCSA, 2021) IEQ 9 Case 2 Summer Clothing (CLO) = 0.95 (GBCSA, 2021)
Natural ventilation min T	24˚C - (GBCSA, 2021) & (SANS , 2010a)

The operational hours are typical to a day office as stipulated by the Green Star SA energy code, any other equipment schedules are assumed to be on the same hours as well. The equipment loads assume standard office equipment and occupancy loads along with outside air loads are assumed as per SANS regulations, these occupancy loads and fresh air loads affect fresh air calculations and cooling load calculations. The indoor temperature is one of the most important parameters as the temperature difference calculated sensible heat, a comfortable environment is assumed at 20-23˚C. Finally the metabolic parameters are taken directly from

Green Star IEQ 9 thermal comfort modelling code which provides detailed guidance on thermal comfort calculations.

Table 3: *Construction data model inputs*

ITEM	COMMENT
Construction (walls)	300mm IEQ 4 concrete, U = 2.296 W/m²-K (GBCSA, 2021)
Construction (roof)	Comb. roof R 3.7 , U = 0.27 W/m²-K (SANS 10400 XA,2008) Green roof R 2.63 , U = 0.38 W/m²-K (Kotsiris. et al., 2012)
Construction (floor)	450mm IEQ 4 concrete + floor screed, U = 1.146 W/m²-K
Construction (partitions)	110mm brickwork and double plaster, U = 1.6 W/m²-K
Infiltration on 24/7	0.5 AC/h (GBCSA, 2021)

The construction model parameters provides the information into the various thermal resistance of the building envelope. For an energy model, aside from properties such as visual light transmission, condensation and thermal bridging, these materials are basically calculated as a mathermatical component in the thermal calculations. Depensing on how the building is designed, the simulation software will accurately calculate the various areas and volumes using the simulation based EnergyPlus™ engine. The properties in table 3 are extracted directly from the architectural building design layouts thus the construction of the thermal model represent correct thermal resistance and improve the simulations accuracy.

The openings data in table 4 provide similar information to the construction data as set in tabe 3, the main difference is that glazing is the main area of focus and thus must be have the correct thermal properties as specified by the glass manufacturer, in this case compass glass provided the information in table 4. As noted in other sections of this study, clear glazing is the worst-case scenario and there are three other performance glazing types considered in the analysis. Low emissivity glazing is denoted with the letter E. Finally, the framing is considered to be typical aluminium frames as per the architect's drawings. The software calculates the gaps along the façade model to build in a thermal resistance any other thermal properties.

Table 4: *Openings/glazing data model inputs*

ITEM	COMMENT
Glazing type 1 – Clear	SHGC = 0.84 , VLT = 0.89, U = 5.8 W/m²-K K (CG, 2021)
Glazing type 2 – NC60E	SHGC = 0.53 , VLT = 0.57, U = 3.8 W/m²-K K (CG, 2021)
Glazing type 3 – NC55E	SHGC = 0.45 , VLT = 0.7, U = 3.8 W/m²-K K (CG, 2021)
Glazing type 4 – NC52	SHGC = 0.59 , VLT = 0.54, U = 5.8 W/m²-K K (CG, 2021)
Frame type – Low E	Al frame U = 5.73 W/m²-K, SHGC = 0.66 (SANS , 2010b)

The HVAC model table is a general cooling system template selected with a minimum supply air of 24˚C and a minimum humidity ratio of 0.96 as per the applicable standards noted. The cooling and heating coefficient of performance (COP) is a typical value set per the energy modelling software template and mainly affects energy use calculations.

Table 5: *HVAC data model inputs*

ITEM	COMMENT
Heating COP	0.85 Standard 4 pipe air-chiller setting(DesignBuilder, 2021)
Cooling COP	1.8 Standard 4 pipe air chiller setting (DesignBuilder, 2021)
Minimum supply air	24˚C - (GBCSA, 2021) & (Splitler, 2014)
Minimum humidity ratio	0.96 - (Splitler, 2014)

3.5.3 Façade zoning and shading and glazing distribution

The façade zoning was analysed over each of the orientations to the sun. A 4m internal zone from the façade face was used as the simulation volume to calculate the heating and cooling loads. The second floor was considered the most appropriate load as the roof heating load meant a maximum cooling capacity that a HVAC system can deliver for space would be required on this floor. In the envelope design recommendations, a 4m shading device was analysed as to how the overall heat gain can be reduced.

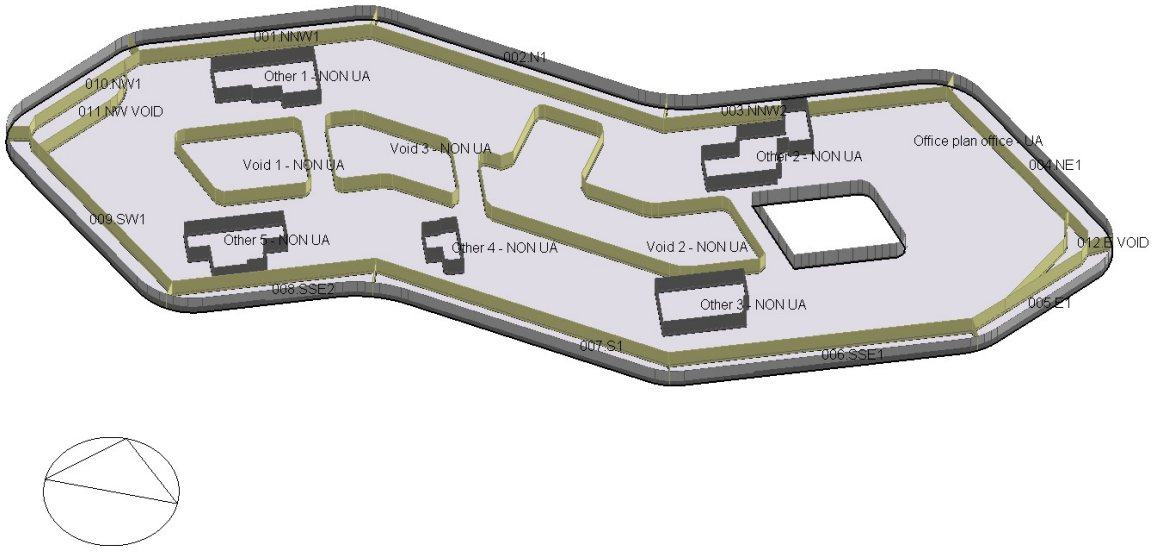

Figure 26: *Perimeter zones for thermal simulations*

The initially estimated percentage of glass distribution along the façade is shown below. While improving the façade performance, the glazing was designed with variable concrete spandrel walls height to reduce the glazing area and thus reduce internal heat gain. This feature of reducing and increasing the spandrel panel height is known as a parametric façade.

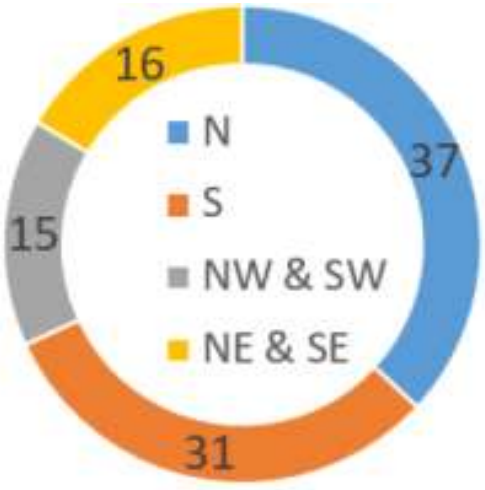

Figure 27: *Estimated percentage distribution of façade orientation*

CHAPTER-4 : SIMULATION & EXPERIMENTAL RESULTS

4.1 Façade analysis energy modelling

The energy modelling for the various glazing types were simulated in a separate model, and each model has a yearly simulation evaluated on an hourly basis. There are more than 20 parameters were extracted within an hourly. This totalled approximately 2 million data points.

4.1.1 Peak simulation load & glazing performance analysis

The peak cooling loads for overheating was limited to anything above or equal to 180W/m².

4.1.1.1 Glazing summary

The glazing summary in table 7 shows that the lowest-performing glazing type was clear glazing which simulated an average of 163.4 W/m², and each of the three performance glazing types was compared to the parameters noted from tables 7-11. The low emissivity glazing types delivered the best thermal performance with a combined average of 126 W/m², and the NC52 glazing resulted in an average of 147.6 W/m². The preferred glazing choice that was selected by the end-user was NC52, as the building envelope design optimisation would ensure that all loads remain below the peak design threshold and the HVAC system energy would perform as expected. The NNW1,N1 and NNW2 zones heat gain needed to be improved.

Table 6: *Peak Cooling Load (W/m²) with 10% margin and 35˚C peak ODBT.*

ZONE	AREA	CLEAR		NC60E		NC55E		NC52	
Direction	m²	TC (kW)	TC (W/m²)	TC (kW)	TC (W/m²)	TC (kW)	TC (W/m²)	TC (kW)	TC (W/m²)
NW1	98,0	19,6	200,0	15,8	161,2	14,7	150,0	17,6	179,6
NNW1	156,0	33,1	212,3	25,1	160,9	23,5	150,6	28,8	184,6
N1	205,0	41,7	203,4	30,8	150,2	29,0	141,5	37,5	182,9
NNW2	180,0	39,4	218,9	29,4	163,3	27,4	152,2	35,0	194,4
NE1	160,0	28,8	180,0	22,7	141,9	21,0	131,3	26,0	162,5
E1	107,0	16,0	149,5	12,8	119,6	12,0	112,1	15,2	142,1
SSE1	200,0	21,8	109,0	19,0	95,0	18,4	92,0	19,7	98,5
S1	206,0	22,3	108,3	19,3	93,7	18,7	90,8	20,7	100,5
SSE2	134,0	15,3	114,2	13,3	99,3	12,9	96,3	14,0	104,5
SW1	158,0	24,1	152,5	19,3	122,2	18,2	115,2	22,3	141,1
TOTAL	1 604	262,1	163,4	207,5	129,4	195,8	122,1	236,8	147,6

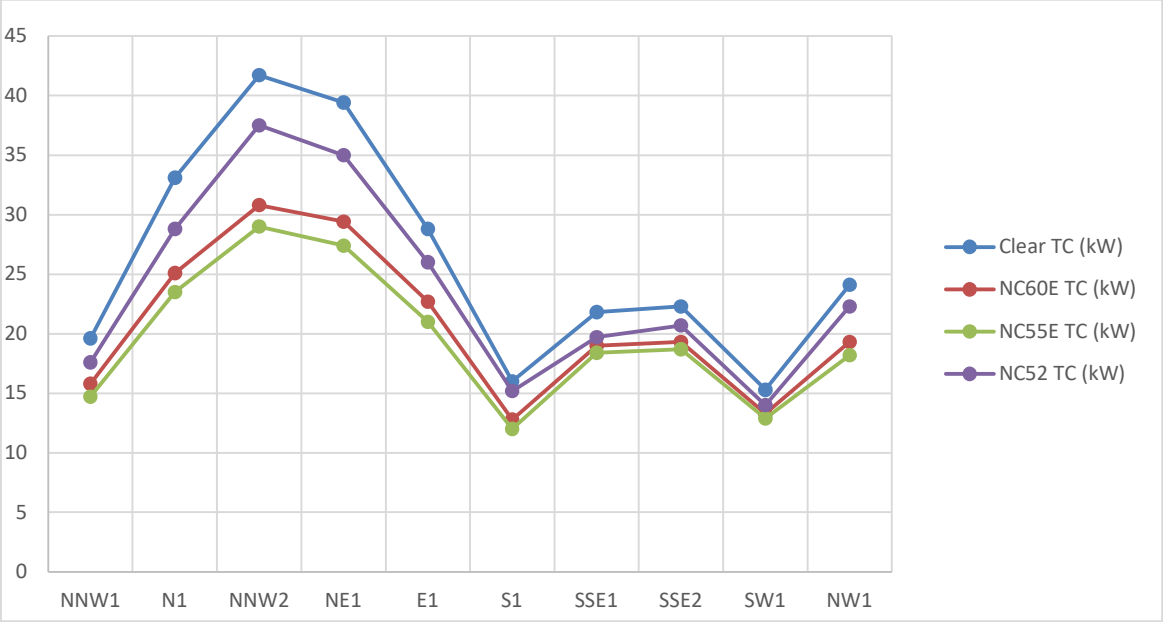

Figure 28: *Peak Cooling load glazing summary (kW) @ 10% margin and 35˚C peak ODBT.*

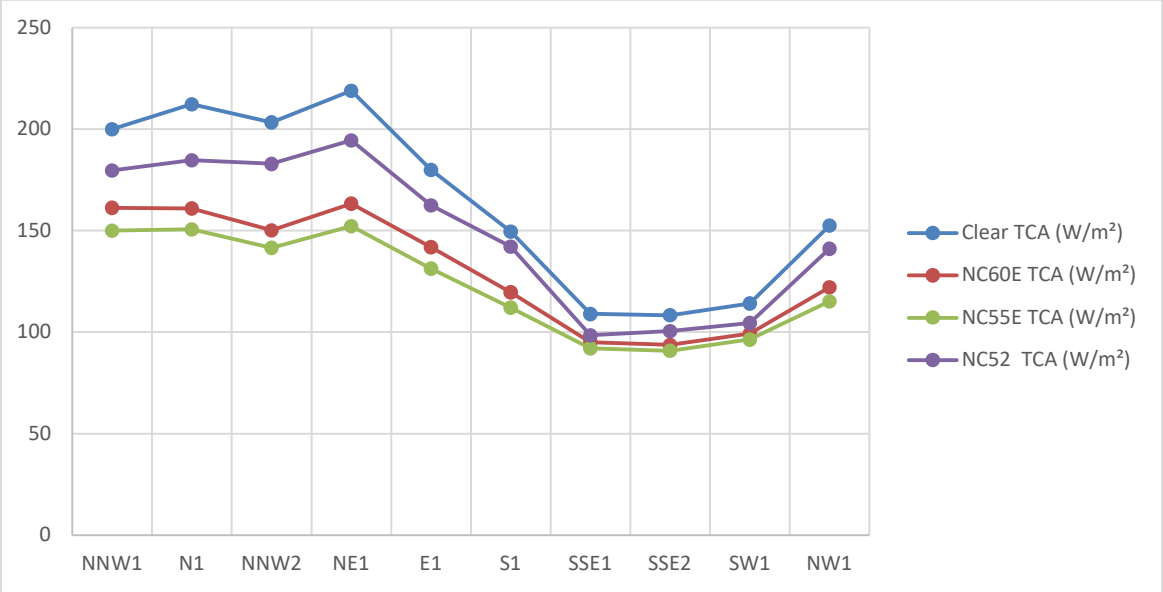

Figure 29: *Peak Cooling load glazing summary (W/m²) @ 10% margin and 35˚C peak ODBT*

4.1.1.2 Clear glazing

The clear glazing simulation results in table 7 represent the worst-case scenario glazing simulation, with the cooling loads in each zone reporting the highest results as expected.

Table 7: *Peak cooling load simulation clear glazing data*

ZONE	DATE	AREA	TC	TCA	SC	LC	ISG	ESG	AT	RT	OT	ODBT
Direction	dd/mm/yy	m²	(kW)	(W/m²)	(kW)	(kW)	(kW)	(kW)	°C	°C	°C	°C
NW1	2002/03/25 16:00	98,0	19,6	200,0	17,9	1,7	5,1	41,3	23,0	38,8	30,9	29,1
NNW1	2002/03/25 16:00	156,0	33,1	212,3	31,0	2,1	7,6	53,0	23,0	40,0	31,5	29,0
N1	2002/03/25 14:00	205,0	41,7	203,4	38,2	3,5	8,5	69,9	23,9	40,6	32,3	30,5
NNW2	2002/03/25 15:00	180,0	39,4	218,9	36,3	3,1	7,7	71,2	23,4	40,3	31,9	30,2
NE1	2002/02/18 12:00	160,0	28,8	180,0	27,4	1,4	5,9	41,9	23,0	37,5	30,3	33,4
E1	2002/01/15 11:00	107,0	16,0	149,5	14,6	1,4	4,4	20,3	23,0	34,9	28,9	29,5
SSE1	2002/01/15 16:00	200,0	21,8	109,0	19,1	2,7	6,4	11,0	23,0	31,0	27,0	32,4
S1	2002/01/15 17:00	206,0	22,3	108,3	19,5	2,8	6,2	15,9	23,0	31,3	27,2	31,1
SSE2	2002/01/15 16:00	134,0	15,3	114,2	13,5	1,8	6,7	7,6	23,0	31,5	27,3	32,4
SW1	2002/01/15 17:00	158,0	24,1	152,5	21,9	2,2	6,1	20,3	23,0	35,3	29,2	31,1
TOTAL	n/a	1 604,0	262,1	163,4	239,4	22,7	64,6	352,4	n/a	n/a	n/a	n/a

The first observation is that each zone peaks at different times according to the sun's orientation, which indicates that occupants along the various zone orientations will collectively experience their respective highest internal solar heat (ISG) gain at these times. The north-north-west (NWW2) zone records the highest total cooling load requirement per metre square of floor area (TCA) of 218.9W/ m², corresponding to a total cooling (TC) of 39,4 kW and a very high external solar heat gain (ESG) of 71,2 kW which exists on the outside surface of the glass panel. As the outer glass face reflects this solar radiation, the simulation produces a 7.7kW of internal transmission heat gain expected on the glass's interior surface.

The outdoor dry bulb temperature (ODBT) at this maximum cooling requirement is iterated by the simulation software from the existing simulation weather file and corresponds to a value of 30.2°C. The supply air temperature (AT) of all the zones in the simulation is modelled at an average of 23°C and a minimum requirement of 24°C, and this was an acceptable comfort temperature as it would remain a control variable to determine the cooling requirements. The radiant temperature (RT), representing the weighted average of the zone inside surface temperature, was recorded at 40.3°C, and an operative temperature (OT) of 31.9°C.

A further observation is that all the north-facing zones are above the 180W/m² design threshold, and as expected, the external solar heat gain is also the highest of all the zones. A higher total cooling load does not mean that the load per area is higher, however, a smaller area footprint tells us that the internal heat gain is concentrated, and the space could experience higher internal temperatures, as per the N1 zone, which has a lower TCA but higher TC over the NNW2 zone.

The east (E1) zone reflects the lowest TC, and the TCA is simulated at 149.59W/ m². This results from the E1 zone having a smaller area along the façade. The AT, OT and ODBT are in the mid-range compared to all the other zones results, and the RT is recorded to be 34.9°C, which is about 5.4°C lower than the NNW2 peak zone. Subject to a thermal comfort analysis, the high-temperature difference in operating temperatures of human thermal comfort could raise concerns about comfort acceptance in one zone and rejection in another.

The south zones except for SW1 all return approximately half the TC and TCA values, this indicates that the south-facing zones experience the lowest heat absorption into the space, and there exist much lower operative and air temperatures. This suggests that the SSE zones can be designed on the same thermostat, noting the SW1 and S1 zones are grouped together.

The total of zone loads also provides a perspective of the average total cooling requirements for all the façade zones, with a TC of 262.1kW over 1604 m², the average TCA is 163.4 W/ m². This result is in the mid-range of the north and south zones, and the total external solar heat gain is much higher than both the TC and total SC load for all the zones. It thus confirms the purpose of the SHGC of glazing to reduce the cooling requirements within the space.

Afram et al. (2014) has analysed predictive model control for HVAC systems and notes that zone control in terms of psychrometric parameters inside a space cannot be adequately controlled if coupling of multi thermal zones is not considered as the results would be inaccurate, thus energy efficiency in zone control is not limited a reduction in ESG and TCA but also the various components of a system and the thermal zone arrangement.

4.1.1.3 NC60E glazing

The NC60E glazing simulation results in table 8 represent the medium performance low emissivity glazing simulation, with the cooling loads in each zone reporting better results as expected, all zones are now below the maximum required TCA.

Table 8:*Peak cooling load simulation NC60E glazing data*

ZONE	DATE	AREA	TC	TCA	SC	LC	ISG	ESG	AT	RT	OT	ODBT
Direction	dd/mm/yy	m²	(kW)	(W/m²)	(kW)	(kW)	(kW)	(kW)	°C	°C	°C	°C
NW1	2002/03/25 16:00	98,0	15,8	161,2	14,2	1,6	2,8	21,3	23,0	36,0	29,5	29,0
NNW1	2002/03/25 15:00	156,0	25,1	160,9	22,5	2,6	4,0	28,9	23,3	36,3	29,8	30,2
N1	2002/03/25 14:00	205,0	30,8	150,2	27,3	3,5	4,6	34,7	24,1	36,6	30,3	30,5
NNW2	2002/03/25 15:00	180,0	29,4	163,3	26,2	3,2	4,2	36,0	23,8	36,8	30,3	30,2
NE1	2002/03/25 12:00	160,0	22,7	141,9	20,2	2,5	3,8	26,8	23,0	34,5	28,8	28,4
E1	2002/01/15 10:00	107,0	12,8	119,6	11,2	1,6	2,4	13,6	23,0	32,5	27,8	27,2
SSE1	2002/01/15 16:00	200,0	19,0	95,0	16,4	2,6	3,4	5,5	23,0	29,5	26,3	32,4
S1	2002/01/15 16:00	206,0	19,3	93,7	16,6	2,7	3,4	6,5	23,0	29,4	26,2	32,4
SSE2	2002/01/15 16:00	134,0	13,3	99,3	11,5	1,8	3,5	3,8	23,0	29,9	26,5	32,4
SW1	2002/01/15 17:00	158,0	19,3	122,2	17,1	2,2	3,3	18,6	23,0	35,5	27,8	31,1
TOTAL	n/a	1 604	207,5	129,4	183,2	24,3	35,4	195,7	n/a	n/a	n/a	n/a

The first observation is that similar to clear glazing, each zone peaks at different times, these dates and times are the same and were expected to remain a control variable with all simulations as there is no change in the building envelope of the orientation to the sun. However, the simulation shows differences, and the peak date and time changed for some of the zones. The NWW2 zone records the highest TCA of 163.3W/ m², corresponding to a TC of 29,4 kW and an ESG of 36 kW, approximately half of the clear glazing load at this zone. The simulation produces a 4.2kW ISG, approximately 45% lower than the clear glazing result.

The ODBT at this maximum cooling requirement corresponds to a value of 30.2°C, and only a 1% change is observed. The supply AT lies in-between 23 - 24°C, as noted for the clear glazing. The RT was recorded at 36.8°C, which is a 3.5°C lower than clear glazing at this zone, and also responded to an OT of 30.3°C, which is approximately 1.6°C lower as well. This sets the precedent that one can expect a lower internal temperatures when low emissivity glazing is used in a façade, the temperature change can impact thermal comfort, and the end-user could apply a higher fan and cooling setting, which would result in higher energy usage.

A further observation is that all the north-facing zones have been reduced below 180W/m², and the ESG is also the highest of all the zones. A higher total cooling load does not mean that the TCA is higher, and a smaller area footprint tells us that the internal heat gain is concentrated, thus the space could experience higher internal temperatures as seen in the north 1 (N1) zone, which has a lower TCA but higher TC.

The E1 zone reflects the lowest TC, and the TCA is simulated at 119.6 W/ m², and a significant reduction of 20% is observed. The internal temperatures are in the mid-range of all the other zones results, and the RT is recorded at 32.5°C, which is about 2.4°C lower than the NNW2 peak zone, compared to clear glazing. The OT is recorded at 27.8°C, which is a 1.1°C difference, and the ODBT responded to a value of 27.2°C, this is slightly above 2°C when compared to clear glazing and is most interesting as the ODBT should not be affected as the energy plus calculates this value.

A further observation is that the peak time of the east zone has changed by one hour, and the ODBT variable has responded accordingly in the energy simulation. Although glazing cannot change the ODBT, the response of ISG & ESG regarding how Low E glazing performs in relation to the suns radiation, it observed that this affects the internal temperature and peak times at which occupants might feel comfortable.

The south zones except for SW1 all return approximately 60% of the cooling and cooling load per area values, the south-facing zones, with regards to temperature and cooling loads, each perform similarly as the clear glazing. However, the cooling load requirements are decreased by 13%, and the temperatures are lower by 1°C. Likewise, to clear glazing, the south-facing zones except SW1 can be designed on the same zone control thermostat and respond collectively to the ODBT.

The total zone loads are considerably lower than clear glazing, with a TC of 207kW over 1604 m², the average TCA is 122.2W/ m². When comparing the result to clear glazing, the TC & TCA reduced by almost 21%. We observed that the total results are in the mid-range of the north and south zones, and the total external solar heat gain is higher than the total SC for all the zones and lower than the total TC. In comparison with clear glazing, it was found that there was a 45% reduction in the ESG and ISG, and the latent load (LC), with little difference noted.

Although the reduction in ESG is significant for Low E glazing, it should be noted that Trcka et al. (2010) has indicated that the actual energy consumption could vary by up to 40%, and a crude thermal analysis should be sufficient, however, the discrepancies in actual thermal performance needs to be considered as a cooling plant could be incorrectly designed to run without adequate capacity. Bhasko et al. (2011) has investigated in great detail the various occupation schedules and adaptive cooling techniques, and the analysis done for the façade types is quite basic in comparison to an adaptive cooling study as the different occupancy schedules and space parameters are far more detailed for a dynamic system, however, as expected heat gain in both this study and that of Bhasko et al. (2011) shows that heat gain dominates all other thermal parameters in thermal simulation, thus sensible cooling is quite close in all the zones.

4.1.1.4 NC55E glazing

The NC55E glazing simulation results in table 9 represent the high-performance, low emissivity glazing simulation, with the cooling loads in each zone reporting slightly better results when compared to NC60E and displaying the best percentage of energy efficiency improvement when compared to the clear glazing results. The NC55E analysis focuses mainly on comparing simulation results between NC60E as their thermal properties are relatively similar, although some relevant comparisons have been noted for clear glazing.

Table 9 : *Peak cooling load simulation NC55E glazing data*

ZONE	DATE	AREA	TC	TCA	SC	LC	ISG	ESG	AT	RT	OT	ODBT
Direction	dd/mm/y	m²	(kW)	(Wm²)	(kW)	(kW)	(kW)	(kW)	°C	°C	°C	°C
NW1	2002/03/	98,0	14,7	150,0	13,0	1,7	2,3	16,7	23,0	35,0	29,0	29,1
NNW1	2002/03/	156,0	23,5	150,6	20,9	2,6	3,2	22,6	23,0	35,0	29,0	30,2
N1	2002/03/	205,0	29,0	141,5	25,5	3,5	3,6	26,9	23,7	35,2	29,4	30,5
NNW2	2002/03/	180,0	27,4	152,2	24,3	3,1	3,3	22,8	23,5	35,6	29,5	30,2
NE1	2002/03/	160,0	21,0	131,3	18,5	2,5	3,0	20,9	23,0	33,6	28,3	28,3
E1	2002/01/	107,0	12,0	112,1	10,4	1,6	1,9	10,5	23,0	31,8	27,4	27,2
SSE1	2002/01/	200,0	18,4	92,0	15,8	2,6	2,7	4,3	23,0	29,2	26,0	32,4
S1	2002/01/	206,0	18,7	90,8	16,0	2,7	2,7	5,0	23,0	29,0	26,0	32,4
SSE2	2002/01/	134,0	12,9	96,3	11,1	1,8	2,8	3,0	23,0	29,6	26,3	32,4
SW1	2002/01/	158,0	18,2	115,2	16,0	2,2	2,6	14,4	23,0	31,9	27,4	31,1
TOTAL	n/a	1 604	195,8	122,1	171,5	24,3	28,1	147,1	n/a	n/a	n/a	n/a

The first observation is that similar to clear glazing, each zone peaks at different times, these dates and times do not change compared to the NC60E peak times, thus the .main advantage of the low emissivity glazing types will only be concerning cooling performance and the other associated variables. The NWW2 zone records the highest TCA of 152.2W/ m², corresponding to a TC of 27,4 kW and ESG of 22.8 kW compared to NC60E, the TCA & TC has only been lowered by 6.8%. As the outer glass face reflects this solar radiation, the simulation produces a 3.3kW of ISG, approximately 21.5% lower than the NC60E result.

The ODBT at this maximum cooling requirement corresponds to a value of 30.2°C, and no change is observed. The supply AT lies in-between 23 - 24°C, as noted for the clear glazing. The RT was recorded at 35.6°C, which is a 1.2°C lower than NC60E at this zone, and also responded to an OT of at 29.5°C, which is approximately 2.4°C lower. A further observation is that all the north-facing zones remain below 180W/m² with improved cooling load requirements, and the ESG is still the highest of all the zones, and when compared to NC60E, a 37% reduction is noted. The N1 zone also continues to have a lower TCA, but higher TC and 31% reduction is indicated for when compared NC60E, a further decrease of 61.5% for clear glazing. Apart from the N1 zone, all the other zones have a notable reduction in the ESG.

The E1 zone continues to reflect the lowest TC, and the TCA is simulated at 112.1 W/ m², a reduction of 6.3%. The internal temperatures are the mid-range of all the other zones results, and the RT is recorded to be 31.8°C, which is about 0.7 °C lower than the NNW2 peak zone. Further to this, similar conclusions for the NC60E results are drawn for that of NC55E glazing.

The south zones except for SW1 all return approximately 60% of the TCA & TC, the south-facing zones, with regards to temperature and cooling loads, each perform similarly as the clear glazing, however, the cooling load requirements are decreased by 16%, and the temperatures are lower by 1°C. Likewise, to clear glazing, the south-facing zones except SW1 can be designed on the same zone control thermostat and respond collectively to the ODBT. Compared to NC60E, the South zones do not have significant changes in the results aside from the ESG, which has an average of 20% reduction.

The total zone loads are considerably lower than clear glazing, with a TC of 195.8kW over 1604 m², the average TCA is 122.2W/ m². When comparing the result to NC60E, the TC & TCA reduced by almost 5.6%. We observed that the totalled results are in the mid-range of the north and south zones, the total ESG is higher than the total SC for all the zones and lower than the TC. It was found that there was a 25% reduction in the ESG and a 20% reduction in the ISG, and the LC did not indicate much of a difference.

Wang et al. (2017) has investigated the effects of spatial distribution and notes that the thermal effects of space arrangement should be considered. The implementation of C02 sensors to improve energy efficiency in zone control. Similarly, Aliahmadipour et al. (2017) has analysed turbulent airflow with CFD and noted that space arrangement could ensure that airflow will be more uniform and decrease the likelihood of unacceptable thermal conditions.

4.1.1.5 NC52 Glazing

The NC52 glazing simulation results in table 10 represent the mid-performance glazing simulation. The cooling loads in each zone report improved results compared to clear glazing. Low emissivity glazing has the best performance. Neither glazing type can provide improved thermal performance on glazing specification alone.

Table 10 : *Peak cooling load simulation NC52 glazing data (base)*

ZONE	DATE	AREA	TC	TCA	SC	LC	ISG	ESG	AT	RT	OT	ODBT
Direction	dd/mm/yy	m²	(kW)	(Wm²)	(kW)	(kW)	(kW)	(kW)	°C	°C	°C	°C
NW1	2002/03/25	98,0	17,6	179,6	15,9	1,7	2,8	22,7	23,0	37,8	30,4	29,0
NNW1	2002/03/25	156,0	28,8	184,6	26,1	2,7	4,0	30,8	23,0	38,2	30,6	30,2
N1	2002/03/25	205,0	37,5	182,9	34,0	3,5	4,6	37,3	23,2	38,6	30,9	30,5
NNW2	2002/03/25	180,0	35,0	194,4	31,9	3,1	4,2	38,5	23,0	38,7	30,8	30,2
NE1	2002/03/25	160,0	26,0	162,5	23,4	2,6	3,8	28,6	23,0	36,6	29,8	28,4
E1	2002/11/30	107,0	15,2	142,1	13,4	1,8	2,4	13,8	23,7	34,9	29,3	27,9
SSE1	2002/01/15	200,0	19,7	98,5	17,0	2,7	3,2	5,9	23,0	29,8	26,4	32,4
S1	2002/01/15	206,0	20,7	100,5	17,9	2,8	3,4	8,4	23,0	30,5	26,8	31,1
SSE2	2002/01/15	134,0	14,0	104,5	12,2	1,8	3,6	4,0	23,0	30,6	26,8	32,4
SW1	2002/01/15	158,0	22,3	141,1	20,2	2,1	3,3	20,2	23,0	34,5	28,8	31,1
TOTAL	n/a	1 604	236,8	147,6	212,0	24,8	35,3	210,2	n/a	n/a	n/a	n/a

The first observation is that similar to clear glazing, each zone peaks at different times, these dates and times only change for the NNW1, NE1 zone and E1 zone. The most interesting difference is that the peak date and time of the E1 zone have shifted by almost a month and a half. This result is not expected as only the glazing performance has changed. Thus, from an energy usage point of view, the E1 zone might require a dedicated thermostat control to manage the heating and cooling to ensure acceptable indoor conditions. The NWW2 zone records the highest TCA of 194.4W/ m², corresponding to a TC of 35 kW and an ESG of 38.5 kW, and when compared to clear glazing, the TCA & TC has only been lowered by 11%. The simulation produces a 4.2 kW of ISG and is approximately 45% lower than clear glazing.

The ODBT at this maximum cooling requirement corresponds to a value of 30.2°C, and no change is observed. The supply AT lies in-between 23 - 24°C, as noted for the clear glazing. The RT was recorded at 38.7°C, which is a 1.9°C lower than NC60E at this zone, and also responded to an OT of at 30.8°C, which is approximately 1.1°C lower. A further observation is that all the north-facing zones except NE1 are above 180W/m² with improved cooling load requirements compared to clear glazing. The results are now above the design threshold and decreased performance when the cooling loads are compared to low emissivity glazing. The ESG has improved, as for the NNW2 zone notes a 6.5% increase is observed. The north 1 (N1) zone also continues to have a lower TCA, but a higher TC, and a 10.1% reduction is noted when compared to clear glazing, and all the other zones have a notable decrease in the ESG.

The E1 zone continues to reflect the lowest TC, and the TCA is simulated at 142.1 W/ m², which is a reduction of 8.2%. The ISG is observed to have a 46% increase which is similar for all the other zones. The internal temperatures are in the mid-range of the other zones results, and the ODBT is calculated at 27.9°C, which has decreased by 1.6°C, and NC52 now has internal temperatures increasing the energy efficiency of the HVAC system in the E1 zone. The RT is recorded to be 34.9°C, and no change is observed regarding clear glazing.

The south zones except for SW1 all return an average TCA & TC increase in performance of approximately 8.4%. Compared to clear glazing, the south zones have significant changes in the ISG, which accounts for an average of 45% increase in performance. Regarding temperatures, the AT and ODBT exhibit no difference, however, the SSE1 zone notes a 3.9% decrease in AT and a 2.2% decrease in OT. The cooling load requirements are decreased by

16%, and the temperatures are lowered by 1°C. The SSE2 zone can be designed on the same thermostat and respond collectively to the ODBT, and both SW1 and S1 are grouped.

The total zone loads are much better than clear glazing but require improvement, with a TC of 236.8kW over 1604 m², the average TCA is 147.6W/m². When comparing the result to clear glazing, we find that the TC & TCA was improved by 9.7%. We observed that the totalled results are in the mid-range of the north and south zones, the total external solar heat gain is lower than the total sensible load and total load. It was found that there was a 40% increase in performance of the ESG and a 45% increase in performance of the ISG, and the latent load (LC), a 9.1% increase in performance was observed.

Touma et al. (2017) provided a solution to increase thermal performance and reduce ESG as noted in figure 1, it was shown that a 10% increase in performance is due to blinds being implemented along the façade. Blinds are highly recommended on a parametric façade and although not included in the simulations, the client installed blinds on the internal space of the building façade to improve energy efficiency via a reduction in internal heat gain.

Colombo et al. (2017) has investigated the effects of blinds on a double glazed façade, and the CFD analysis shows that a façade can significantly improve the internal cooling load requirements and should be investigated later. The effects of green roofs with indoor ventilation have been analysed by Ran et al. (2017). It was noted that 26.7% energy saving is theoretically possible, which is a high saving compared to the green modelled in this study with NC52 glazing. Finally, Kotsiris et al. (2016) looks further into the values and note that various additional materials, such as coarse aggregates on green roofs, can cause improved thermal performance inside the space. The NC52 green roof simulation only analysed a general U value, and further in-depth analyses into the performance of green roofs is required.

4.1.2 Sustainable design optimisation for improved energy performance

The building envelope was required to be Optimised by reducing the glazing area and 1m external louvre shading devices on each window. A simulation was also done that analyses a green roof's passive thermal Optimisation effect and measures the thermal performance.

4.1.2.1 NC52 Glazing Optimised with building envelope shading

The NC52 glazing and building envelope shading simulation in table 11 represent the selected glazing zones with improved thermal performance to ensure a maximum of 180 W/m².

Table 11: *Peak cooling load simulation NC52 glazing and combined shading data*

ZONE	DATE	AREA	TC	TCA	SC	LC	ISG	ESG	AT	RT	OT	ODBT
Direction	dd/mm/yy	m²	(kW)	(Wm²)	(kW)	(kW)	(kW)	(kW)	°C	°C	°C	°C
NW1	2002/03/25	98,0	14,4	146,9	12,7	1,7	1,7	17,3	23,0	34,8	28,9	29,0
NNW1	2002/03/25	156,0	21,9	140,4	19,3	2,6	3,1	20,7	23,0	34,4	28,7	29,0
N1	2002/03/25	205,0	28,3	138,0	24,9	3,4	3,6	25,5	23,0	34,2	28,6	30,5
NNW2	2002/03/25	180,0	26,7	148,3	23,7	3,0	3,2	26,9	23,0	34,7	28,9	30,2
NE1	2002/03/25	160,0	19,8	123,8	17,2	2,6	2,9	21,6	23,0	33,2	28,0	28,8
E1	2002/01/15	107,0	11,4	106,5	9,8	1,6	1,9	8,1	23,0	31,2	27,1	27,2
SSE1	2002/01/15	200,0	19,7	98,5	17,0	2,7	2,7	5,7	23,0	29,9	26,5	32,4
S1	2002/01/15	206,0	20,3	98,5	17,5	2,8	2,7	8,3	23,0	30,3	26,6	31,1
SSE2	2002/01/15	134,0	13,6	101,5	11,8	1,8	2,8	3,9	23,0	30,3	26,6	32,4
SW1	2002/01/15	158,0	17,8	112,7	15,7	2,1	2,6	12,1	23,0	31,6	27,3	31,1
TOTAL	n/a	1 604	193,9	120,9	169,6	24,3	27,2	150,1	n/a	n/a	n/a	n/a

The first observation is that each zone peaks at different times according to the orientation to the sun, and changes were observed concerning the NC52 base simulation. The shading device, whose function is to limit solar radiation, ensured that the peak times of the NNW1 and NE1 zones were shifted by an hour, and within such a short period, it is not expected that there would be any changes to zone control. The NWW2 zone records the highest TCA of 148.3W/ m², corresponding to a TC of 26.7 kW and an ESG of 26.9 kW, with a 23.7% improvement for the TC and TCA, also a 30.1% ESG and 23.8% ISG decrease in cooling requirements, these are substantial gains in thermal performance in the peak zone.

The ODBT at this maximum cooling requirement corresponds to a value of 30.2°C, and no change is observed. The RT was recorded at 34.7°C, and a 10.7% decrease was noted. Further to this, the OT of 28.9°C was 6.2% lower. The N1 zone, similar to other simulations, has a lower TCA, but TC, an improvement of 24.5% was noted.

The E1 zone now reflects the second-lowest TC & TCA at 11.4kW and 106.5W/ m² respectively, with an impressive 25% performance improvement. The AT, OT and ODBT also remain in the mid-range compared to all the other zones results, and the RT is recorded at 31.2°C, about 10.6% lower than the NNW2 peak zone.

The south zones except for SW1 are all simulated as the lowest TCA, with a 98.5 W/ m² at zones S1 & SSE2, it is observed that the south-facing zones experience the most inadequate heat absorption into the space, and there exist the lowest OT and AT in these zones. However, the performance increase due to the shading on the south-facing zones seems to have the least performance benefit in terms of their TC and ESG percentage improvements. The south-southeast facing zones, as per the base case, can thus be designed on the same zone thermostat and respond collectively to the ODBT, with the SW1 and S1 zones are on the same thermostat.

According to the total zones averages, there is a TC of 193.9kW over 1604 m², and the average TCA is 120.9 W/ m². Compared to the base simulation, it is observed that there was an improvement of 18.1% for the TC & TCA, however, considering the north zones only, this average is around 25%. This result is in the mid-range of the north and south zones. The total ESG is much lower than all the previous simulation total averages with a reported load of 150.1 W/ m², with a 28.6% average increase in thermal performance noted. Finally, the average ISG reported at 27.2kW with a 22.9% average increase is indicated.

4.1.2.2 NC52 Glazing Optimised with building envelope shading and a green roof

The NC52 glazing and building envelope shading simulation in table 12 represent the improved thermal performance envelope with NC52 glazing and a green roof element modelled as thermal resistance the lowest possible cooling requirements within each zone.

Table 12: *Peak cooling load simulation NC52 glazing and Optimised shading structure with green roof*

ZONE	DATE	AREA	TC	TCA	SC	LC	ISG	ESG	AT	RT	OT	ODBT
Direction	dd/mm/yy	m²	(kW)	(Wm²)	(kW)	(kW)	(kW)	(kW)	°C	°C	°C	°C
NW1	2002/03/25	98,0	15,0	153,1	13,4	1,6	1,7	17,3	23,0	35,6	29,3	29,0
NNW1	2002/03/25	156,0	21,9	140,4	19,2	2,7	3,1	20,7	23,7	35,3	29,5	29,0
N1	2002/03/25	205,0	28,0	136,6	24,5	3,5	3,6	23,5	23,9	35,3	29,6	30,4
NNW2	2002/03/25	180,0	26,0	144,4	22,9	3,1	3,2	21,5	24,0	35,7	29,9	30,2
NE1	2002/03/25	160,0	20,9	130,6	18,3	2,6	2,9	21,6	23,0	34,0	28,5	28,8
E1	2002/01/15	107,0	11,6	108,4	9,9	1,7	1,9	8,1	23,0	31,5	27,2	27,2
SSE1	2002/01/15	200,0	19,9	99,5	17,2	2,7	2,7	5,8	23,0	30,0	26,5	32,4
S1	2002/01/15	206,0	20,2	98,1	17,5	2,7	2,7	8,3	23,0	30,3	26,6	30,1
SSE2	2002/01/15	134,0	13,8	103,0	12,0	1,8	2,8	3,9	23,0	30,4	26,7	32,4
SW1	2002/01/15	158,0	17,9	113,3	15,7	2,2	2,6	12,1	23,0	31,7	27,4	31,1
TOTAL	n/a	1 604	195,2	121,7	170,6	24,6	27,2	142,8	n/a	n/a	n/a	n/a

The first observation is that each zone peaks at the exact times as per simulation in table 12, where there is no green roof, and thus in this instance, there are no effects observed in the peak time intervals. The NWW2 zone remains the highest TCA of 144.4W/ m², corresponding to a TC of 26 kW and an ESG of 21.5 kW, with a 2.6% improvement for the TC and TCA, also a 20.1% ESG and 0% ISG decrease in cooling requirements, these are minimal gains in thermal performance for the façade in the peak zone in relation to all of the other simulations. The ODBT at this maximum cooling requirement corresponds to a value of 30.2°C, and no change is observed. The RT was recorded at 35.7°C, and a 2.9% increase is noted. Further to this, the OT of 29.9°C was 3.5% higher. The N1 zone also has a lower TCA, but TC, improvement of 1.1% is noted.

The E1 zone continues to reflect the second-lowest TC & TCA at 11.6kW and 108.4W/ m², respectively, with a minor 1.8% performance decrease noted. The AT, OT and ODBT have either decreased or shown no performance increase, the RT is recorded at 31.5°C, which is a 1.6% increase in temperature.

The south zones except for SW1 are all simulated as the lowest TCA, with a 98.1 W/ m² at zones S1, it is observed that the south-facing zones experience the most inadequate heat absorption into the space, and there is now an increase in the cooling requirement, which is under 1.5% on average, there also exist the lowest OT and AT in these zones but no changes are observed in relation to space temperatures, with the exception of the S1 zone where a 3.2% decrease in temperature is noted.

According to the total zones averages, there is a TC of 195.0kW over 1604 m², the average TCA is 121.7 W/ m². When compared to the simulation without the green roof, it is observed that there was a decrease of 0.7% for the TC & TCA. However, considering the north zones only, this average is around 2.7%, the results are scattered as the NW1 zone has a 4.2% decrease, and the NNW1 remains the same. The total ESG is 4.9% better than all the previous simulation total averages with a reported load of 142.8 W/ m², however, the results are also scattered as the NNW2 exhibits a 20.1% decrease in ESG, but the majority of the zones remain constant, and no change is observed. The average ISG reported at 27.2kW reported remains the same according to the simulation for all zones. Temperatures on average also remain similar, with slight differences.

The green roof shows a minimal effect on reducing the total load in this simulation and this can be attributed to the small area of each façade zone as the entire floor area was not simulated, Zhang et al. (2016) has also analysed green roofs and also noted advantages with regards to improved thermal insulation and indoor temperatures with a 75% reduction in heat gain, comparing this to the simulation above there is only a 0.7% improvement noted and needs to be analysed further in respect to the various green roof insulation values. It is also pointed out that a green roof retains heat inside the space during the night hours, and additional cooling or night ventilation strategies will have to be implemented to maintain ideal thermal conditions. It is not expected that the space would be occupied in an office thus green roof is low risk.

Damian et al. (2020), uses the shading system S3, as shown in figure 2 to arrive at an energy saving of 60%, it is noted that for this analysis, the clear glazing total reduction from 262.1kW to 195.2kW is approximated at a 74.5% increase in energy saving.

4.1.3 Thermal comfort analysis

The thermal comfort assessment was done following the Green Star new building technical manual, as described in IEQ9. This modelling standard references the ASHRAE 55-2004 thermal comfort as shown in table 13 to define the acceptable temperature levels in relation to occupants' comfort inside the space. The second and most important tool used to determine acceptable comfort levels is the Fanger predicted mean vote (PMV) scale as defined in ISO7730. The simulated values were compared to these tables as a weighted average and discomfort hours to determine comfort acceptance for NC52 glazing.

The results in table 15 are the weighted average simulation hours for CLO60 and CLO95 thermal insulation, respectively. These hours were calculated using each simulated hour in each zone along the façade over an entire year using the best performing energy model with NC52 glazing and a green roof and combined with an improved shading envelope. The CLO60 insulation value, as shown in the metabolic rates in table 2, is used to determine the weighted average of a zone within the summer period, and the CLO95 applies to the winter timeframe. To comply with the IEQ9 green star point system, the simulation results would have to strictly follow the recommended operation schedule and produce fewer hours of performance data than a complete yearly simulation, as shown in figures 30 -31 below. The simulation thus considers an entire year and combines both winter and summer periods for each insulation parameter.

Table 13: *IEQ-9.1 Adaptive comfort temperatures as per ASHRAE 55*-2004 *(GBCSA, 2021)*

MEAN MONTHLY OUTDOOR TEMP.	MINIMUM INTERNAL TEMP. (80%) ACCEPTABLE	MINIMUM INTERNAL TEMP. (90%) ACCEPTABLE	MINIMUM INTERNAL TEMP. (90%) ACCEPTABLE	MINIMUM INTERNAL TEMP. (80%) ACCEPTABLE
°C	°C	°C	°C	°C
10	17.5	18.5	23.5	24.5
15	19	20	25	26
20	20.5	21.5	26.5	27.5
25	22	23	28	29
30	23.5	24.5	29.5	30.5

Table 14: *IEQ-9.1 PMV index as defined in ISO7730 (GBCSA, 2021)*

PMV (PREDICTED MEAN VOTE)	PPD (PREDICTED PERCENTAGE	THERMAL SCALE
+3		Hot
+2	70%	Warm
+1	25%	Slightly warm
+0.5	10%	-
0	5%	Neutral
-0.5	10%	-
-1	25%	Slightly cool
-2	70%	Cool
-3		Cold

4.1.3.1 Thermal analysis of peak and best TCA performance zones per insulation

The NNW2 zone notes the highest TCA, and in this zone, it is observed that over a yearly period, the CLO60 Fanger PMV indicated by the green line in figure 29, ranges between approximately 0 and -1.5 on the index chart, with the lowest level of comfort acceptance observed in between June and July, according to table 14 on the comfort scale, this amounts to a 50% predicted percentage dissatisfied of occupants in this zone.

Analysing the discomfort hours (red line in figure 29), we observe that the amount of discomfort hours corresponds to 100 hours, and the trendline indicates that the Fanger index does not have a directly proportional relationship to the number of hours that one feels, thus a higher discomfort index does not mean one experiences longer time of discomfort.

The relative humidity indicated by the blue line in figure 29 is modelled between 43% - 50%, with the lowest between June and July. The trendline is similar to the Fanger index, and this is expected as humidity has a significant role in acceptable comfort conditions. The temperatures which are banded together in the first graph of figure 29, also follow a similar trendline to the Fanger and humidity as expected, however, the results are not scattered, a relatively smooth trendline is observed, the ODBT, on the other hand, results are scattered away from the internal temperatures, and colder temperature is observed.

For the CLO60 and CLO95 simulations, the only differences are noted in the discomfort hours and Fanger PMV index value, a CLO95 insulation value produced a higher low in the June period and the majority of other periods have positive values, and this means a higher CLO value indicates warmer temperature on the discomfort scale.

Buratti et al. (2017) has analysed ventilated brick walls using CFD. The velocity and temperature profile on buildings' indoor and outdoor surfaces have significantly varying effects on how the outer wall of a façade is constructed. In this respect, the thermal analysis done is very basic compared to a full CFD simulation which could then be used to calculate the change in velocity, which is paramount to a PMV study.

A detailed CFD analysis would yield an array of data which could then be used in EnergyPlus to account for these variations and produce a much more accurate PMV profile for each zone. Youseff et al. (2015) also investigated comfort conditions with CFD, and used a constant 0.8m/s for the velocity, and produced various results based on different temperature profiles. Thus, the façade thermal simulation for Appendices A - Q is limited to 0.3m/s and 0.15m/s as per the Greenstar IEQ9 standard, although it does not consider different additional setpoints for the occupants will indeed require to meet their thermal comfort needs. In that respect, the PMV investigation is limited in helping one understand the effects of improving the HVAC system's thermal comfort and energy efficiency.

It was found along the NNW2 zone, and for clothing insulation of 0.6, as seen in figure 30 in February , the PMV closest to -0.5 is noted at -0.64 which corresponds to an AT of 24.36°C and MRT of 25.94°C. For clothing insulation of 0.95 , it was found that during February, the PMV closest to 0.5 is noted at 0.62 and the same temperatures are noted. When the results of this analysis is compared to that of Song et al. (2022) in figure 3, the -0.5 PMV corresponds to an AT of 24.7°C and MRT of 20.8°C, while the 0.5 PMV corresponds to an AT of 24.7°C and MRT of 28.2°C. In terms of AT, there is less than a 1.5°C temperature difference, and this points to accurate simulation results, for the MRT, however, there is approximately a 3°C difference, and this can be attributed to a variety of factors. The most important fact is that as Song et al. (2022) noted, AT & MRT should be as close as possible for a comfortable environment which is the case for the NNW2 zone in both clothing insulation simulations. This however, does not take into consideration the number of discomfort hours which is what thermal comfort acceptance is based on, this is why the entire year is assessed for a weighted average as done in chapter 4.1.3.2.

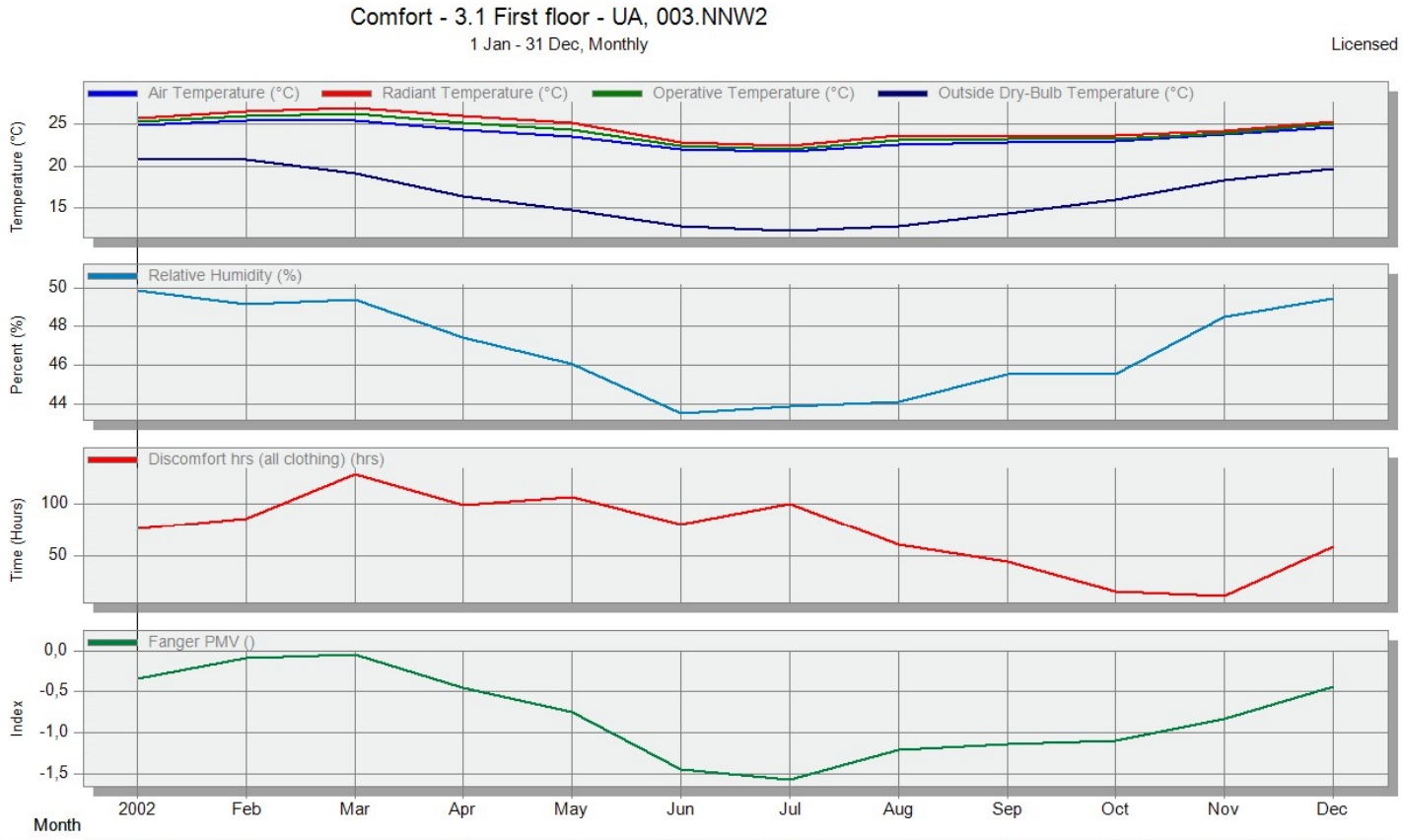

	2002	Feb	Mar	Apr	May	Jun	Jul	Aug	Sep	Oct	Nov	Dec
Air Temperature (°C)	24,92	25,46	25,44	24,36	23,60	22,06	21,69	22,54	22,88	22,98	23,78	24,69
Radiant Temperature (°C)	25,71	26,60	26,97	25,94	25,18	22,79	22,40	23,66	23,50	23,62	24,16	25,37
Operative Temperature (°C)	25,31	26,03	26,21	25,15	24,39	22,42	22,04	23,10	23,19	23,30	23,97	25,03
Outside Dry-Bulb Temperature (°C)	20,82	20,86	19,11	16,48	14,79	12,83	12,31	12,89	14,34	15,96	18,33	19,77
Relative Humidity (%)	49,87	49,14	49,39	47,45	46,06	43,49	43,87	44,12	45,53	45,54	48,47	49,48
Discomfort hrs (all clothing) (hrs)	75,33	85,50	127,83	99,00	106,00	80,50	99,83	60,50	44,33	16,67	11,83	58,17
Fanger PMV ()	-0,34	-0,09	-0,04	-0,45	-0,75	-1,44	-1,58	-1,21	-1,14	-1,11	-0,83	-0,44

Figure 30: *CLO60 NNW2 comfort simulation graphs (Appendix G)*

25,07

EnergyPlus Output

Comfort - 4.1 Second floor - UA, 003.NNW2

1 Jan - 31 Dec, Monthly

Licensed

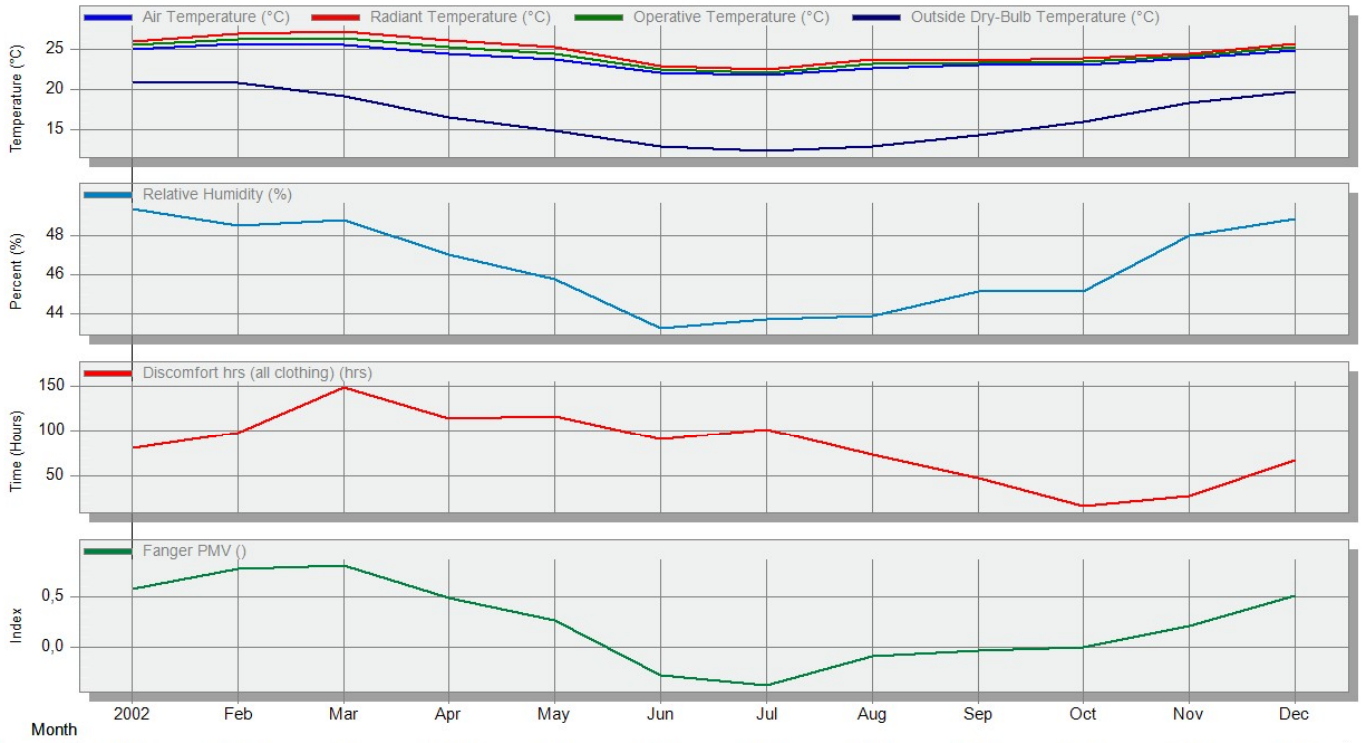

	2002	Feb	Mar	Apr	May	Jun	Jul	Aug	Sep	Oct	Nov	Dec
Air Temperature (°C)	25,07	25,67	25,65	24,51	23,71	22,15	21,75	22,64	23,02	23,12	23,93	24,88
Radiant Temperature (°C)	26,01	26,97	27,28	26,18	25,36	22,90	22,47	23,79	23,69	23,87	24,44	25,71
Operative Temperature (°C)	25,54	26,32	26,46	25,34	24,53	22,53	22,11	23,21	23,36	23,50	24,19	25,30
Outside Dry-Bulb Temperature (°C)	20,82	20,86	19,11	16,48	14,79	12,83	12,31	12,89	14,34	15,96	18,33	19,77
Relative Humidity (%)	49,39	48,50	48,81	47,04	45,78	43,27	43,72	43,89	45,19	45,15	48,00	48,89
Discomfort hrs (all clothing) (hrs)	80,50	97,17	148,33	114,00	116,17	90,83	100,83	73,50	47,00	16,33	27,00	67,17
Fanger PMV ()	0,58	0,78	0,82	0,49	0,27	-0,28	-0,38	-0,10	-0,04	-0,01	0,21	0,51

Figure 31: *CLO95 NNW2 comfort simulation graphs (Appendix G)*

The S1 zone notes the lowest TCA, and in this zone, it is observed that over a yearly period, the CLO60 Fanger PMV in figure 32 ranges between approximately 0 and -2.6 on the index chart, with the lowest level of comfort acceptance observed in between June and July, according to table 14 on the comfort scale, this amounts to over 85% predicted percentage dissatisfied of occupants in this zone in this period. Considering the PMV for the NNW2 zone, the shift in orientation to the sun angle has caused a significant loss of comfort for the occupants , and greater energy use is expected to cool down the S1 zone to an acceptable comfort level.

The discomfort hours notes that the amount of discomfort hours corresponds to 240 hours and this is approximately double the amount of time of discomfort when compared to the S1 zone, also the change in building orientation has increased the amount of time which the occupant feels comfortable. The relative humidity in figure 27 is modelled between 47% -54%, with the lowest in between October and December. The trendline is not similar compared to the Fanger index, which is unexpected as the humidity now peaks between March and May. This indicates the importance of zone control and arrangement of the thermostat is key to a functional HVAC design, and a poorly designed system would be highly inefficient to the energy efficiency

The temperatures banded together in the first graph of figure 27 are similar in trendline when compared to the NNW2 zone, but there are lower temperatures extremes in the June period noted for the S1 zone, thus the occupants would require additional cooling in the June period to maintain higher comfort temperature and reduce the amount of time discomfort is reported. Similar to the NNW2 zone, a higher low is reported on the discomfort index for the CLO95 insulation, but the trend is distributed more evenly between hot and cold discomfort than the CLO60 simulation, which produces colder temperature discomfort extremes.

It was found along the S1 zone and for a clothing insulation of 0.6 as seen in figure 31 in the month of February , the PMV closest to -0.5 is noted at -0.64 which corresponds to an AT of 24.26°C and MRT of 24.42°C. For a clothing insulation of 0.95 , it was found that during February the PMV closest to 0.5 is noted at 0.62 and the same temperatures are noted. When the results of this analysis is compared to that of Song et al. (2022) in figure 3, the -0.5 PMV corresponds to an AT of 24.7°C and MRT of 20.8°C, while the 0.5 PMV corresponds to an AT of 24.7°C and MRT of 28.2°C. In terms of AT, there is less than a 1.5°C temperature difference and this points to accurate simulation results, for the MRT however, there is approximately 4°C difference and this can be attributed to a variety of factors. AT & MRT for the S1 zone in both clothing insulation simulations are almost equal. Again this is not the the weighted average performance , which is assessed to provide a wholistic outview on thermal comfort.

25,25

EnergyPlus Output

Comfort - 4.1 Second floor - UA, 007.S1

1 Jan - 31 Dec, Monthly

Licensed

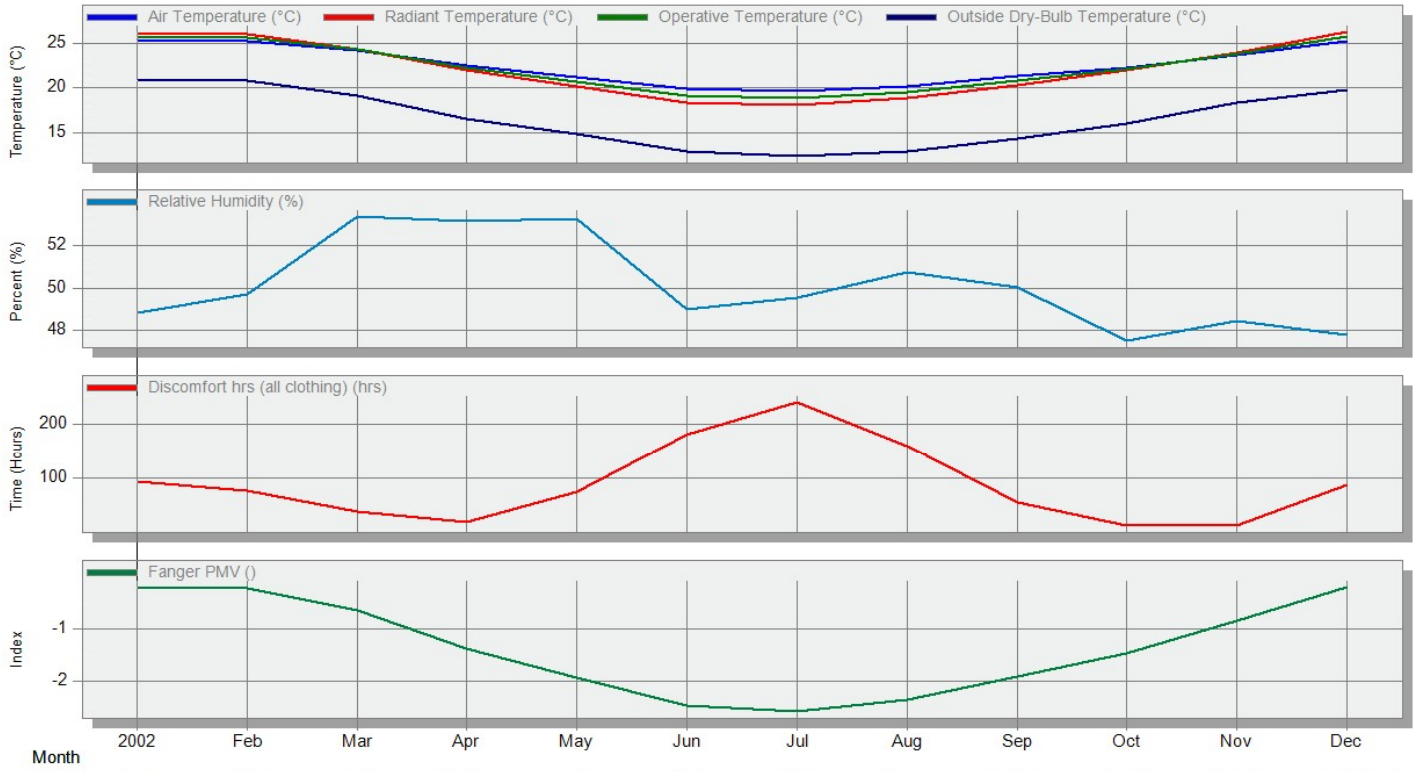

Air Temperature (°C)	25,25	25,27	24,26	22,55	21,22	19,94	19,61	20,18	21,31	22,33	23,77	25,26
Radiant Temperature (°C)	26,25	26,06	24,42	22,01	20,12	18,40	18,09	18,86	20,31	22,03	24,00	26,35
Operative Temperature (°C)	25,75	25,66	24,34	22,28	20,67	19,17	18,85	19,52	20,81	22,18	23,89	25,80
Outside Dry-Bulb Temperature (°C)	20,82	20,86	19,11	16,48	14,79	12,83	12,31	12,89	14,34	15,96	18,33	19,77
Relative Humidity (%)	48,85	49,74	53,40	53,20	53,29	49,00	49,53	50,78	50,04	47,51	48,45	47,80
Discomfort hrs (all clothing) (hrs)	93,67	77,17	38,00	20,33	75,50	180,17	240,67	159,17	55,83	13,17	13,17	87,67
Fanger PMV ()	-0,20	-0,21	-0,64	-1,37	-1,93	-2,47	-2,58	-2,35	-1,90	-1,45	-0,85	-0,19

Figure 32: *CLO60 S1 comfort simulation graphs (Appendix J)*

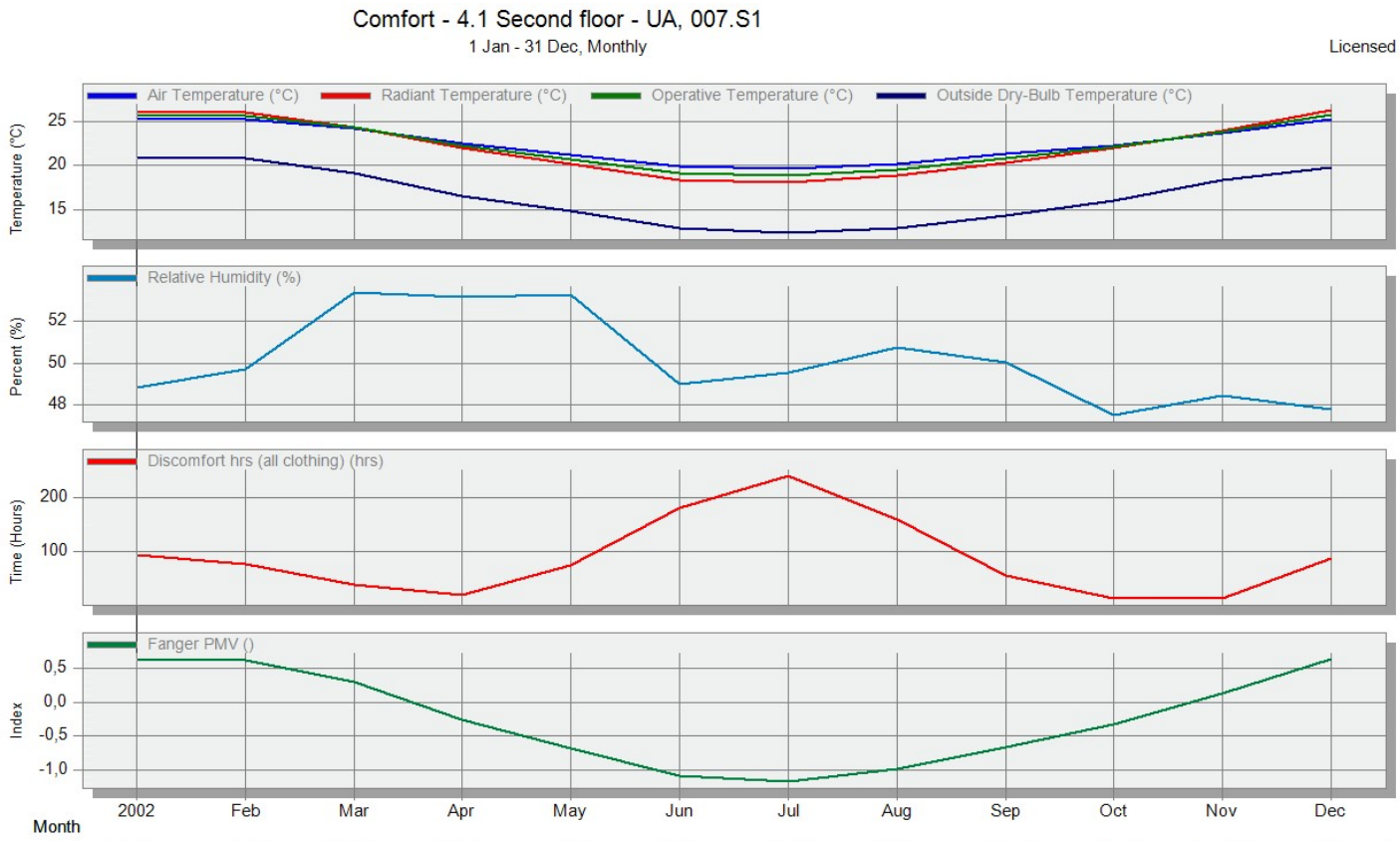

Month	2002	Feb	Mar	Apr	May	Jun	Jul	Aug	Sep	Oct	Nov	Dec
Air Temperature (°C)	25,25	25,27	24,26	22,55	21,22	19,94	19,61	20,18	21,31	22,33	23,77	25,26
Radiant Temperature (°C)	26,25	26,06	24,42	22,01	20,12	18,40	18,09	18,86	20,31	22,03	24,00	26,35
Operative Temperature (°C)	25,75	25,66	24,34	22,28	20,67	19,17	18,85	19,52	20,81	22,18	23,89	25,80
Outside Dry-Bulb Temperature (°C)	20,82	20,86	19,11	16,48	14,79	12,83	12,31	12,89	14,34	15,96	18,33	19,77
Relative Humidity (%)	48,85	49,74	53,40	53,20	53,29	49,00	49,53	50,78	50,04	47,51	48,45	47,80
Discomfort hrs (all clothing) (hrs)	93,67	77,17	38,00	20,33	75,50	180,17	240,67	159,17	55,83	13,17	13,17	87,67
Fanger PMV ()	0,63	0,62	0,30	-0,25	-0,68	-1,09	-1,17	-0,99	-0,66	-0,32	0,13	0,64

Figure 33: *CLO95 S1 comfort simulation graphs (Appendix J)*

4.1.3.2 Weighted average & PMV simulation for a 10% & 25% PPD

The Green Star SA technical standard requires at least 98% of occupants to be within the -0.5 to 0.5 index range for the best overall thermal comfort performance. The second-best result would be if 98% PMV levels could be maintained between -1 to 1 for the occupied hours. The weighted average is used to determine the acceptable levels of discomfort hours according to the combined zones simulated PMV values for each hour of a year. These hours are carefully sorted into a 10% and 25% predicted percentage dissatisfied array as a weighted average.

It is observed in figure 34, which has been derived from appendix Q, that a CLO60 simulation produces an average of 77.84% of weighted hours outside the range of -0.5 to 0.5 or 10% PPD. This means that the majority of hours which 10% of occupants, will feel highly uncomfortable. It is expected that there would be significantly increased energy usage to raise the temperature to comfortable levels. The weighted hours for the 25% or -1 to 1 index levels indicate that 46.88% of the hours are observed outside the acceptable range and unacceptable on the comfort scale. The CLO95 simulation in figure 35 derived from appendix Q, yielded much better results in both the 10% and 25% index scale. Although still not acceptable for good comfort conditions, it was observed that for the -0.5 to 0.5 PMV range, the weighted average was simulated at 54.27%, a 30% reduction in dissatisfaction hours. The -1 to 1 PMV range was reduced to 17.18%, a significant reduction of 63% in the average weighted hours.

Kusaik et al. (2014) have developed a data-driven approach to ensure energy performance increases by 20.15% and maintains satisfactory thermal comfort. The various zones inside an office space also affect the PMV and discomfort hours, as shown by Mochinda et al. (2005), where internal features caused increased turbulence, decreasing the discomfort hours for areas where thermal comfort is of critical importance. Using a CFD analysis would be required to increase air movement and reduce dead spots, which will require additional cooling capacity and further decrease energy efficiency. Another method proposed by Wang et al. (2017) has indicated the importance of combining novel indoor positioning CO_2 occupancy sensors with data-driven occupancy schedules. This is an effort to remove instances of overcooling and fine-tune the HVAC system performance to decrease operational hours in areas. A 20% energy saving was observed in an actual office with improved thermal comfort conditions, and this study needs to investigate these effects in further research.

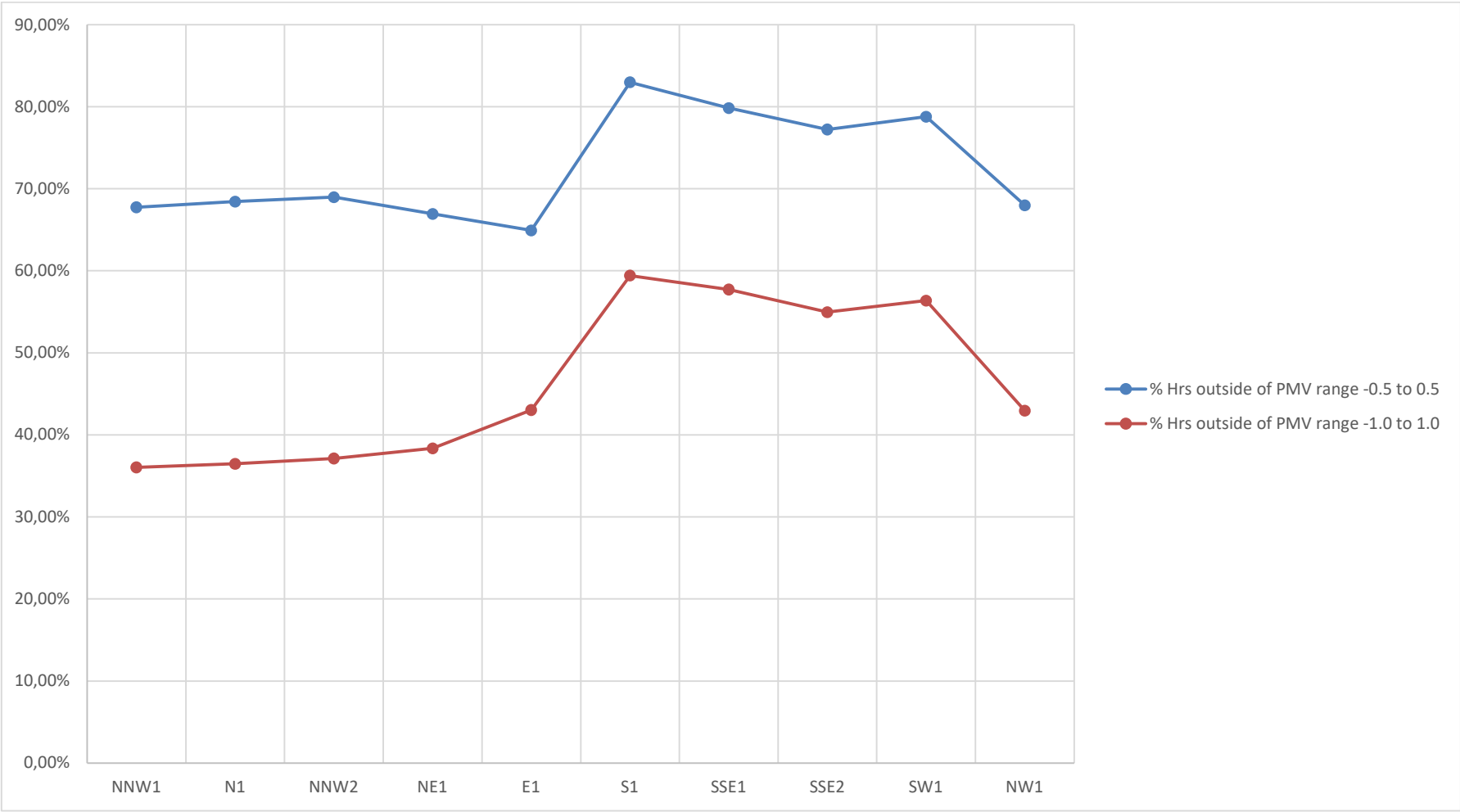

Figure 34: *PMV weighted average results for CLO60*

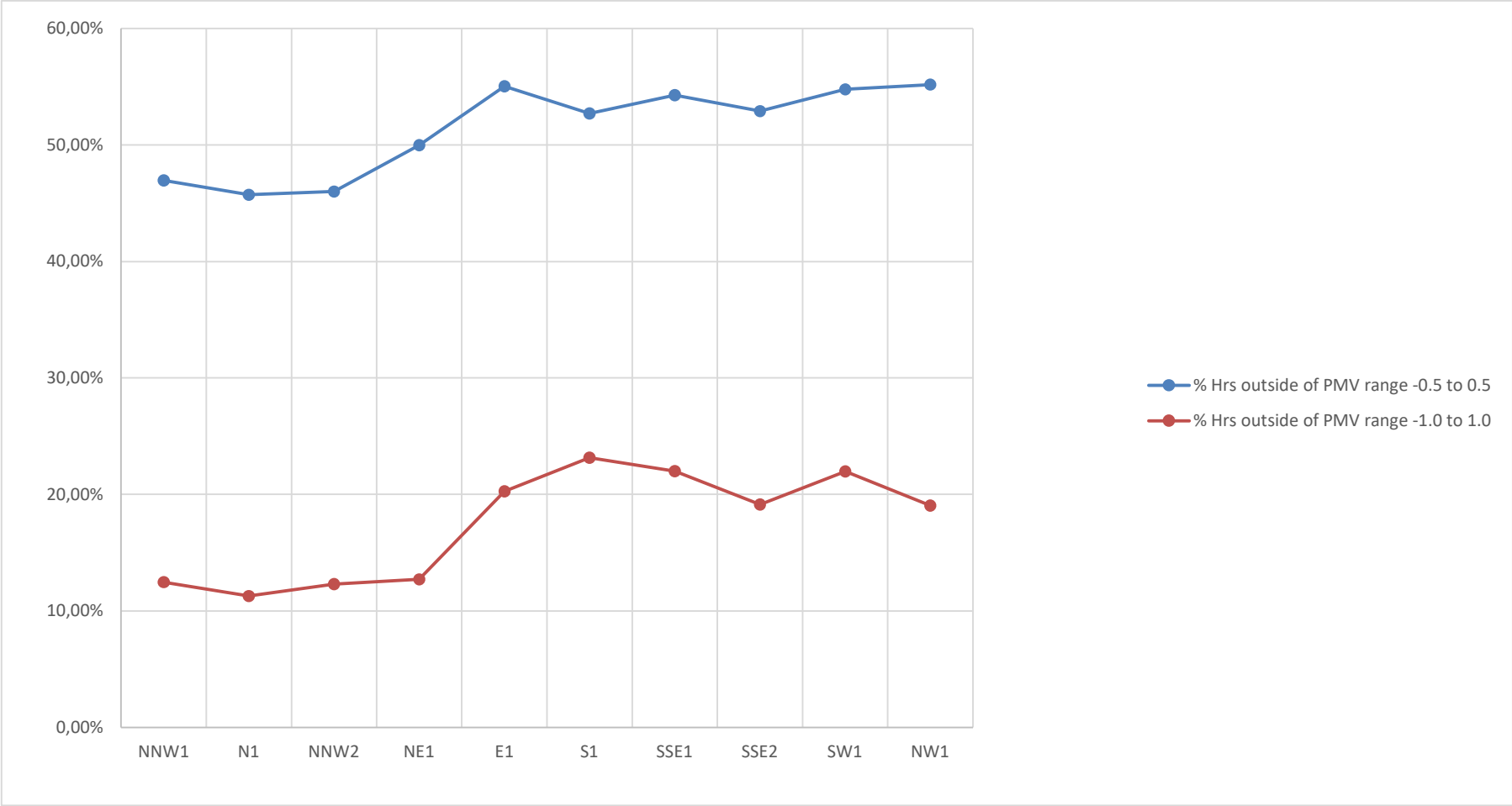

Figure 35: *PMV weighted average results for CLO95*

CHAPTER-5 : CONCLUSIONS & RECOMMENDATIONS

5.1 Conclusions and recommendations

The main aim of this thesis was to understand the difference in the performance of four glazing types in a parametric façade using thermal modelling simulation tools. The various sub-disciplines of building physics in a façade analysis was also a key aspect of this research to understand how they each play a role in an overheating thermal analysis. These were classified into the following three categories:

a) A Peak simulation load & glazing performance analysis of a parametric façade
b) The Sustainable design Optimisation of a building architectural design for improved energy performance
c) Perform a thermal comfort analysis to understand the importance of psychrometric charts.

5.1.1 Peak simulation load & glazing performance analysis

Thermal modelling was done for four glazing types: Clear, NC60E, NC55E & NC52. The purpose was to identify the best performing glazing type for the Capitec head office in Stellenbosch that could ensure a HVAC design threshold of 180W/ m² could be adhered to sizing a smaller HVAC design for the building.

It was observed that clear glazing on its own presented the worst-case scenario for a building with a large glazing area. The external solar heat gain is borderline close to the sensible heat gain and total cooling load, and this indicates that the surface of the glass absorbs the majority of solar radiation, which entails higher internal temperatures and needs more cooling capacity reducing, considerably energy efficiency.

NC60E is a low emissivity performance glazing and, based on the results, has performed exceptionally well by ensuring that not only is the design threshold adhered to in all zone, but the external solar heat gains have been reduced by approximately 45% if not more. The internal temperatures were lower as expected, and a change in peak zone times were observed in some zones, which will affect the HVAC design in terms of the zone thermostat and perhaps the number of fan coil units and, in turn, the energy efficiency.

NC55E is a better performance low emissivity glazing and, based on the results, has performed better than all the other glazing types. Not only is the design threshold adhered to in all zones, but the external solar heat gains have been reduced by approximately 58%. The internal temperatures were much lower when compared to clear glazing, and a change in peak zone

times was observed in some zones. Compared to the NC60E glazing, the performance results were very close however, there was a considerable reduction in external solar gain. If low emissivity were the only option, NC60E would be sufficient, and NC50E would benefit from the glazing area that would suit a high rise building façade where the additional cost could be offset by saving on additional HVAC plant room sizing.

NC52 is much better performance glazing, and alternative to low emissivity as NC52 performed much better than clear glazing, there was an 11% performance improvement on the total cooling load in the peak zone along the façade. The majority of the north zone were either above or at the peak design threshold, even though up to 46% improvement in the internal and external solar heat gains were observed. Internal temperatures were slightly lower than clear glazing as the performance glazing reduced the thermal gains.

The analysis was a complex thermal analysis however, when compared to other literature, many limitations and variables have not been adopted into the study, such as zone control and adaptive occupancy scheduling. The zones need to be checked against the predicted model results as discrepancies of up to 40% are observed in some studies where measurement and verification were done. For HVAC design, the final load analysis summarised below was sufficient to design an HVAC plant with an appropriate safety factor.

5.1.2 Sustainable design Optimisation for improved energy performance

The results in the glazing comparison identified the peak glazing performance values concerning the design threshold 180W/ m², NC52 was selected as the glazing type by the client as passive architecture, and a parametric façade would prove helpful in reducing the peak results below this design threshold. Two separate analyses were carried out, including a façade design with external shading devices, and a second simulation was done with a green roof component modelled as an additional resistance in the thermal roof makeup.

The shading component added to the façade resulted in considerable performance improvements in every aspect of the thermal results. The total peak load in the peak zone, when compared to NC52 glazing without shading, resulted in a 23.7% decrease in cooling load requirements and up to 30.1% improvement in the external solar gains, along with this, a 10.7% decrease in radiant temperature was noted which means the air conditioning unit reaches the set point much faster and uses less energy from the chilled water plant.

The green roof in this instance resulted in minor performance improvements in selected variables of the thermal results. The total peak load in the peak zone, when compared to NC52

glazing with shading, resulted in a 2.6% decrease in cooling load requirements and up to 20.1% improvement in the external solar gains, along with this, a 3.5% increase in radiant temperature was noted. Retention of heat means that inside the space, the air conditioning unit works slightly harder and reaches the set point much slower and uses more energy from the chilled water plant. The results are not uniform as each zone now has a more complex thermal external roof component, and a green roof acts as in a passive cooling capacity and thus requires careful consideration as to the effects on thermal vs the reduction in cooling capacity. The total improvement in energy performance is noted at approximately 74.5% from clear glazing to a fully optimised building structure with shading and NC52 glazed parametric façade.

When comparing the results to other literature, the green roof does not perform as expected as 75% performance gains are noted where studies combine night ventilation and more complex green materials with better resistance values. In this respect, the analysis was fundamental and required a more detailed approach to better green roof material and placement of the various types of trees and objects. This could then lead to the involvement of CFD analysis, which would provide more information on external wind velocities and thermal heat gains, and surface temperature profiles could provide a more accurate result.

In essence, the addition of a green roof was not implemented in this project as the majority of the roof are required for the services plant room area, however, we learned that green roofs or any objects placed on a roof provide insulation and that insulation can benefit in some instances and also work against the goal of improving energy efficiency in the long run.

5.1.3 Thermal comfort analysis

The thermal comfort analysis was done only to understand the fundamental aspects of comfort studies. The results obtained provide the reader with the necessary tools to understand that analysing comfort in a zone is a deeply misunderstood subject. Simply guessing whether a system would perform according to the expectations of what it was designed for is not as easy as turning the knob on a remote thermostat.

In this study, the thermal comfort results were unsatisfactory under Green Star and ASHRAE recommendations. It proves that comfort can only be designed statistically in the hope that spatial planning, occupancy densities, and scheduling are considered. Noting that it can only be substantiated through measurement and verification to improve trial and error iterations for acceptability even if done correctly.

Thermal comfort calculated to the Fanger PMV index was analysed as to the weighted average of hours outside the acceptable limits of a 10% and 25% acceptability limit, the Green star guideline which references ASHRAE literature, which requires that 98% of hours are inside the limits for either a $-0.5 < PMV < 0.5$ or $-1 < PMV < 1$ respectively. These hours were simulated for each zone using CLO60 and CLO95 insulation values, representing the winter and summer clothes, respectively, and the best and worst zone were analysed.

The NNW2 zone with a CLO60 was found to have a 50% predicted percentage of dissatisfaction in June to July period, with the lowest level of thermal comfort observed in this time. The variation in discomfort hours also helps one understand that time of discomfort is not determined by a higher discomfort index. The relative humidity in the space seems to follow the same trendline in this instance, and this makes sense as humidity is a significant factor in both comfort and health issues inside residential spaces.

Internal temperatures are closely banded together in a smooth trendline and indicate that temperature is maintained as closely as possible to the required set point. The NNW2 zone with a CLO95 was found to have the same performance as a CLO60, but the Fanger index produced more positive values, which means temperatures were still uncomfortable in some instances. Still, the discomfort was felt for higher temperatures, whereas a CLO60 simulation mainly reports data on colder extremes.

The S1 zone with a CLO60 was found to have an average of 85% predicted percentage of dissatisfaction in June to July period, with the lowest level of thermal comfort observed in this time, and the discomfort hours have more than doubled concerning the NNW2 zone. The relative humidity in the space notes the same trendline in this instance, and now it peaks between Mach – May. The scattering of data means humidity level seems to scatter away from the times in other zones, which means more complicated zone control issues during the design phase and possibly an increase in energy utilisation.

Internal temperatures are still closely banded together in a smooth trendline, indicating that temperature is maintained as closely as possible to the required set point. However, there are lower internal temperatures, and additional cooling might be required in June if higher comfort temperatures are maintained. The CLO95 simulation changes the discomfort levels to higher lowers and a more evenly distributed Fanger index.

The weighted average analysis analysed all the hours of a CLO60 and CLO95 simulation in each zone over a year. A CLO60 simulation with NC52 glazing, including a parametric façade

with reduced glazing area, external shading devices and a green roof, resulted in 77.84 % of weighted average hours outside a 10% PPD and 46.88 % of weighted average hours outside a 25% PPD. A CLO95 simulation with NC52 glazing, including a parametric façade with reduced glazing area, external shading devices and a green roof, resulted in 54.27 % of weighted average hours outside a 10% PPD and 17.18 % of weighted average hours outside a 25% PPD.

The CLO60 results are highly unacceptable to any standard of thermal comfort, however, it needs to be noted that an entire year was simulated, and different occupancy schedules will produce different results. Even though the CLO95 simulation produced better results, the building physics based improvements need to be considered on a broader spectrum. The following has not been considered in this analysis:

- CO_2 zone control sensors
- Computational fluid dynamic based velocities and temperatures,
- Adaptive comfort scheduling,
- Increasing supply air airflow velocities,
- Night ventilation,
- Spatial arrangement through CFD analysis
- Data-driven based energy improvement models.

These considerations above are all critical to ensuring that an HVAC system can be designed correctly and respond to the thermal comfort requirements of the occupants in multi-space and multi-zone applications. The HVAC system is expected to utilise energy closer to the upper band of the design threshold as the Stellenbosch region is hot and uncomfortable. Ensuring acceptable thermal comfort in this space would mean higher flow rates of chilled water usage.

The limitations of this study, as mentioned above, is that the analysis requires a CFD study and data-driven approach across the energy spectrum of the building services of the facility. In addition to a measurement and verification over a certain period, this is the only way to gauge the true impact of solar heat gains on the internal temperatures, along with the actual utilisation of the chiller plant for a specific zone.

For theoretical analysis, it would be of further benefit to do a detailed analysis of how much additional TCA capacity is required to meet the 10% PPD GreenStar acceptable thermal comfort levels. Similarly, a CFD study would further provide more information on what airflow velocities might be required by the fan coil unit to ensure a 10% PPD can be achieved.

BIBLIOGRAPHY

AHLEM, Z., ZILI-GHEDIRA, L. & BEN NASRALLAH, S. 2015 Desiccant-based dehumidification and direct/indirect evaporative cooling technologies. *IREC2015 The Sixth International Renewable Energy Congress*,6, 1-6.

AL-BADRI, A.R. & AL-WAALY, A.A.Y. 2017 The influence of chilled water on the performance of direct evaporative cooling. *Energy and Buildings*, 155, 143-150.

AL TOUMA, A. & OUHRANI,,D. Experimental analysis of double and triple glazed façades with different shading devices in Qatar. 2017 *2nd International Conference Sustainable and Renewable Energy Engineering (ICSREE)* , 38-41.

ANDERSON, K. 2014b *Design energy simulation for architects: a guide to 3D graphics*. London, Routledge.

ASHRAE. 2013a *2013 ASHRAE handbook*. Atlanta, ASHRAE.

ASHRAE. 2015a *2015 ASHRAE handbook: heating, ventilating, and air-conditioning applications*. Atlanta, ASHRAE.

ASHRAE. 2016 *2016 ASHRAE handbook: heating, ventilating, and air-conditioning systems and equipment*. Atlanta , ASHRAE.

ASHRAE. 2013b *District cooling guide*. Atlanta, ASHRAE.

ASHRAE. 2013c *District heating guide*. Atlanta, ASHRAE.

ASHRAE. 2015c *Thermal guidelines for data processing environments*. Atlanta,ASHRAE.

ASHRAE. 2013e *UFAD guide design, construction, and operation of underfloor air distribution systems*. Atlanta, ASHRAE.

AFRAM, A. & SHARIFI, F. 2014 Review of modelling methods for HVAC systems, *Applied Thermal Engineering*, 67(1-2), 507-519.

ALIAHMADIPOUR, M., ABDOLZADEH, M. & LARI, K. 2017 Airflow simulation of HVAC system in a compartment of a passenger coach, *Applied Thermal Engineering*, 123,973-990.

BHASKORO, P.T., UL HAQ GILANI, S.I. & ARIS, M.S., 2013, Simulation of energy-saving potential of a centralized HVAC system in an academic building using an adaptive cooling technique, *Energy Conversion and Management*, 75 617-628.

BURATTI, C., PALLADINO, D., MORETTI, E. & DI PALMA, R. 2018 Development and

Optimisation of a new ventilated brick wall: CFD analysis and experimental validation, *Energy and Buildings*, 168, 284-297.

CAPITEC. 2021. From 25 000 to 15 million clients: 20 years of capitec. [ONLINE] Available at: https://www.capitecbank.co.za/bank-better-live better/articles/ experiences/from-25-000-to-15-million-clients-20-years-of-capitec/.

ÇENGEL, Y. A. & CIMBALA, J. M. 2006 *Fluid mechanics: fundamentals and applications*. Boston, McGraw-Hill Higher Education.

ÇENGEL, Y. A., TURNER, R. H. & CIMBALA, J. M. 2008 *Fundamentals of thermal-fluid sciences*. Boston, McGraw-Hill Education.

ÇENGEL, Y. A., & BOLES, M. A. 2001 *Thermodynamics: an engineering approach*. Boston, McGraw-Hill Higher Education.

ÇENGEL, Y. A. 2007 *Heat and mass transfer: a practical approach*. Boston, McGraw-Hill.

COLOMBO, E., ZWAHLEN, M., FREY, M., & JOHANN, L. 2017, Design of a glazed double-façade by means of coupled CFD and building performance simulation, *Energy Procedia*, 122, 355-360.

CG. 2021. Composition of commercial glass. [ONLINE] Available at: https://compassglass.co.za/technical/. [Accessed 1 May 2021].

DAMIAN, A., FILIP, R-G., CATALINA, R., FRUNZULICA, R. & NOTTO, G. *2020* The influence of solar-shading systems on an office building cooling load. *2020 7th International Conference on Energy Efficiency and Agricultural Engineering (EE&AE)*, 1-4.

DE ANTONELLIS, S., JOPPOLO, C.M., LEONE, C., LIBERATI, P. & MILANI, S. 2017, Indirect evaporative cooling systems: an experimental analysis in summer condition, *Energy Procedia*, 140, 467-474.

DESIGNBUILDER. 2021 DesignBuilder product overview. [ONLINE] Available at: https://www.designbuilder.co.uk/. [Accessed 1 May 2021].

ETHERIDGE, D. 2012 *Natural ventilation of buildings: theory, measurement and design*. Chichester, West Sussex, Wiley.

GBCSA. 2010 *Technical manual green star SA office design & office as built*. *1,1*. South Africa, GBCSA.

GRONDZIK, G. 2007 *Air-Conditioning System Design Manual*. Elsevier Science.

GARG, V., MATHUR, J., TATALI, S., & BHATIA, A. 2017 *Building energy simulation: a workbook using DesignBuilder.* Boca Raton, CRC Press.

HAW, L. C., SAADATIAN, O., BAHARUDDIN, A. H., MAT, S., SULAIMAN, M. Y., & HWANG, RH. & AN CHEN, W., 2022 *Creating glazed facades performance map based on energy and thermal comfort perspective for office building design strategies in Asian hot-humid climate zone.* Applied Energy, 311.

HOWELL, R. H., COAD, W. J. & SAUER, H. J. 2013 *Principles of heating ventilating and air conditioning, 7th edition*. Atlanta, ASHRAE.

JIANG, L. & TANG. M., 2017.Thermal analysis of extensive green roofs combined with night ventilation for space cooling, Energy and Buildings, 156, 238-249.

KOTSIRIS, G., ANDROUTSOPOULOS, A., POLYCHRONI, E., NEKTARIOS, P.A. 2012 Dynamic U-value estimation and energy simulation for green roofs, *Energy and Buildings, 45, 240-249.*

KUSIAK, A., XU, G., ZHANG, Z. 2014 Minimization of energy consumption in HVAC systems with data-driven models and an interior-point method, *Energy Conversion and Management*, 85, 146-153.

LOMBARD, L.P., ORTIZ, MAESTRE, I.R., 2011, The map of energy flow in HVAC systems, *Applied Energy*, 88(12),, 5020-5031.

MA. J. & GAO, Y.,2010, "Study on the radiant cooling system with Water Flow on Roof, *2010 International Conference on Mechanic Automation and Control Engineering*, 1,1940-1943.

MOCHIDA, A., YOSHINO, H., TAKEDA, T., KAKEGAWA, T., MIYAUCHI, S., 2005 Methods for controlling airflow in and around a building under cross-ventilation to improve indoor thermal comfort, *Journal of Wind Engineering and Industrial Aerodynamics*, 93, 6.

MCDOWALL, R., & MONTGOMERY, R. 2011 *Fundamentals of HVAC control systems*. Atlanta, ASHRAE.

NICOL, F. 2013 *The limits of thermal comfort: avoiding overheating in European buildings*. London, CIBSE.

RAN, J.& TANG. M. 2017 Effect of Green Roofs Combined with Ventilation on Indoor Cooling and Energy Consumption, *4th International Conference on Power and Energy Systems Engineering*, 4, 25-29

SANS.2010a *The application of the National Building Regulations Part O: Lighting and ventilation,* 4,1 Pretoria, SABS.

SANS. 2010b.Energy efficiency in buildings SANS 204: *Energy use in buildings* 1, Pretoria, SABS.

SANTAMOURIS, M. 2008 *Advances in passive cooling*. London, Earthscan.

SEO, J., OOKA, R., KIM, J.T. & NAM, Y., 2014 Optimisation of the HVAC system design to minimize primary energy demand, *Energy and Buildings*, 76, 102-108.

SIMMONDS, P. 2015 *ASHRAE design guide for tall, supertall, and megatall building systems*. Atlanta, ASHRAE.

SONG, B., BAI, A. & YANG, L. *2020* *Analysis of the long term effects of solar radiation on the indoor thermal comfort in office buildings*. Energy, 247.

SPLITLER, J. D. 2014 *Load calculation applications manual*. Atlanta, ASHRAE.

TRČKA, M. &HENSEN, J.L.M., 2010, Overview of HVAC system simulation, *Automation in Construction*, 19(2), 93-99.

UNDERWOOD, C. & YIK, F. 2008 *Modelling Methods for Energy in Buildings*. John Wiley & Sons.

WOOD, A., SALIB, R. 2017 *Guide to natural ventilation in high rise office buildings*. New York, Routledge.

WANG, W., CHEN, J., HUANG, G.& LU, Y. 2017 Energy-efficient HVAC control for an IPS-enabled large space in commercial buildings through dynamic spatial occupancy distribution, *Applied Energy*, 207, 305-323.

YOUSSEF, A.A., MINA, E.M., ELBAZ, A.R., ABDEL MESSIH, R.N. 2017 Studying comfort in a room with cold air system using computational fluid dynamics, *Ain Shams Engineering Journal*.

ZHANG, Y., KACIRA, M., & LING, L. 2016 A CFD study on improving airflow uniformity in the indoor plant factory system, *Biosystems Engineering*, 147, 193-205.

APPENDIX A - *Capitec Bank first floor layout*

APPENDIX B – *GBCSA schedules for thermal model*

Schedule:Compact,

ZA-GBCSA Office_Occ,

Fraction,

Through: 31 Dec,

For: Weekdays SummerDesignDay WinterDesignDay,

Until: 07:00, 0,

Until: 08:00, 0.15,

Until: 09:00, 0.60,

Until: 17:00, 1,

Until: 18:00, 0.5,

Until: 19:00, 0.15,

Until:21:00, 0.05,

Until: 24:00, 0,

For: Saturday,

Until: 08:00, 0,

Until: 17:00, 0.05,

Until: 24:00, 0,

For: Sunday Holidays AllOtherDays,

Until: 08:00, 0,

Until: 17:00, 0.05,

Until: 24:00, 0;

APPENDIX C – *Site simulation data*

20,82

EnergyPlus Output

Site Data - 3.1 First floor - UA, 001.NNW1

1 Jan - 31 Dec, Monthly

Licensed

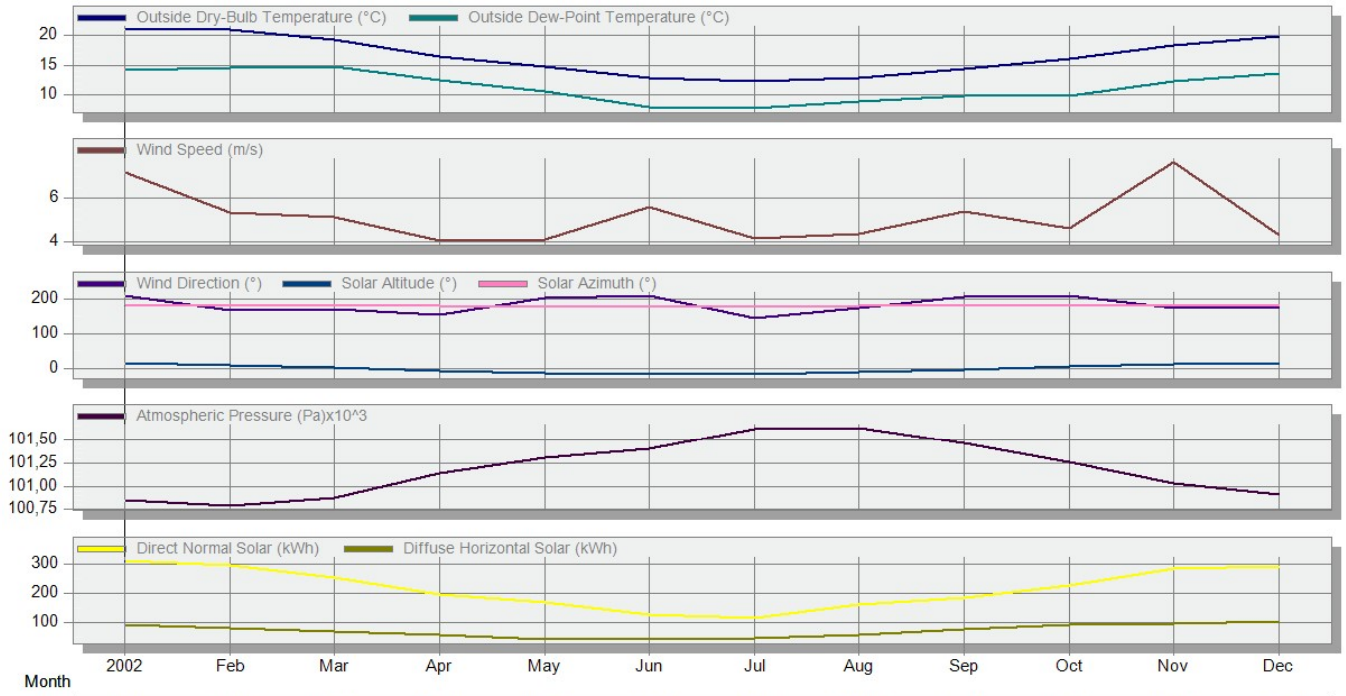

Outside Dry-Bulb Temperature (°C)	20,82	20,86	19,11	16,48	14,79	12,83	12,31	12,89	14,34	15,96	18,33	19,77
Outside Dew-Point Temperature (°C)	14,10	14,55	14,82	12,45	10,68	8,09	7,86	8,92	9,81	9,93	12,23	13,60
Wind Speed (m/s)	7,19	5,35	5,13	4,04	4,10	5,60	4,16	4,34	5,40	4,59	7,67	4,28
Wind Direction (°)	208,22	167,59	169,32	154,65	201,67	208,30	146,42	174,14	205,93	209,54	173,01	173,97
Solar Altitude (°)	14,89	9,41	1,47	-6,97	-13,44	-16,39	-15,18	-10,01	-2,25	6,22	13,10	16,37
Solar Azimuth (°)	179,69	180,44	179,14	179,56	178,46	178,92	178,07	178,92	179,53	179,65	179,88	179,86
Atmospheric Pressure (Pa)x10^3	100,85	100,79	100,88	101,14	101,31	101,41	101,62	101,63	101,47	101,26	101,03	100,91
Direct Normal Solar (kWh)	312,96	297,66	255,49	197,53	170,31	128,71	117,59	164,08	187,39	227,06	286,22	294,23
Diffuse Horizontal Solar (kWh)	91,52	82,61	69,21	58,69	43,98	42,62	47,56	56,43	76,84	94,19	97,02	102,65

APPENDIX D – *CLO-0.60 & CLO-0.95 NNW1*

CLO 0.60

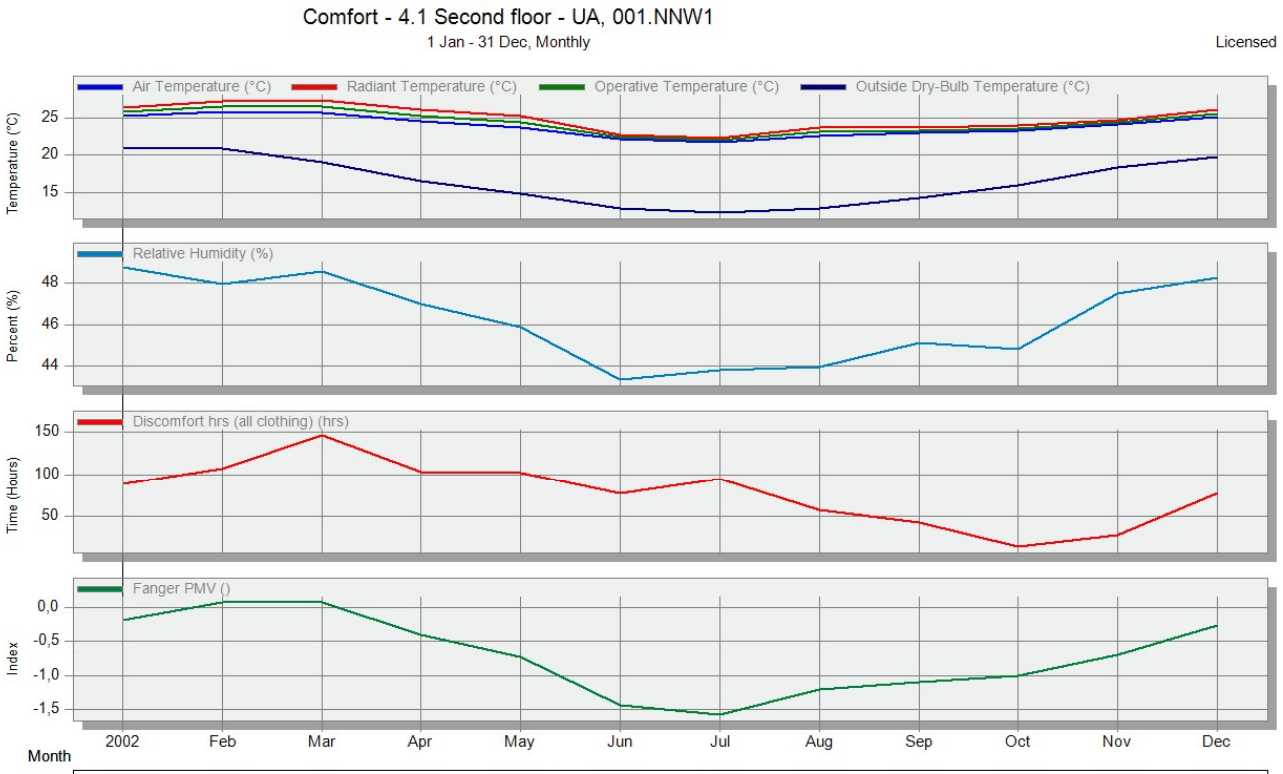

Air Temperature (°C)	25,27	25,86	25,73	24,51	23,67	22,12	21,73	22,61	23,04	23,24	24,10	25,10
Radiant Temperature (°C)	26,32	27,25	27,37	26,10	25,20	22,75	22,33	23,65	23,65	24,00	24,68	26,05
Operative Temperature (°C)	25,80	26,56	26,55	25,30	24,43	22,43	22,03	23,13	23,34	23,62	24,39	25,57
Outside Dry-Bulb Temperature (°C)	20,82	20,86	19,11	16,48	14,79	12,83	12,31	12,89	14,34	15,96	18,33	19,77
Relative Humidity (%)	48,78	47,96	48,55	47,01	45,86	43,32	43,76	43,93	45,11	44,82	47,50	48,25
Discomfort hrs (all clothing) (hrs)	88,33	107,00	146,17	102,83	102,50	77,17	94,33	57,83	43,50	14,83	28,83	77,50
Fanger PMV ()	-0,18	0,08	0,07	-0,40	-0,73	-1,44	-1,58	-1,20	-1,09	-1,00	-0,69	-0,26

CLO 0.95

25,27

EnergyPlus Output

Comfort - 4.1 Second floor - UA, 001.NNW1

1 Jan - 31 Dec, Monthly

Licensed

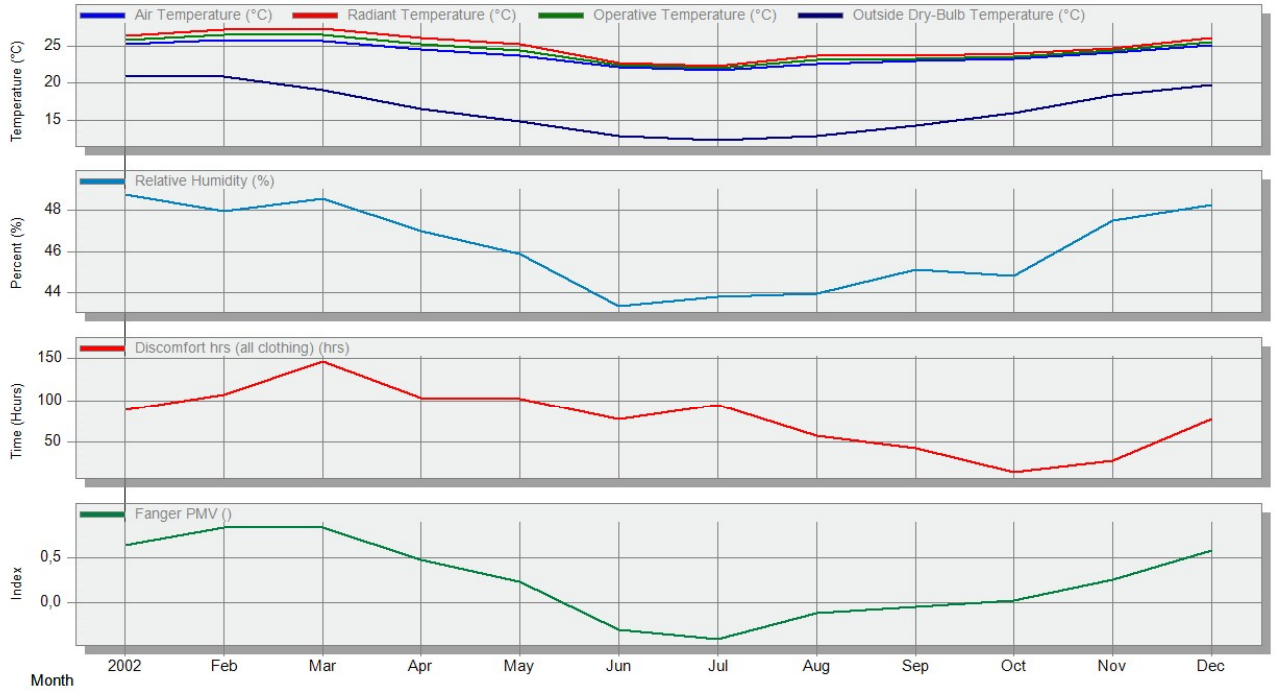

	2002	Feb	Mar	Apr	May	Jun	Jul	Aug	Sep	Oct	Nov	Dec
Air Temperature (°C)	25,27	25,86	25,73	24,51	23,67	22,12	21,73	22,61	23,04	23,24	24,10	25,10
Radiant Temperature (°C)	26,32	27,25	27,37	26,10	25,20	22,75	22,33	23,65	23,65	24,00	24,68	26,05
Operative Temperature (°C)	25,80	26,56	26,55	25,30	24,43	22,43	22,03	23,13	23,34	23,62	24,39	25,57
Outside Dry-Bulb Temperature (°C)	20,82	20,86	19,11	16,48	14,79	12,83	12,31	12,89	14,34	15,96	18,33	19,77
Relative Humidity (%)	48,78	47,96	48,55	47,01	45,86	43,32	43,76	43,93	45,11	44,82	47,50	48,25
Discomfort hrs (all clothing) (hrs)	88,33	107,00	146,17	102,83	102,50	77,17	94,33	57,83	43,50	14,83	28,83	77,50
Fanger PMV ()	0,64	0,84	0,84	0,48	0,24	-0,30	-0,40	-0,12	-0,04	0,02	0,26	0,58

APPENDIX E – *CLO-0.60 & CLO-0.95 N1*

CLO 0.60

25,03

EnergyPlus Output

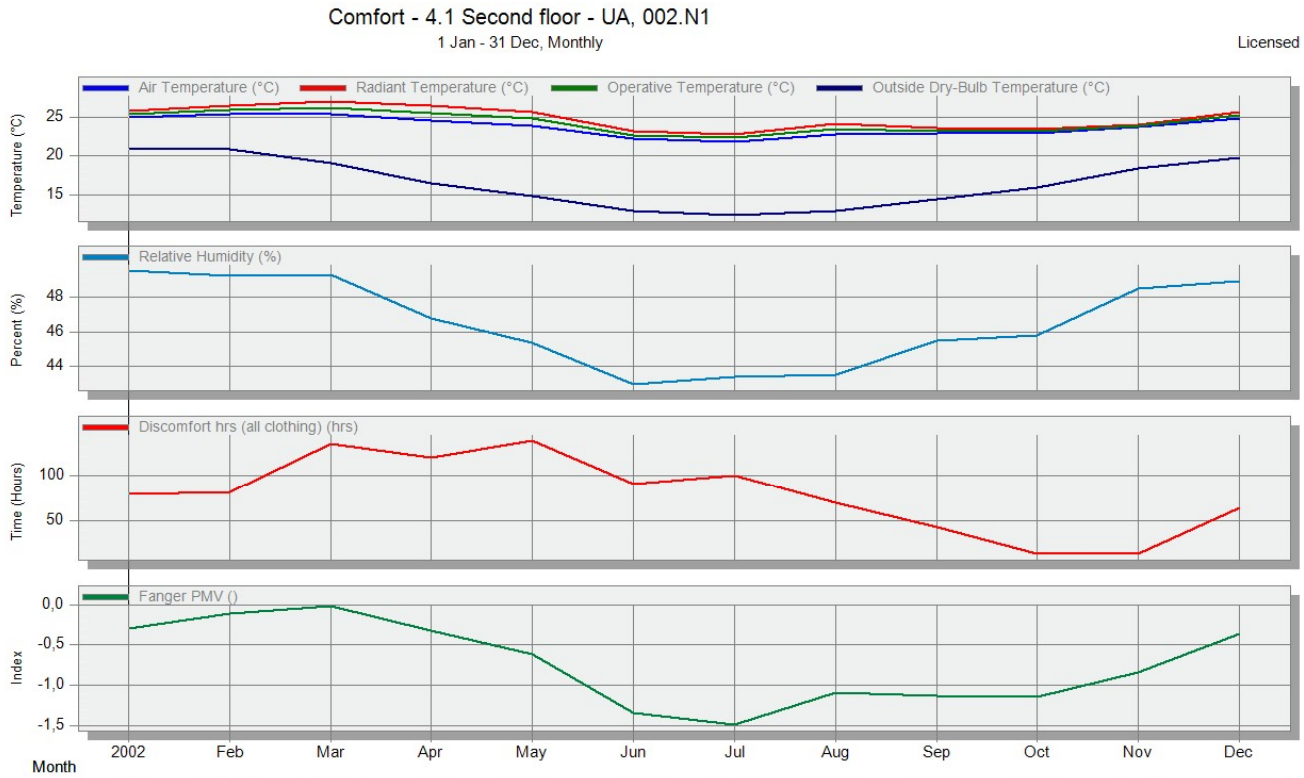

Air Temperature (°C)	25,03	25,44	25,49	24,59	23,87	22,28	21,89	22,78	22,90	22,91	23,77	24,88
Radiant Temperature (°C)	25,84	26,49	27,09	26,52	25,76	23,16	22,76	24,15	23,57	23,45	24,03	25,63
Operative Temperature (°C)	25,44	25,96	26,29	25,55	24,81	22,72	22,32	23,46	23,23	23,18	23,90	25,25
Outside Dry-Bulb Temperature (°C)	20,82	20,86	19,11	16,48	14,79	12,83	12,31	12,89	14,34	15,96	18,33	19,77
Relative Humidity (%)	49,55	49,22	49,28	46,78	45,35	42,96	43,40	43,53	45,47	45,77	48,49	48,94
Discomfort hrs (all clothing) (hrs)	79,00	80,67	134,33	119,17	137,50	90,00	99,00	69,83	43,00	14,33	14,50	63,50
Fanger PMV ()	-0,30	-0,11	-0,02	-0,33	-0,61	-1,35	-1,48	-1,09	-1,13	-1,14	-0,84	-0,37

CLO 0.95

25,03

EnergyPlus Output

Comfort - 4.1 Second floor - UA, 002.N1

1 Jan - 31 Dec, Monthly

Licensed

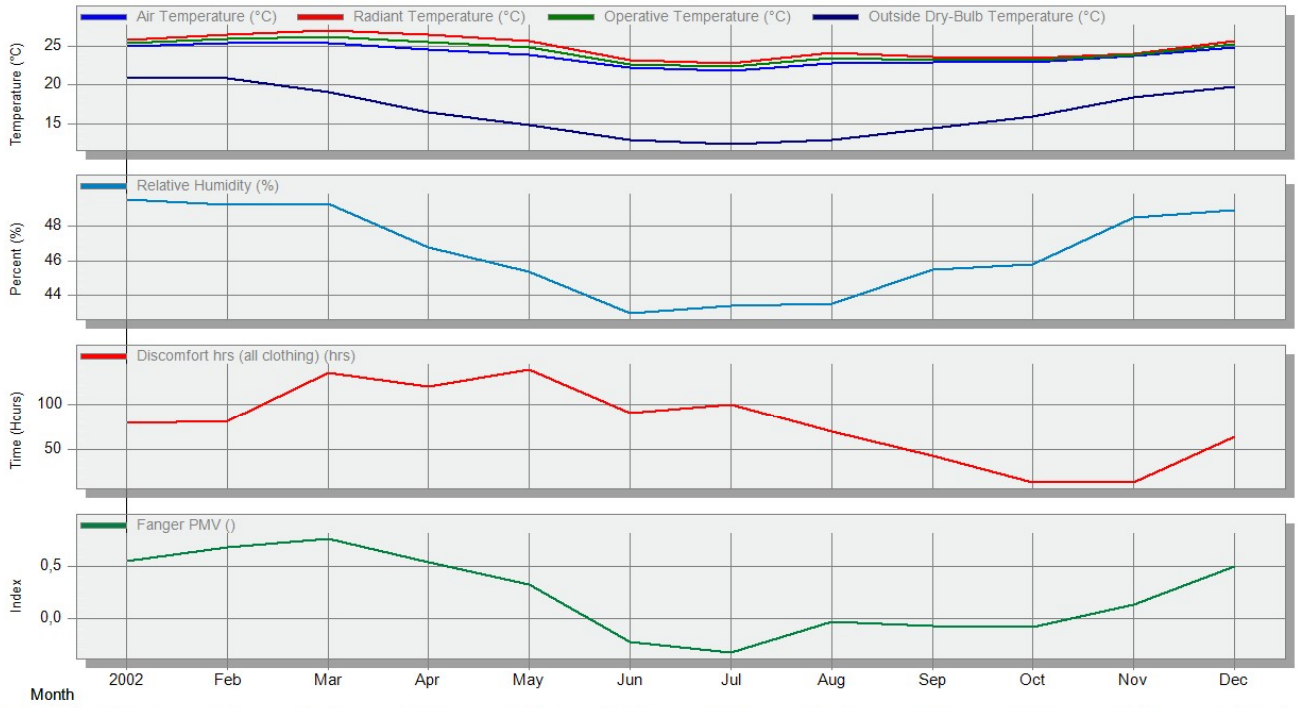

	2002	Feb	Mar	Apr	May	Jun	Jul	Aug	Sep	Oct	Nov	Dec
Air Temperature (°C)	25,03	25,44	25,49	24,59	23,87	22,28	21,89	22,78	22,90	22,91	23,77	24,88
Radiant Temperature (°C)	25,84	26,49	27,09	26,52	25,76	23,16	22,76	24,15	23,57	23,45	24,03	25,63
Operative Temperature (°C)	25,44	25,96	26,29	25,55	24,81	22,72	22,32	23,46	23,23	23,18	23,90	25,25
Outside Dry-Bulb Temperature (°C)	20,82	20,86	19,11	16,48	14,79	12,83	12,31	12,89	14,34	15,96	18,33	19,77
Relative Humidity (%)	49,55	49,22	49,28	46,78	45,35	42,96	43,40	43,53	45,47	45,77	48,49	48,94
Discomfort hrs (all clothing) (hrs)	79,00	80,67	134,33	119,17	137,50	90,00	99,00	69,83	43,00	14,33	14,50	63,50
Fanger PMV ()	0,55	0,69	0,77	0,55	0,33	-0,23	-0,33	-0,04	-0,07	-0,08	0,14	0,50

APPENDIX F – *CLO-0.60 & CLO-0.95 NE1*

CLO 0.60

25,52

EnergyPlus Output

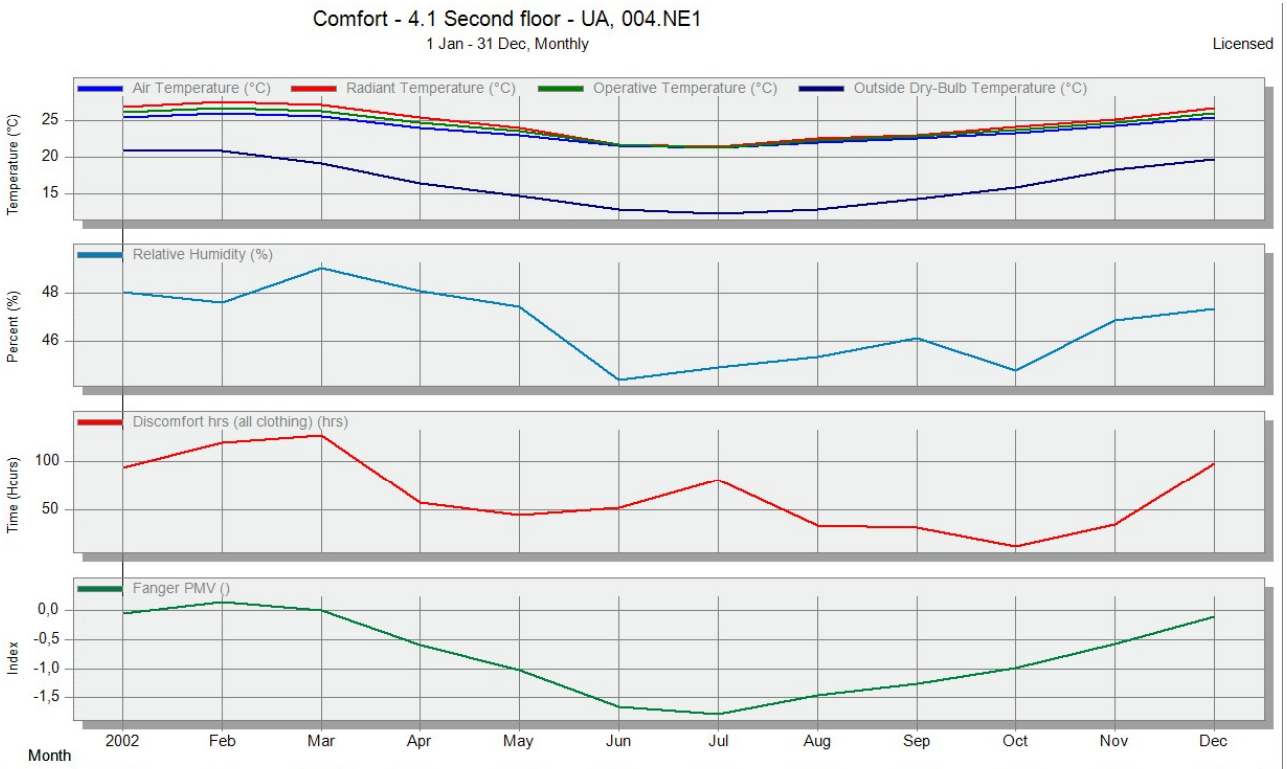

	2002	Feb	Mar	Apr	May	Jun	Jul	Aug	Sep	Oct	Nov	Dec
Air Temperature (°C)	25,52	25,96	25,54	24,09	23,07	21,67	21,31	22,07	22,64	23,26	24,31	25,41
Radiant Temperature (°C)	26,86	27,62	27,16	25,43	24,02	21,80	21,42	22,62	22,99	24,12	25,20	26,69
Operative Temperature (°C)	26,19	26,79	26,35	24,76	23,54	21,73	21,37	22,34	22,82	23,69	24,75	26,05
Outside Dry-Bulb Temperature (°C)	20,82	20,86	19,11	16,48	14,79	12,83	12,31	12,89	14,34	15,96	18,33	19,77
Relative Humidity (%)	48,02	47,60	49,03	48,07	47,42	44,37	44,87	45,31	46,10	44,77	46,85	47,33
Discomfort hrs (all clothing) (hrs)	93,83	118,33	126,17	58,00	45,33	52,67	81,17	34,00	32,33	13,17	35,33	97,50
Fanger PMV ()	-0,05	0,15	0,00	-0,58	-1,02	-1,66	-1,79	-1,45	-1,26	-0,98	-0,57	-0,11

CLO 0.95

25,19

EnergyPlus Output

Comfort - 3.1 First floor - UA, 004.NE1

1 Jan - 31 Dec, Monthly

Licensed

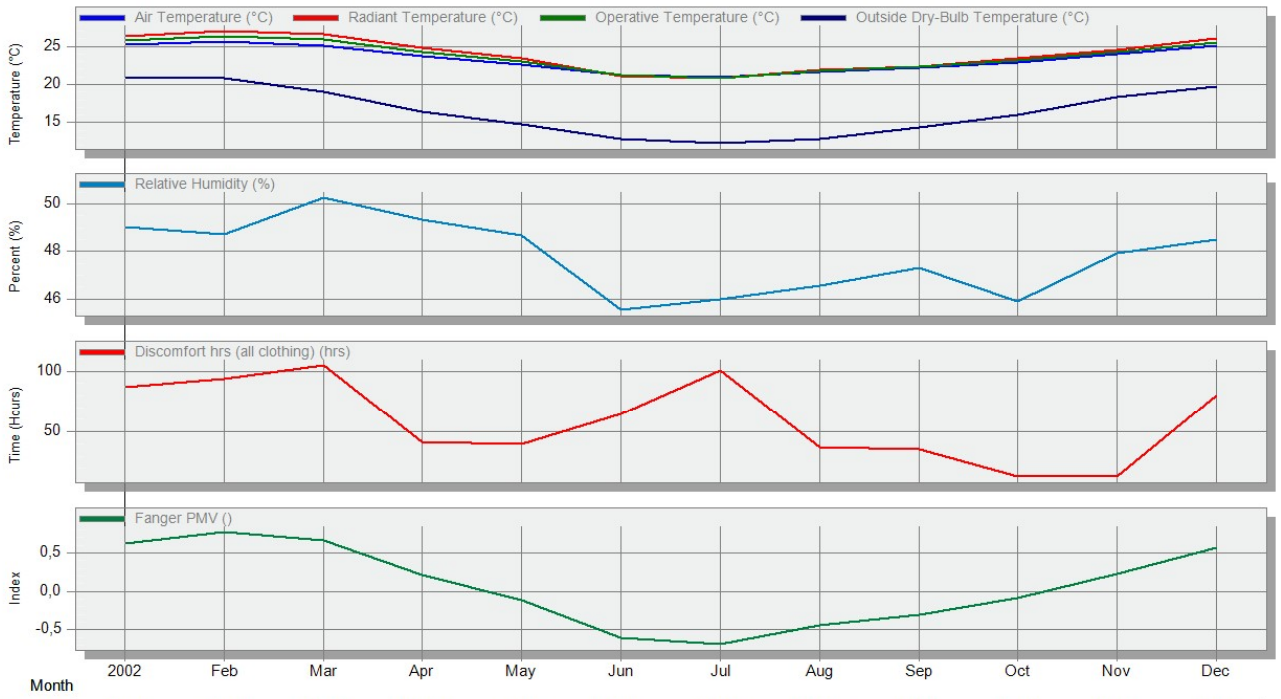

	2002	Feb	Mar	Apr	May	Jun	Jul	Aug	Sep	Oct	Nov	Dec
Air Temperature (°C)	25,19	25,58	25,12	23,67	22,64	21,23	20,92	21,63	22,21	22,86	23,94	25,02
Radiant Temperature (°C)	26,30	27,01	26,53	24,77	23,37	21,16	20,82	21,97	22,34	23,48	24,59	26,05
Operative Temperature (°C)	25,74	26,29	25,83	24,22	23,00	21,19	20,87	21,80	22,28	23,17	24,26	25,53
Outside Dry-Bulb Temperature (°C)	20,82	20,86	19,11	16,48	14,79	12,83	12,31	12,89	14,34	15,96	18,33	19,77
Relative Humidity (%)	49,02	48,72	50,27	49,35	48,69	45,54	45,98	46,55	47,32	45,89	47,93	48,49
Discomfort hrs (all clothing) (hrs)	86,67	94,00	104,83	42,00	39,67	65,00	100,67	37,00	36,00	13,33	13,83	80,17
Fanger PMV ()	0,63	0,77	0,66	0,22	-0,11	-0,60	-0,69	-0,44	-0,31	-0,09	0,22	0,57

APPENDIX G – *CLO-0.60 & CLO-0.95 NNW2*

CLO 0.60

24,92

EnergyPlus Output

Comfort - 3.1 First floor - UA, 003.NNW2

1 Jan - 31 Dec, Monthly

Licensed

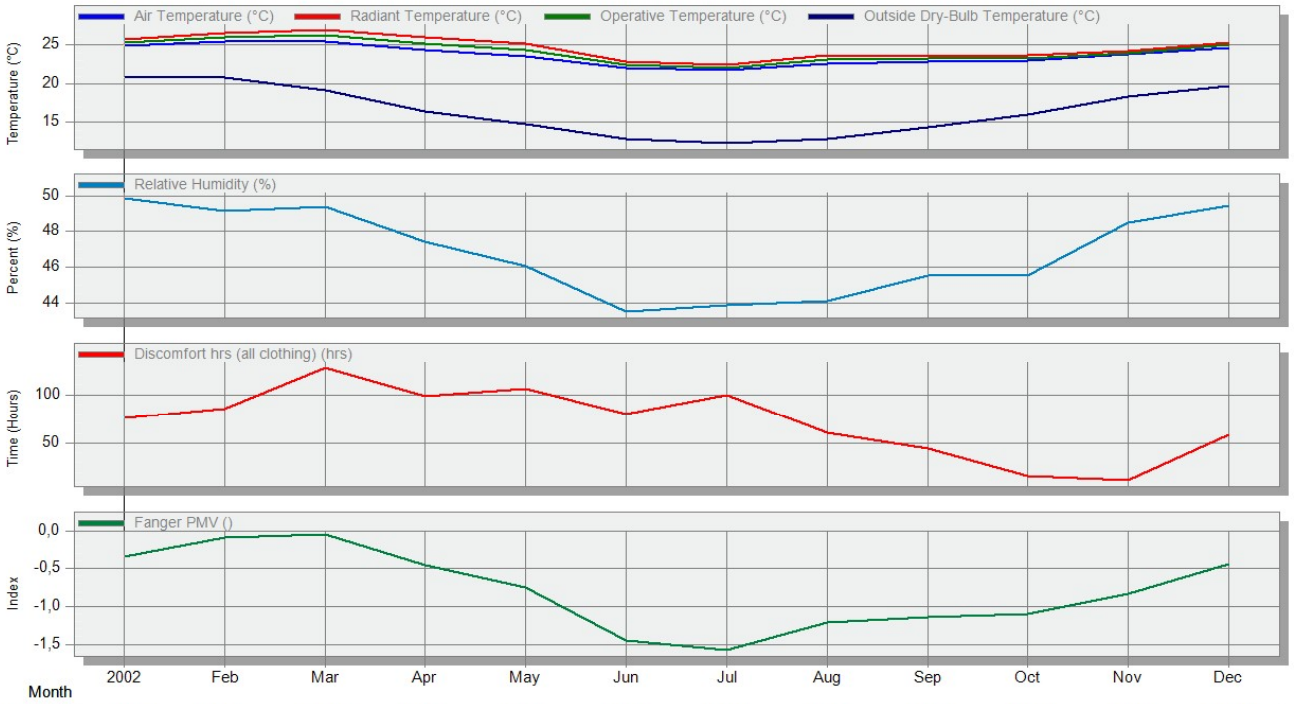

Air Temperature (°C)	24,92	25,46	25,44	24,36	23,60	22,06	21,69	22,54	22,88	22,98	23,78	24,69
Radiant Temperature (°C)	25,71	26,60	26,97	25,94	25,18	22,79	22,40	23,66	23,50	23,62	24,16	25,37
Operative Temperature (°C)	25,31	26,03	26,21	25,15	24,39	22,42	22,04	23,10	23,19	23,30	23,97	25,03
Outside Dry-Bulb Temperature (°C)	20,82	20,86	19,11	16,48	14,79	12,83	12,31	12,89	14,34	15,96	18,33	19,77
Relative Humidity (%)	49,87	49,14	49,39	47,45	46,06	43,49	43,87	44,12	45,53	45,54	48,47	49,48
Discomfort hrs (all clothing) (hrs)	75,33	85,50	127,83	99,00	106,00	80,50	99,83	60,50	44,33	16,67	11,83	58,17
Fanger PMV ()	-0,34	-0,09	-0,04	-0,45	-0,75	-1,44	-1,58	-1,21	-1,14	-1,11	-0,83	-0,44

CLO 0.95

25,07

EnergyPlus Output

Comfort - 4.1 Second floor - UA, 003.NNW2

1 Jan - 31 Dec, Monthly

Licensed

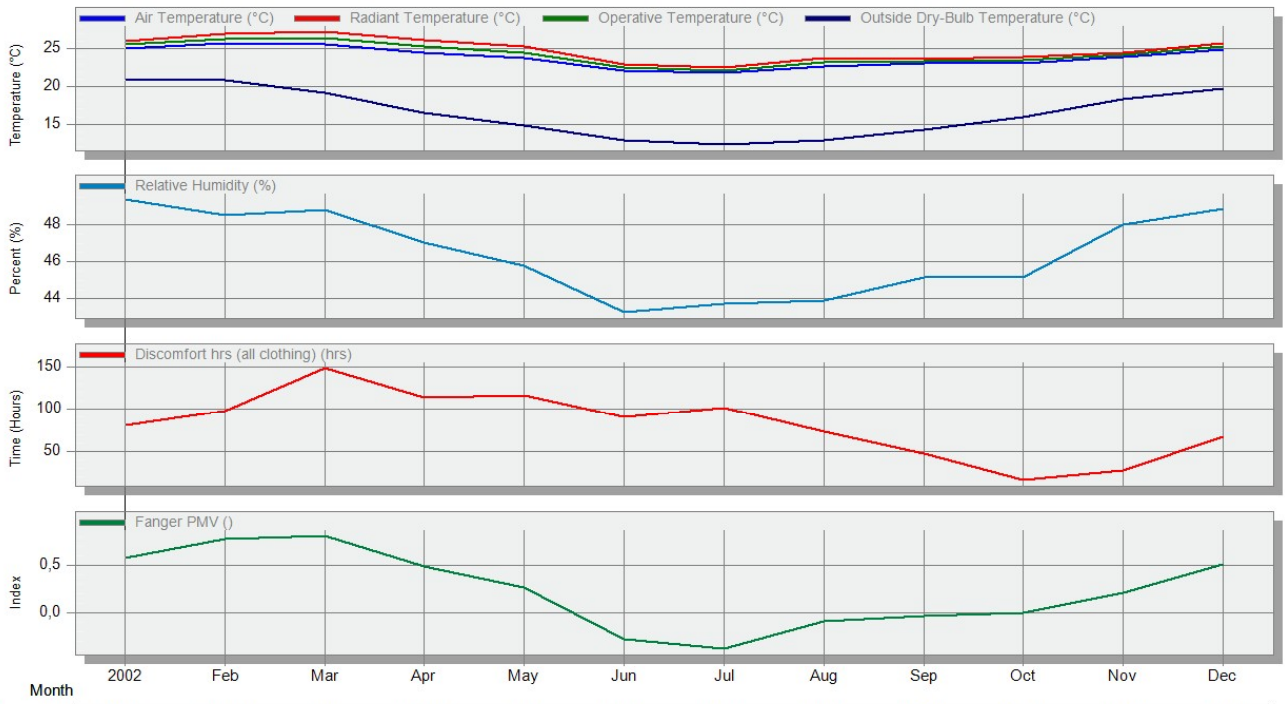

	2002	Feb	Mar	Apr	May	Jun	Jul	Aug	Sep	Oct	Nov	Dec
Air Temperature (°C)	25,07	25,67	25,65	24,51	23,71	22,15	21,75	22,64	23,02	23,12	23,93	24,88
Radiant Temperature (°C)	26,01	26,97	27,28	26,18	25,36	22,90	22,47	23,79	23,69	23,87	24,44	25,71
Operative Temperature (°C)	25,54	26,32	26,46	25,34	24,53	22,53	22,11	23,21	23,36	23,50	24,19	25,30
Outside Dry-Bulb Temperature (°C)	20,82	20,86	19,11	16,48	14,79	12,83	12,31	12,89	14,34	15,96	18,33	19,77
Relative Humidity (%)	49,39	48,50	48,81	47,04	45,78	43,27	43,72	43,89	45,19	45,15	48,00	48,89
Discomfort hrs (all clothing) (hrs)	80,50	97,17	148,33	114,00	116,17	90,83	100,83	73,50	47,00	16,33	27,00	67,17
Fanger PMV ()	0,58	0,78	0,82	0,49	0,27	-0,28	-0,38	-0,10	-0,04	-0,01	0,21	0,51

APPENDIX H – *CLO-0.60 & CLO-0.95 E1*

CLO 0.60

25,62

EnergyPlus Output

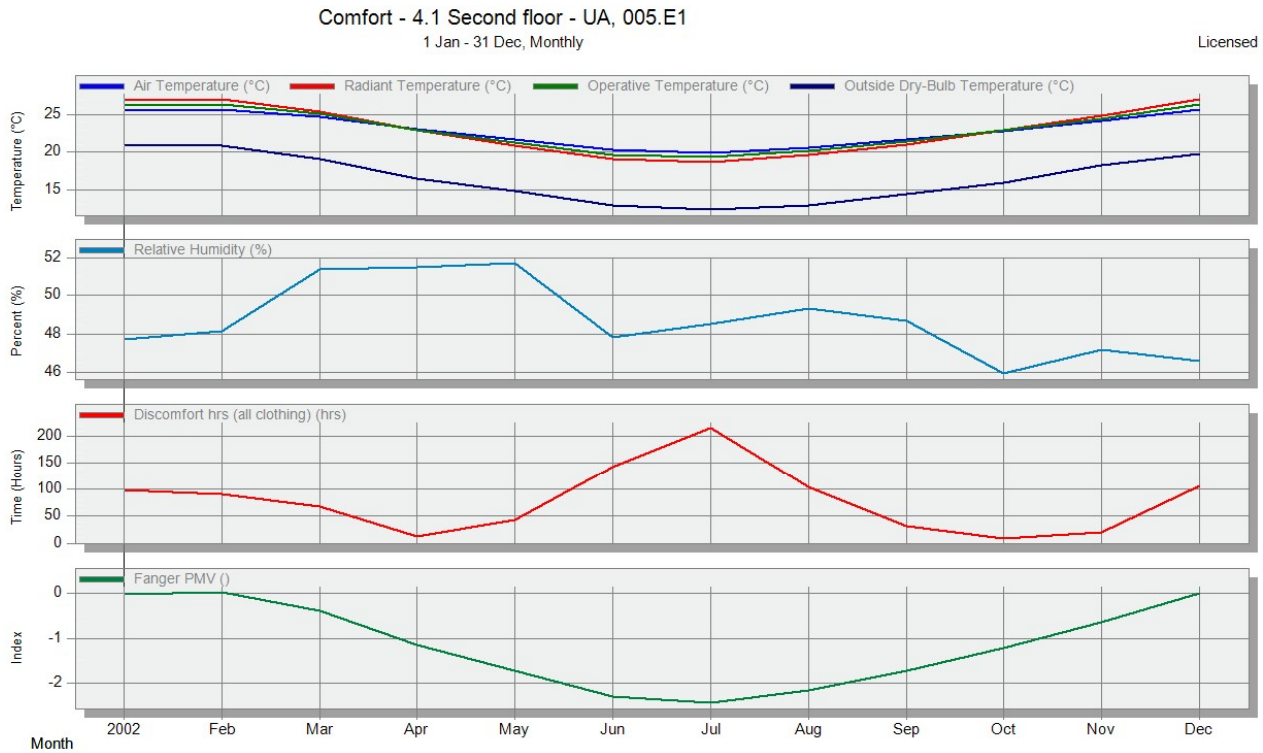

	2002	Feb	Mar	Apr	May	Jun	Jul	Aug	Sep	Oct	Nov	Dec
Air Temperature (°C)	25,62	25,77	24,81	23,03	21,70	20,34	19,95	20,65	21,74	22,85	24,19	25,66
Radiant Temperature (°C)	26,98	27,05	25,44	22,89	20,94	19,05	18,66	19,62	21,05	22,99	24,83	27,11
Operative Temperature (°C)	26,30	26,41	25,12	22,96	21,32	19,70	19,30	20,13	21,39	22,92	24,51	26,39
Outside Dry-Bulb Temperature (°C)	20,82	20,86	19,11	16,48	14,79	12,83	12,31	12,89	14,34	15,96	18,33	19,77
Relative Humidity (%)	47,70	48,17	51,34	51,46	51,69	47,85	48,55	49,35	48,71	45,96	47,18	46,63
Discomfort hrs (all clothing) (hrs)	98,83	91,67	67,50	12,00	43,83	142,83	215,83	104,33	30,83	7,83	19,33	106,67
Fanger PMV ()	-0,02	0,03	-0,39	-1,15	-1,72	-2,30	-2,44	-2,15	-1,71	-1,22	-0,65	0,00

CLO 0.95

25,62

EnergyPlus Output

Comfort - 4.1 Second floor - UA, 005.E1

1 Jan - 31 Dec, Monthly

Licensed

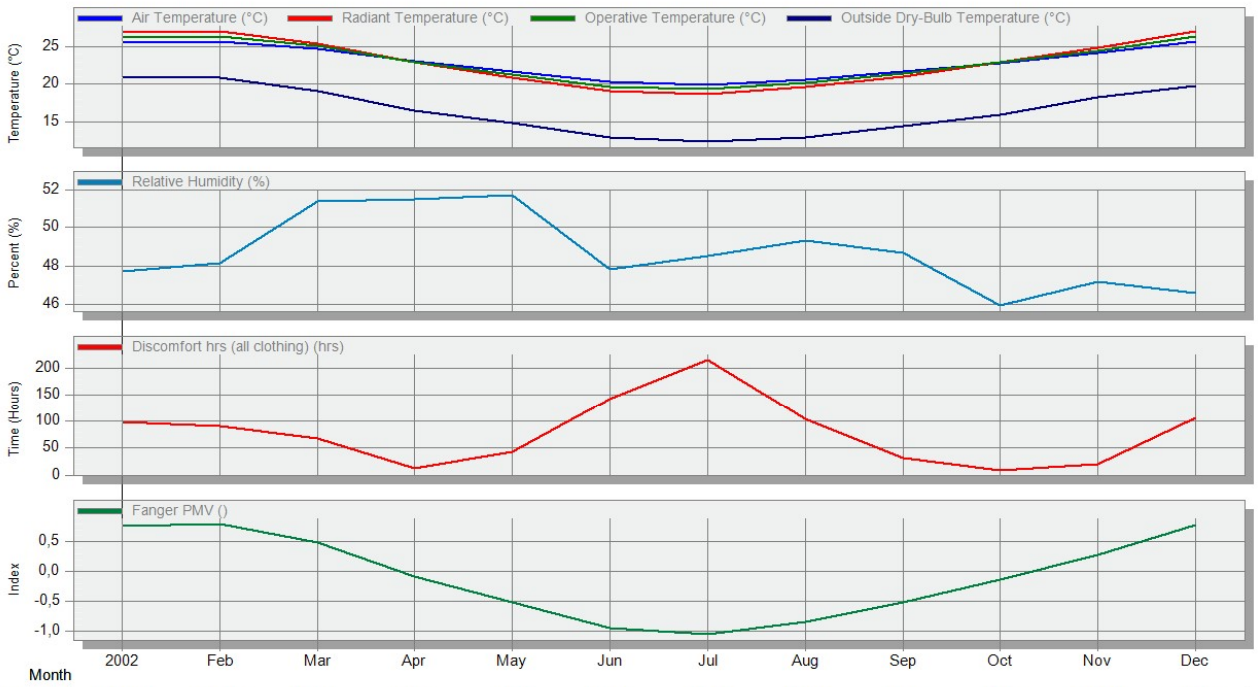

	2002	Feb	Mar	Apr	May	Jun	Jul	Aug	Sep	Oct	Nov	Dec
Air Temperature (°C)	25,62	25,77	24,81	23,03	21,70	20,34	19,95	20,65	21,74	22,85	24,19	25,66
Radiant Temperature (°C)	26,98	27,05	25,44	22,89	20,94	19,05	18,66	19,62	21,05	22,99	24,83	27,11
Operative Temperature (°C)	26,30	26,41	25,12	22,96	21,32	19,70	19,30	20,13	21,39	22,92	24,51	26,39
Outside Dry-Bulb Temperature (°C)	20,82	20,86	19,11	16,48	14,79	12,83	12,31	12,89	14,34	15,96	18,33	19,77
Relative Humidity (%)	47,70	48,17	51,34	51,46	51,69	47,85	48,55	49,35	48,71	45,96	47,18	46,63
Discomfort hrs (all clothing) (hrs)	98,83	91,67	67,50	12,00	43,83	142,83	215,83	104,33	30,83	7,83	19,33	106,67
Fanger PMV ()	0,77	0,80	0,49	-0,09	-0,52	-0,96	-1,06	-0,84	-0,52	-0,14	0,29	0,78

APPENDIX I – *CLO-0.60 & CLO-0.95 SSE1*

CLO 0.60

25,37

EnergyPlus Output

Comfort - 4.1 Second floor - UA, 006.SSE1

1 Jan - 31 Dec, Monthly

Licensed

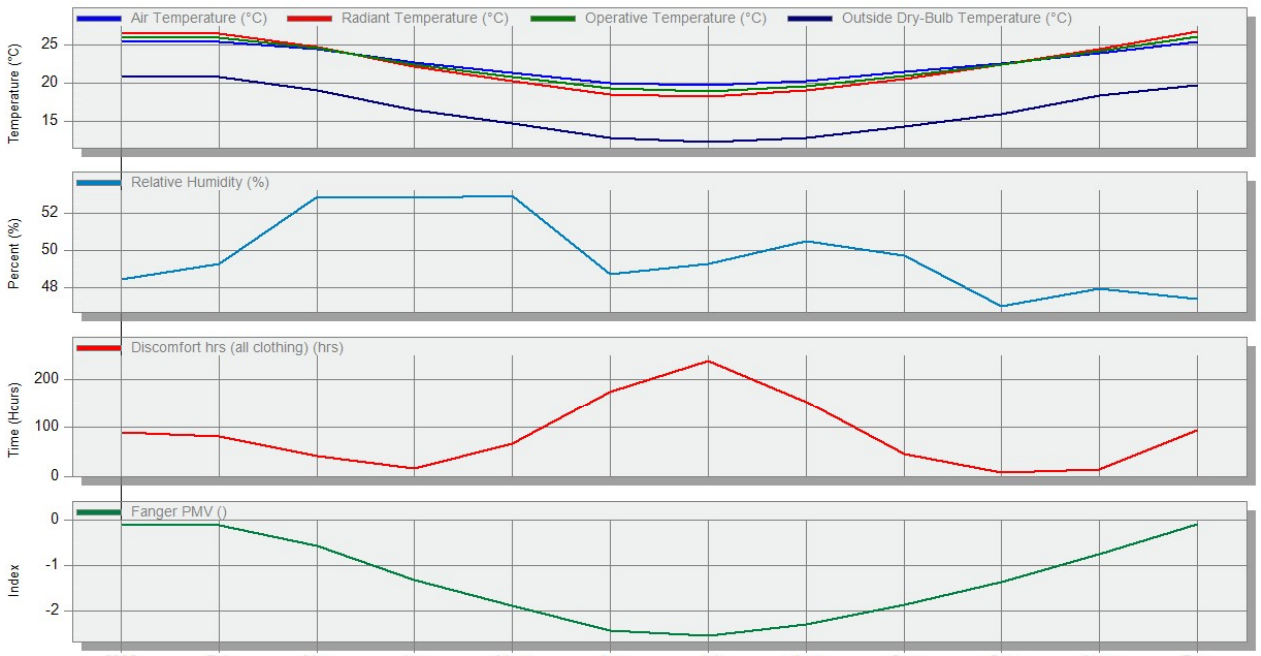

	2002	Feb	Mar	Apr	May	Jun	Jul	Aug	Sep	Oct	Nov	Dec
Air Temperature (°C)	25,37	25,42	24,39	22,65	21,32	20,04	19,71	20,29	21,41	22,51	23,93	25,39
Radiant Temperature (°C)	26,60	26,42	24,67	22,18	20,29	18,57	18,24	19,02	20,48	22,35	24,39	26,74
Operative Temperature (°C)	25,98	25,92	24,53	22,42	20,81	19,31	18,97	19,65	20,95	22,43	24,16	26,06
Outside Dry-Bulb Temperature (°C)	20,82	20,86	19,11	16,48	14,79	12,83	12,31	12,89	14,34	15,96	18,33	19,77
Relative Humidity (%)	48,45	49,24	52,86	52,83	52,93	48,68	49,25	50,45	49,70	46,97	47,94	47,38
Discomfort hrs (all clothing) (hrs)	89,50	80,50	40,33	16,67	67,00	173,17	237,17	152,00	45,67	8,33	14,00	94,33
Fanger PMV ()	-0,12	-0,13	-0,58	-1,32	-1,88	-2,43	-2,54	-2,30	-1,86	-1,37	-0,76	-0,11

CLO 0.95

25,37

EnergyPlus Output

Comfort - 4.1 Second floor - UA, 006.SSE1

1 Jan - 31 Dec, Monthly

Licensed

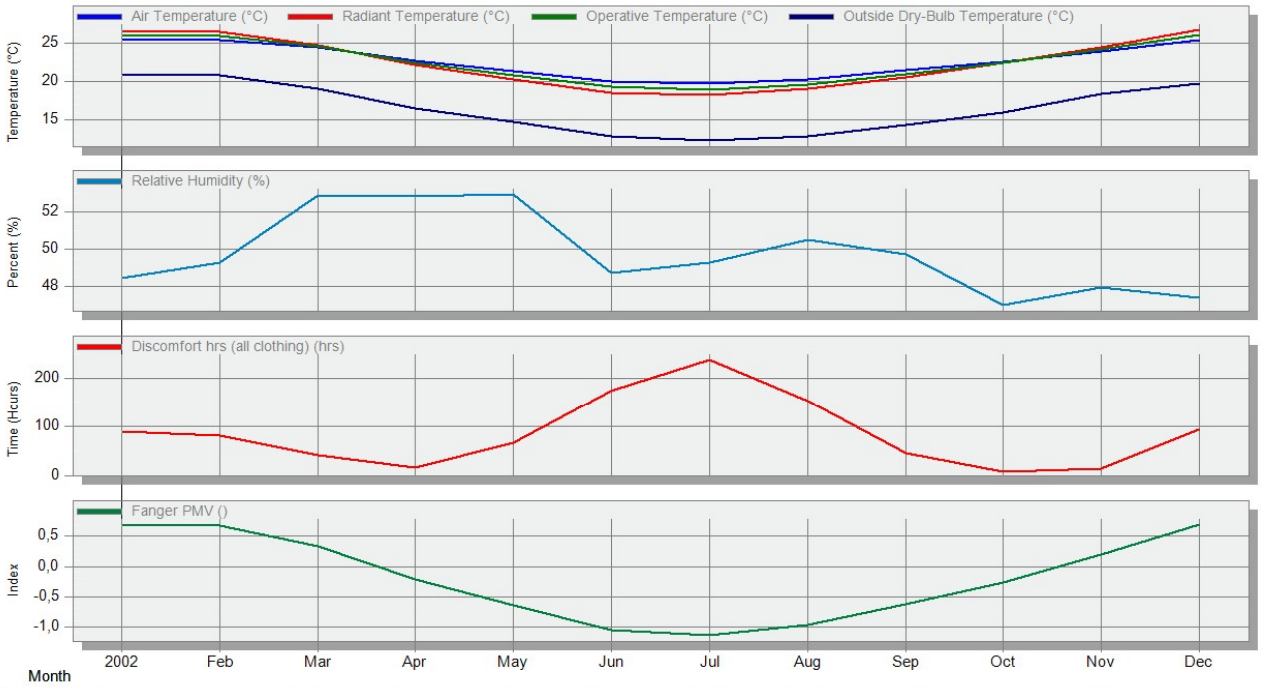

	2002	Feb	Mar	Apr	May	Jun	Jul	Aug	Sep	Oct	Nov	Dec
Air Temperature (°C)	25,37	25,42	24,39	22,65	21,32	20,04	19,71	20,29	21,41	22,51	23,93	25,39
Radiant Temperature (°C)	26,60	26,42	24,67	22,18	20,29	18,57	18,24	19,02	20,48	22,35	24,39	26,74
Operative Temperature (°C)	25,98	25,92	24,53	22,42	20,81	19,31	18,97	19,65	20,95	22,43	24,16	26,06
Outside Dry-Bulb Temperature (°C)	20,82	20,86	19,11	16,48	14,79	12,83	12,31	12,89	14,34	15,96	18,33	19,77
Relative Humidity (%)	48,45	49,24	52,86	52,83	52,93	48,68	49,25	50,45	49,70	46,97	47,94	47,38
Discomfort hrs (all clothing) (hrs)	89,50	80,50	40,33	16,67	67,00	173,17	237,17	152,00	45,67	8,33	14,00	94,33
Fanger PMV ()	0,69	0,68	0,34	-0,22	-0,64	-1,06	-1,14	-0,96	-0,63	-0,26	0,20	0,70

APPENDIX J– *CLO-0.60 & CLO-0.95 S1*

CLO 0.60

25,25

EnergyPlus Output

Comfort - 4.1 Second floor - UA, 007.S1

1 Jan - 31 Dec, Monthly

Licensed

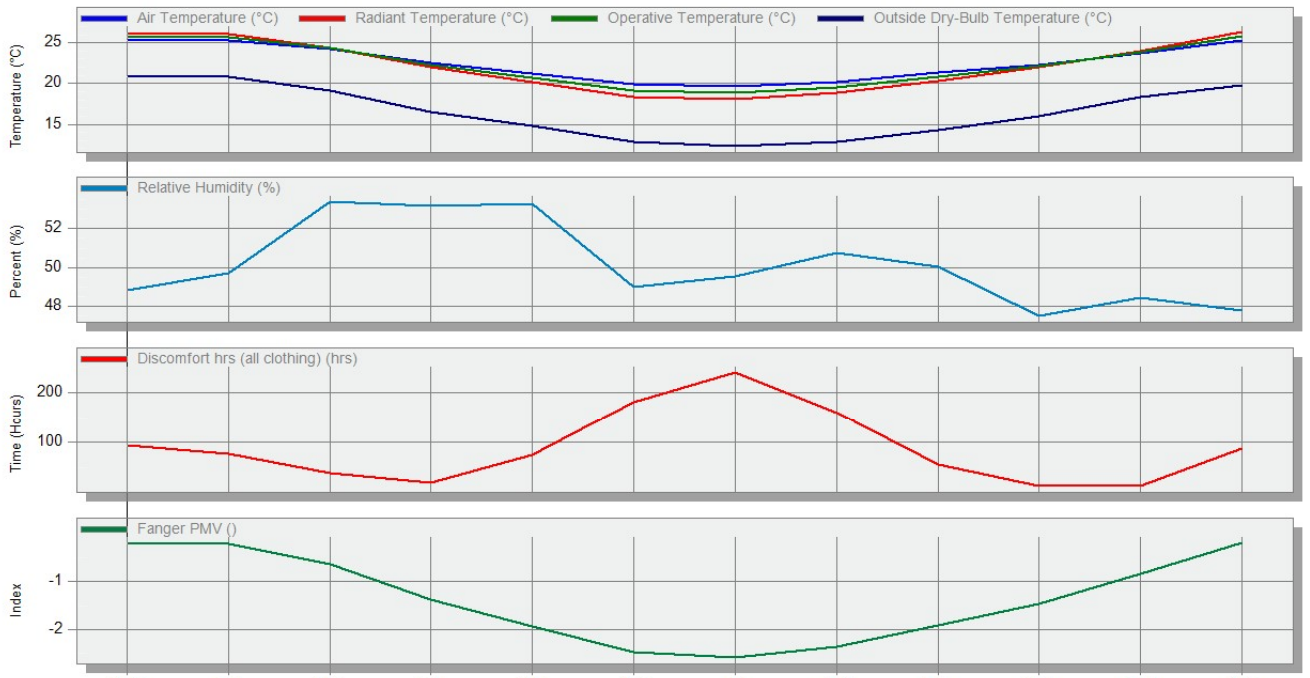

Air Temperature (°C)	25,25	25,27	24,26	22,55	21,22	19,94	19,61	20,18	21,31	22,33	23,77	25,26
Radiant Temperature (°C)	26,25	26,06	24,42	22,01	20,12	18,40	18,09	18,86	20,31	22,03	24,00	26,35
Operative Temperature (°C)	25,75	25,66	24,34	22,28	20,67	19,17	18,85	19,52	20,81	22,18	23,89	25,80
Outside Dry-Bulb Temperature (°C)	20,82	20,86	19,11	16,48	14,79	12,83	12,31	12,89	14,34	15,96	18,33	19,77
Relative Humidity (%)	48,85	49,74	53,40	53,20	53,29	49,00	49,53	50,78	50,04	47,51	48,45	47,80
Discomfort hrs (all clothing) (hrs)	93,67	77,17	38,00	20,33	75,50	180,17	240,67	159,17	55,83	13,17	13,17	87,67
Fanger PMV ()	-0,20	-0,21	-0,64	-1,37	-1,93	-2,47	-2,58	-2,35	-1,90	-1,45	-0,85	-0,19

CLO 0.95

25,25

EnergyPlus Output

Comfort - 4.1 Second floor - UA, 007.S1

1 Jan - 31 Dec, Monthly

Licensed

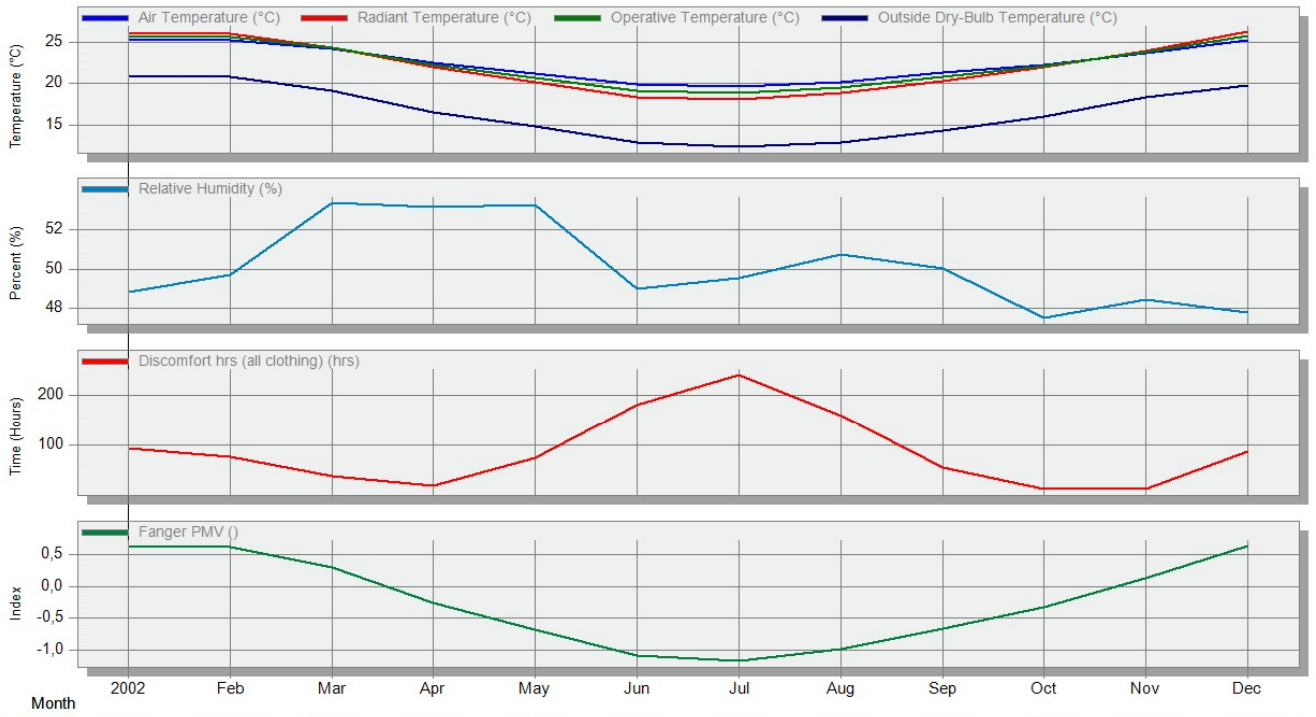

	2002	Feb	Mar	Apr	May	Jun	Jul	Aug	Sep	Oct	Nov	Dec
Air Temperature (°C)	25,25	25,27	24,26	22,55	21,22	19,94	19,61	20,18	21,31	22,33	23,77	25,26
Radiant Temperature (°C)	26,25	26,06	24,42	22,01	20,12	18,40	18,09	18,86	20,31	22,03	24,00	26,35
Operative Temperature (°C)	25,75	25,66	24,34	22,28	20,67	19,17	18,85	19,52	20,81	22,18	23,89	25,80
Outside Dry-Bulb Temperature (°C)	20,82	20,86	19,11	16,48	14,79	12,83	12,31	12,89	14,34	15,96	18,33	19,77
Relative Humidity (%)	48,85	49,74	53,40	53,20	53,29	49,00	49,53	50,78	50,04	47,51	48,45	47,80
Discomfort hrs (all clothing) (hrs)	93,67	77,17	38,00	20,33	75,50	180,17	240,67	159,17	55,83	13,17	13,17	87,67
Fanger PMV ()	0,63	0,62	0,30	-0,25	-0,68	-1,09	-1,17	-0,99	-0,66	-0,32	0,13	0,64

APPENDIX K – *CLO-0.60 & CLO-0.95 SSE2*

CLO 0.60

25,51

EnergyPlus Output

Comfort - 4.1 Second floor - UA, 008.SSE2

1 Jan - 31 Dec, Monthly

Licensed

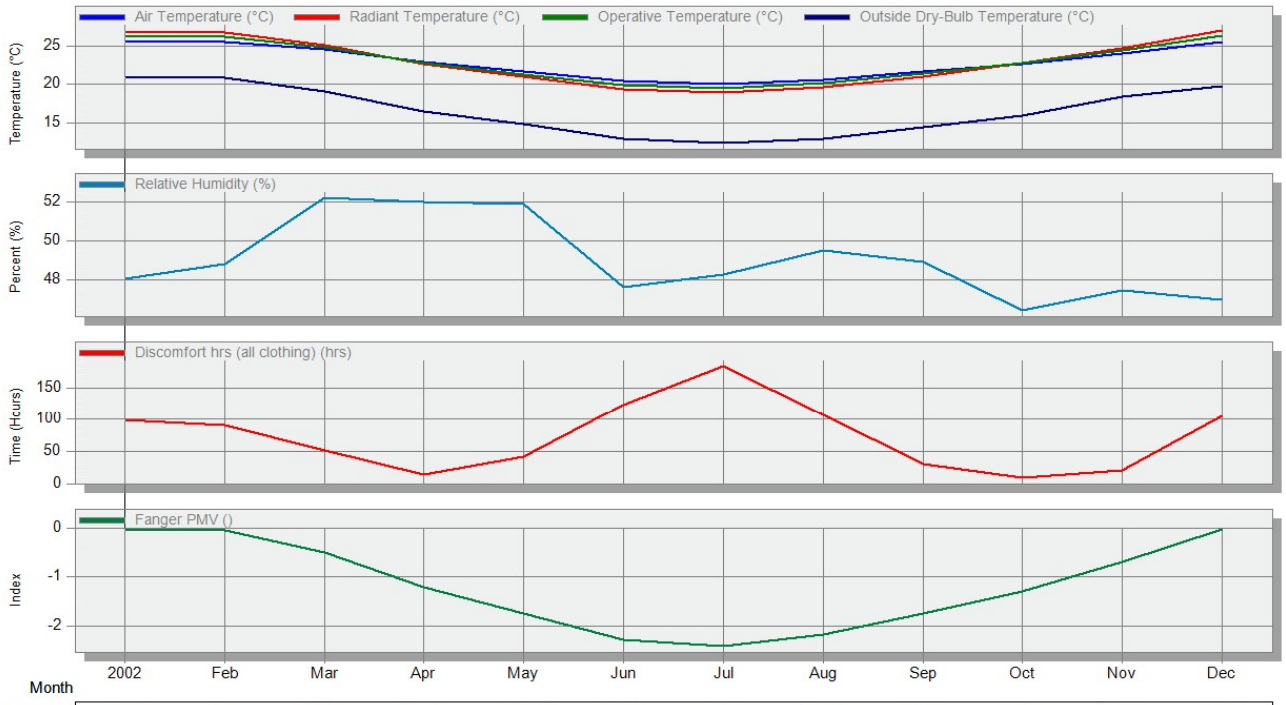

	2002	Feb	Mar	Apr	May	Jun	Jul	Aug	Sep	Oct	Nov	Dec
Air Temperature (°C)	25,51	25,56	24,56	22,88	21,63	20,40	20,03	20,59	21,66	22,69	24,08	25,54
Radiant Temperature (°C)	26,91	26,75	25,07	22,71	20,96	19,27	18,87	19,64	21,02	22,79	24,75	27,06
Operative Temperature (°C)	26,21	26,16	24,81	22,79	21,29	19,84	19,45	20,12	21,34	22,74	24,42	26,30
Outside Dry-Bulb Temperature (°C)	20,82	20,86	19,11	16,48	14,79	12,83	12,31	12,89	14,34	15,96	18,33	19,77
Relative Humidity (%)	48,04	48,79	52,24	52,00	51,91	47,64	48,29	49,51	48,93	46,43	47,49	46,96
Discomfort hrs (all clothing) (hrs)	98,50	91,00	50,67	14,50	42,33	122,33	183,67	106,00	30,17	8,50	20,67	104,50
Fanger PMV ()	-0,05	-0,05	-0,49	-1,21	-1,73	-2,26	-2,39	-2,16	-1,73	-1,28	-0,68	-0,03

CLO 0.95

25,51

EnergyPlus Output

Comfort - 4.1 Second floor - UA, 008.SSE2

1 Jan - 31 Dec, Monthly

Licensed

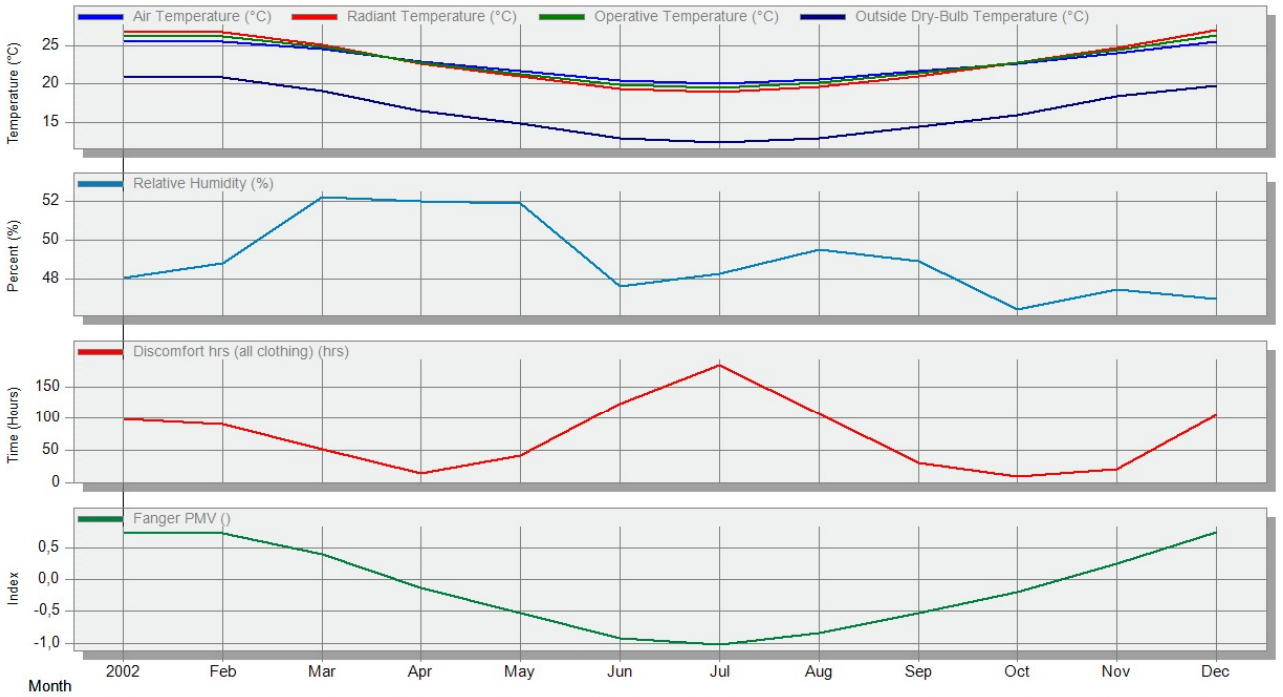

Air Temperature (°C)	25,51	25,56	24,56	22,88	21,63	20,40	20,03	20,59	21,66	22,69	24,08	25,54
Radiant Temperature (°C)	26,91	26,75	25,07	22,71	20,96	19,27	18,87	19,64	21,02	22,79	24,75	27,06
Operative Temperature (°C)	26,21	26,16	24,81	22,79	21,29	19,84	19,45	20,12	21,34	22,74	24,42	26,30
Outside Dry-Bulb Temperature (°C)	20,82	20,86	19,11	16,48	14,79	12,83	12,31	12,89	14,34	15,96	18,33	19,77
Relative Humidity (%)	48,04	48,79	52,24	52,00	51,91	47,64	48,29	49,51	48,93	46,43	47,49	46,96
Discomfort hrs (all clothing) (hrs)	98,50	91,00	50,67	14,50	42,33	122,33	183,67	106,00	30,17	8,50	20,67	104,50
Fanger PMV ()	0,74	0,74	0,41	-0,13	-0,53	-0,93	-1,03	-0,85	-0,53	-0,19	0,26	0,76

APPENDIX L – *CLO-0.60 & CLO-0.95 SW1*

CLO 0.60

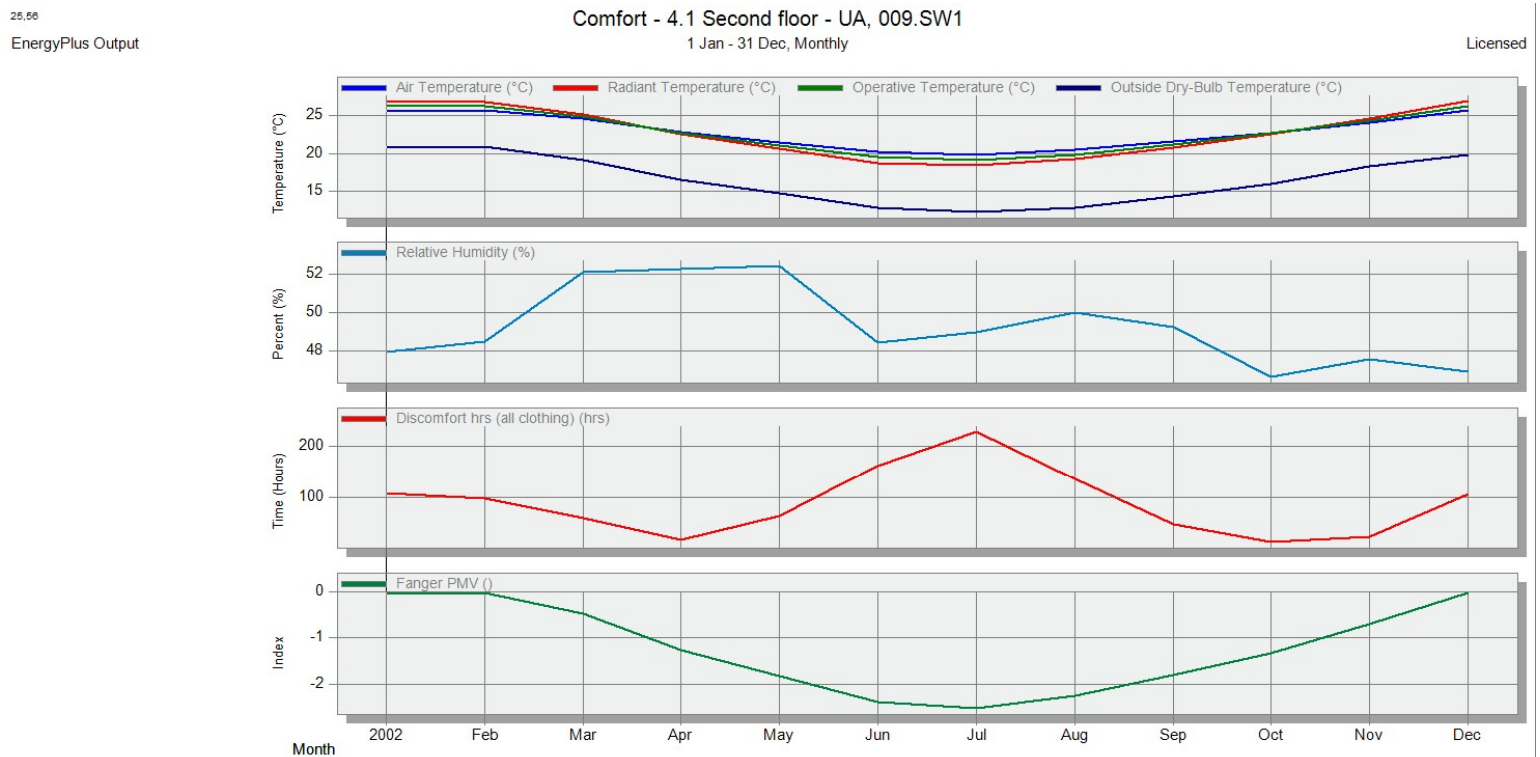

	2002	Feb	Mar	Apr	May	Jun	Jul	Aug	Sep	Oct	Nov	Dec
Air Temperature (°C)	25,56	25,68	24,61	22,80	21,47	20,15	19,80	20,43	21,56	22,62	24,08	25,60
Radiant Temperature (°C)	26,78	26,77	25,05	22,47	20,58	18,79	18,43	19,29	20,74	22,58	24,57	26,90
Operative Temperature (°C)	26,17	26,23	24,83	22,63	21,03	19,47	19,12	19,86	21,15	22,60	24,32	26,25
Outside Dry-Bulb Temperature (°C)	20,82	20,86	19,11	16,48	14,79	12,83	12,31	12,89	14,34	15,96	18,33	19,77
Relative Humidity (%)	47,94	48,49	52,11	52,30	52,45	48,38	48,96	50,00	49,24	46,60	47,51	46,87
Discomfort hrs (all clothing) (hrs)	108,00	96,33	58,00	16,83	62,67	162,50	228,50	136,33	47,33	12,17	22,00	106,17
Fanger PMV ()	-0,06	-0,02	-0,48	-1,25	-1,81	-2,38	-2,50	-2,24	-1,79	-1,32	-0,71	-0,04

CLO 0.95

25,56

EnergyPlus Output

Comfort - 4.1 Second floor - UA, 009.SW1

1 Jan - 31 Dec, Monthly

Licensed

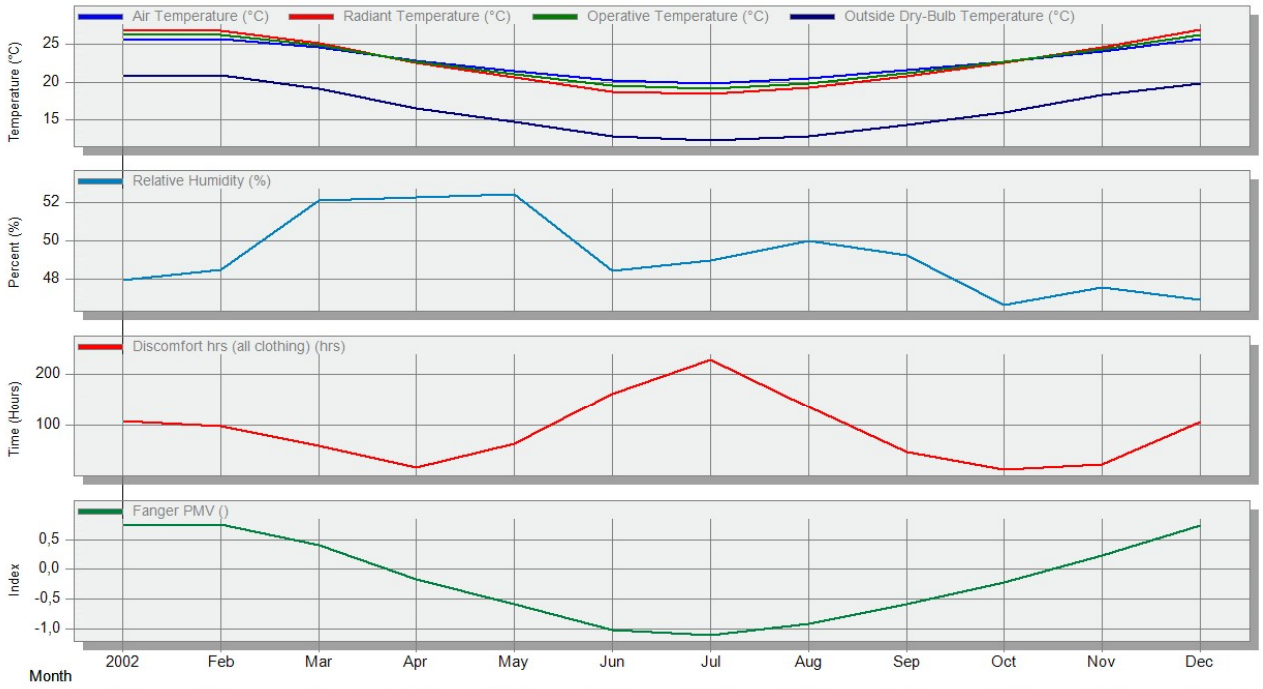

	2002	Feb	Mar	Apr	May	Jun	Jul	Aug	Sep	Oct	Nov	Dec
Air Temperature (°C)	25,56	25,68	24,61	22,80	21,47	20,15	19,80	20,43	21,56	22,62	24,08	25,60
Radiant Temperature (°C)	26,78	26,77	25,05	22,47	20,58	18,79	18,43	19,29	20,74	22,58	24,57	26,90
Operative Temperature (°C)	26,17	26,23	24,83	22,63	21,03	19,47	19,12	19,86	21,15	22,60	24,32	26,25
Outside Dry-Bulb Temperature (°C)	20,82	20,86	19,11	16,48	14,79	12,83	12,31	12,89	14,34	15,96	18,33	19,77
Relative Humidity (%)	47,94	48,49	52,11	52,30	52,45	48,38	48,96	50,00	49,24	46,60	47,51	46,87
Discomfort hrs (all clothing) (hrs)	108,00	96,33	58,00	16,83	62,67	162,50	228,50	136,33	47,33	12,17	22,00	106,17
Fanger PMV ()	0,73	0,76	0,42	-0,17	-0,59	-1,02	-1,11	-0,91	-0,58	-0,22	0,24	0,75

APPENDIX M – *CLO-0.60 & CLO-0.95 SW1*

CLO 0.60

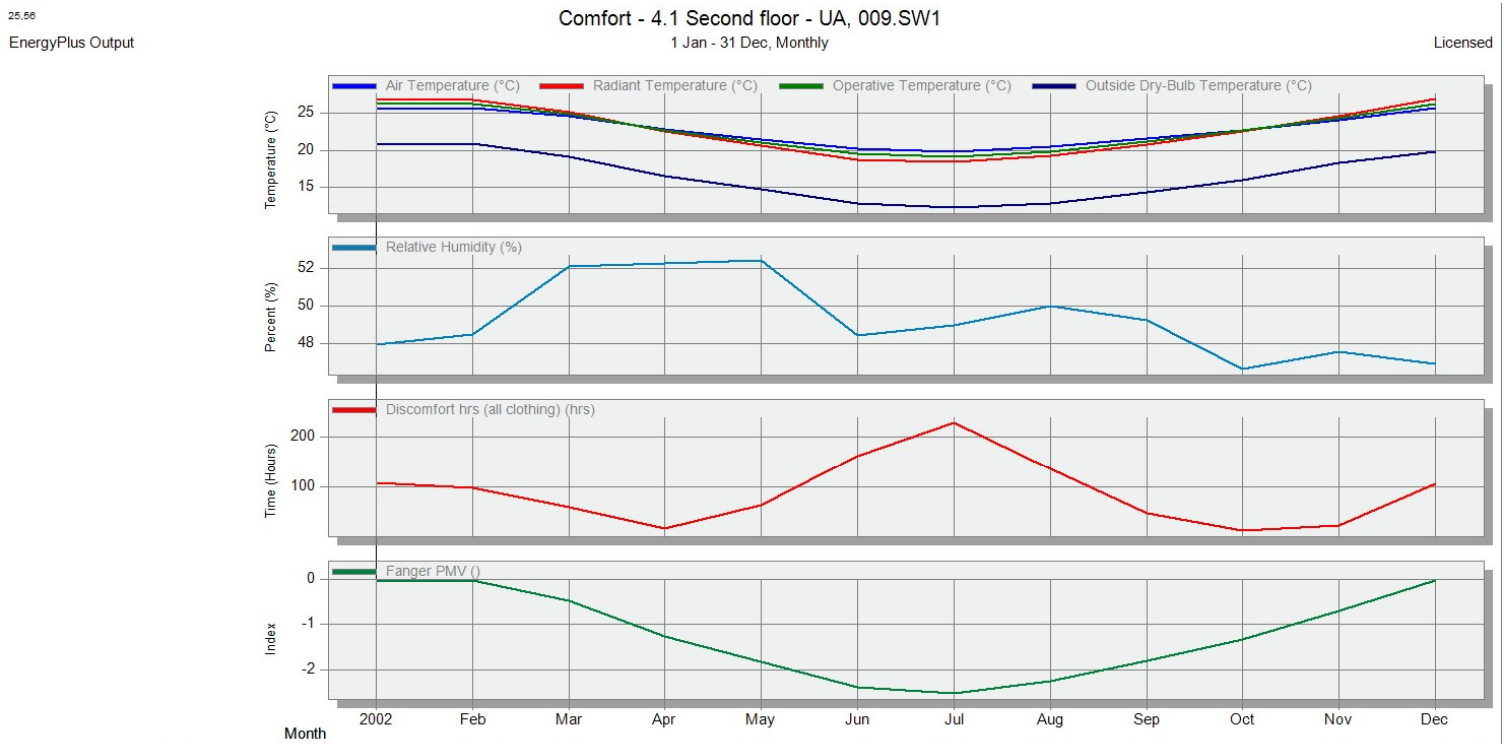

Air Temperature (°C)	25,56	25,68	24,61	22,80	21,47	20,15	19,80	20,43	21,56	22,62	24,08	25,60
Radiant Temperature (°C)	26,78	26,77	25,05	22,47	20,58	18,79	18,43	19,29	20,74	22,58	24,57	26,90
Operative Temperature (°C)	26,17	26,23	24,83	22,63	21,03	19,47	19,12	19,86	21,15	22,60	24,32	26,25
Outside Dry-Bulb Temperature (°C)	20,82	20,86	19,11	16,48	14,79	12,83	12,31	12,89	14,34	15,96	18,33	19,77
Relative Humidity (%)	47,94	48,49	52,11	52,30	52,45	48,38	48,96	50,00	49,24	46,60	47,51	46,87
Discomfort hrs (all clothing) (hrs)	108,00	96,33	58,00	16,83	62,67	162,50	228,50	136,33	47,33	12,17	22,00	106,17
Fanger PMV ()	-0,06	-0,02	-0,48	-1,25	-1,81	-2,38	-2,50	-2,24	-1,79	-1,32	-0,71	-0,04

CLO 0.95

26,13

EnergyPlus Output

Comfort - 4.1 Second floor - UA, 010.NW1

1 Jan - 31 Dec, Monthly

Licensed

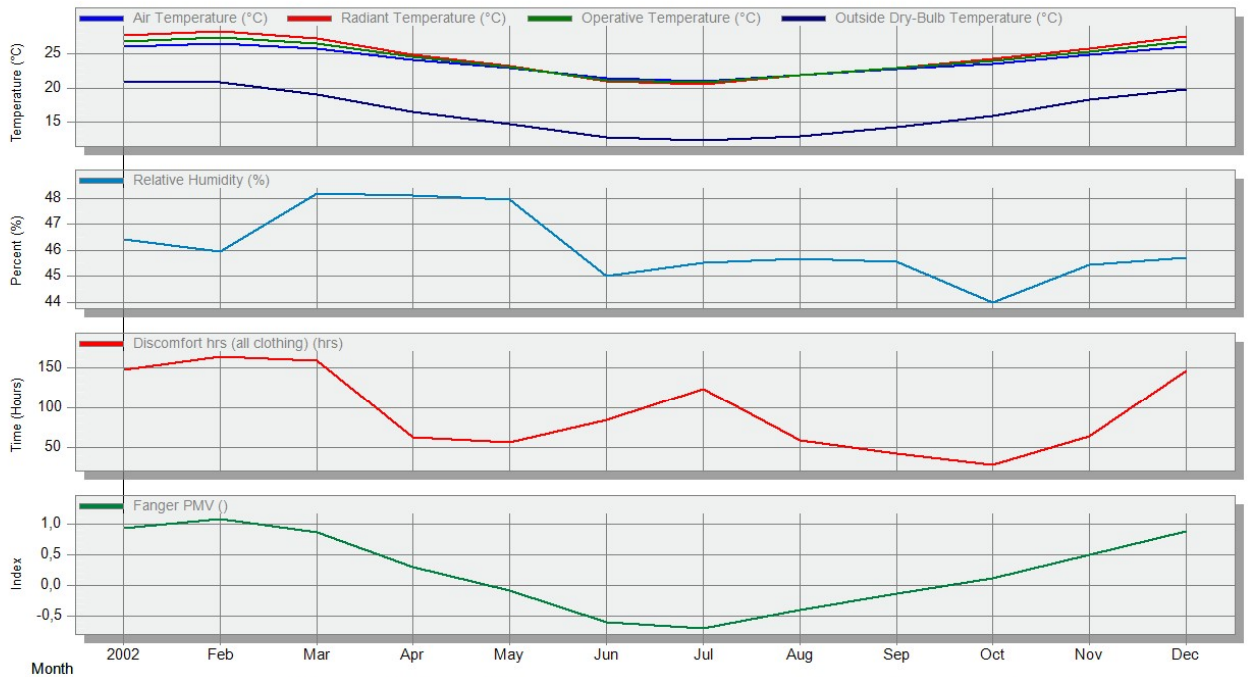

	2002	Feb	Mar	Apr	May	Jun	Jul	Aug	Sep	Oct	Nov	Dec
Air Temperature (°C)	26,13	26,62	25,87	24,12	22,94	21,42	21,03	21,95	22,89	23,57	24,85	26,06
Radiant Temperature (°C)	27,70	28,39	27,33	24,96	23,32	20,99	20,59	21,99	23,04	24,37	25,86	27,55
Operative Temperature (°C)	26,91	27,50	26,60	24,54	23,13	21,20	20,81	21,97	22,97	23,97	25,35	26,80
Outside Dry-Bulb Temperature (°C)	20,82	20,86	19,11	16,48	14,79	12,83	12,31	12,89	14,34	15,96	18,33	19,77
Relative Humidity (%)	46,43	45,95	48,19	48,11	47,93	45,02	45,54	45,66	45,55	43,98	45,45	45,71
Discomfort hrs (all clothing) (hrs)	147,50	164,00	158,33	63,50	56,50	84,83	123,83	58,67	43,33	28,67	64,00	145,67
Fanger PMV ()	0,92	1,08	0,85	0,30	-0,08	-0,60	-0,70	-0,40	-0,13	0,11	0,50	0,88

APPENDIX N - *MEAN RADIANT TEMPERATURE OPERATION HOURS*

LOCATION	FLOOR AREA (m^2)	MEAN RADIANT TEMPERATURE (MRT)											
		<18	18 to 19	19 to 20	20 to 21	21 to 22	22 to 23	23 to 24	24 to 25	25 to 26	26 to 27	27 to 28	> 28
NNW1	156	26,0	176	314	527	647	790	972	1065	1080	955	769	1439
N1	205	28,0	170	331	567	697	835	1030	1146	1055	822	603	1476
NNW2	180	30,0	182	335	547	682	824	1059	1082	1006	894	673	1446
NE1	160	57,0	280	435	574	694	723	826	981	1041	993	772	1384
E1	107	690,0	632	762	796	782	702	667	864	843	717	557	748
S1	206	1110,0	792	823	766	762	683	783	891	778	562	391	419
SSE1	200	945,0	782	830	811	733	683	719	854	820	596	457	530
SSE2	134	629,0	638	809	801	772	773	721	881	872	680	511	673
SW1	158	837,0	717	822	780	752	693	669	840	856	711	470	613
NW1	98	203,0	396	443	642	713	712	689	782	862	936	739	1643

APPENDIX O – *AIR TEMPERATURE (AT) THERMAL OPERATION HOURS*

LOCATION	FLOOR AREA (m^2)	AIR TEMPERATURE					
		< 20	20 to 21	21 to 22	22 to 23	23 to 24	> 24
NNW1	156	357,00	545,00	603,00	936,00	3095,00	3224,00
N1	205	345,00	571,00	617,00	921,00	3188,00	3118,00
NNW2	180	366,00	574,00	624,00	928,00	3124,00	3124,00
NE1	160	540,00	559,00	700,00	839,00	3073,00	3049,00
E1	107	1215,00	876,00	728,00	880,00	2552,00	2509,00
S1	206	1579,00	945,00	698,00	893,00	2467,00	2178,00
SSE1	200	1469,00	951,00	719,00	877,00	2470,00	2274,00
SSE2	134	1234,00	909,00	720,00	906,00	2592,00	2399,00
SW1	158	1362,00	948,00	715,00	881,00	2466,00	2388,00
NW1	**98**	**609,00**	**603,00**	**719,00**	**843,00**	**2820,00**	**3166,00**

APPENDIX P – *RELATIVE HUMIDITY (RH) THERMAL OPERATION HOURS*

LOCATION	FLOOR AREA (m^2)	RELATIVE HUMIDITY (RH)									
		0 to 10	10 to 20	20 to 30	30 to 40	40 to 50	50 to 60	60 to 70	70 to 80	80 to 90	90 to 100
NNW1	156	0,0	516	7657	587	0,0	0,0	0,0	0,0	0,0	0,0
N1	205	0,0	529	7543	688	0,0	0,0	0,0	0,0	0,0	0,0
NNW2	180	0,0	547	7541	672	0,0	0,0	0,0	0,0	0,0	0,0
NE1	160	0,0	772	7647	341	0,0	0,0	0,0	0,0	0,0	0,0
E1	107	0,0	2084	6552	124	0,0	0,0	0,0	0,0	0,0	0,0
S1	206	0,0	2725	6019	16	0,0	0,0	0,0	0,0	0,0	0,0
SSE1	200	0,0	2557	6158	45	0,0	0,0	0,0	0,0	0,0	0,0
SSE2	134	0,0	2076	6612	72	0,0	0,0	0,0	0,0	0,0	0,0
SW1	158	0,0	2376	6271	113	0,0	0,0	0,0	0,0	0,0	0,0
NW1	98	0,0	1042	7003	715	0,0	0,0	0,0	0,0	0,0	0,0

APPENDIX Q – *CLO60 AND CLO95 THERMAL SIMULATION DATA SUMMARY*

PMV weighted average results for CLO60

ZONE	FLOOR AREA (m^2)	HRS OUTSIDE OF PMV RANGE -0.5 TO 0.5	%HRS OUTSIDE OF PMV RANGE -0.5 TO 0.5	WEIGHTED HRS OUTSIDE OF PMV RANGE -0.5 TO 0.5	HRS OUTSIDE OF PMV RANGE -1.0 AND 1.0	%HRS OUTSIDE OF PMV RANGE -1.0 TO 1.0	WEIGHTED HRS OUTSIDE OF PMV RANGE -1.0 TO 0.1.0
NNW1	156	5937	67,77%	0,070204	3159	36,06%	0,03735
N1	205	5997	68,46%	0,093188	3195	36,47%	0,04965
NNW2	180	6043	68,98%	0,082451	3253	37,13%	0,04438
NE1	160	5866	66,96%	0,071143	3362	38,38%	0,04077
E1	107	5690	64,95%	0,046149	3771	43,05%	0,03059
S1	206	7271	83,00%	0,113536	5206	59,43%	0,08129
SSE1	200	6997	79,87%	0,106075	5058	57,74%	0,07668
SSE2	134	6765	77,23%	0,068714	4815	54,97%	0,04891
SW1	158	6904	78,81%	0,082685	4939	56,38%	0,05915
NW1	98	5958	68,01%	0,044259	3763	42,96%	0,02795
TOTAL	1604	%W.A outside PMV range -0.5 to 0.5		77,84%	N/A	N/A	46,88%

PMV weighted average results for CLO95

ZONE	FLOOR AREA (m^2)	HRS OUTSIDE OF PMV RANG -0.5 TO 0.5	% HRS OUTSIDE OF PMV RANG -0.5 TO 0.5	WEIGHTED HRS OUTSIDE OF PMV RANG -0.5 TO 0.5	HRS OUTSIDE OF PMV RANG -1.0 AND 1.0	% HRS OUTSIDE OF PMV RANG -1.0 TO 1.0	WEIGHTED HRS OUTSIDE OF PMV RANG -1.0 TO 0.1.0
NNW1	156	4114	46,96%	0,048647	1092	12,47%	0,01291
N1	205	4006	45,73%	0,062249	988	11,28%	0,01535
NNW2	180	4030	46,00%	0,054986	1077	12,29%	0,01469
NE1	160	4377	49,97%	0,053084	1113	12,71%	0,01350
E1	107	4821	55,03%	0,039101	1775	20,26%	0,01440
S1	206	4617	52,71%	0,072094	2028	23,15%	0,03167
SSE1	200	4754	54,27%	0,072071	1926	21,99%	0,02920
SSE2	134	4634	52,90%	0,047069	1677	19,14%	0,01703
SW1	158	4798	54,77%	0,057463	1925	21,97%	0,02305
NW1	98	4834	55,18%	0,035909	1669	19,05%	0,01240
TOTAL	1604	%W.A outside PMV range -0.5 to 0.5		54,27%	N/A	N/A	17,18%